

UCLA

UCLA Electronic Theses and Dissertations

Title

Overlapping and Discrete Functions of the Matricellular Proteins CCN1 and CCN2 during Endochondral Bone Formation

Permalink

<https://escholarship.org/uc/item/1cf7827n>

Author

Ong, Jessica Renee

Publication Date

2013

Peer reviewed|Thesis/dissertation

UNIVERSITY OF CALIFORNIA

Los Angeles

Overlapping and Discrete Functions of the Matricellular
Proteins CCN1 and CCN2 during Endochondral Bone Formation

A thesis submitted in partial satisfaction
of the requirements for the Degree Master of Arts
in Molecular, Cell, and Developmental Biology

by

Jessica Renee Ong

2013

ABSTRACT OF THE THESIS

Overlapping and Discrete Functions of the Matricellular Proteins CCN1 and CCN2 during Endochondral Bone Formation

by

Jessica Renee Ong

Master of Arts in Molecular, Cell, and Developmental Biology

University of California, Los Angeles, 2013

Professor Karen Lyons, Chair

The CCN (Cyr61/Ctgf/Nov) family of matricellular proteins integrates the extracellular environment with the intracellular environment, with involvement in many cellular processes such as adhesion, proliferation, mechanical stretch, fibrosis, and more. A large question lurks regarding how these CCNs interact with each other to regulate many normal physiological events, as well as disease pathogenesis. While CCN1 and CCN2 are two of the best-studied CCN family members, it remains elusive whether they have similar roles in endochondral bone formation despite similar patterns of mRNA and protein expression within developing bones. Furthermore, *in vivo* data have already shown the significance of CCN2 for endochondral bone formation, but a role for CCN1 in chondrogenesis has only been shown *in vitro*. In order to study whether CCN1 and CCN2 have overlapping functions in endochondral bone formation, we utilized a collagen II/cartilage-selective deletion of *Ccn1* and/or *Ccn2* to analyze the phenotypes of *Ccn1* and *Ccn2* single and double mutant mice. A generally more severe skeletal phenotype was evident in the double mutant axial skeletons, implying the possibility that CCN1 and CCN2 may

have overlapping functions. Surprisingly, in the appendicular skeletons there was not a more severe double mutant phenotype but rather a phenotype closely resembling that of *Ccn2* single mutants, indicating that CCN2 plays a more dominant role within the appendicular skeleton. This supports the new idea that CCN2 is epistatic to CCN1. In addition, CCN1 and CCN2 may work antagonistically to regulate chondrocyte proliferation in the resting zone of tibial growth plates. Also, a novel phenotype was discovered as the double mutant exhibited increased apoptosis in cells at the perichondrial border. These studies will facilitate the understanding of embryonic bone development and how the proteins CCN1 and CCN2 are involved in this process.

The thesis of Jessica Renee Ong is approved.

Jau-Nian Chen

Daniel Cohn

Karen Lyons, Committee Chair

University of California, Los Angeles

2013

TABLE OF CONTENTS

Abstract of the thesis	ii
Acknowledgements	vii
Chapter 1: An introduction to CCN1 and CCN2.....	1
1.1 A background to the CCN family of proteins	1
1.2 Known roles of CCN1 and CCN2 during endochondral bone formation	1
1.3 Similar and opposing roles of CCN1 and CCN2.....	4
Chapter 2: A skeletal analysis of CCN1 and CCN2 in <i>Col2a1</i> expressing cells	9
2.1 Rationale and hypothesis	9
2.2 <i>Ccn1/Ccn2</i> double mutants have more severe axial skeleton defects	9
2.3 CCN1 and CCN2 are vital for proper growth plate formation.....	11
2.4 CCN1 and CCN2 are not essential for apoptosis at the chondro-osseus junction.....	12
2.5 CCN1 and CCN2 may work conversely to maintain proper proliferation in the reserve zone.....	13
2.6 Discussion.....	15
Chapter 3: Remaining questions and future directions.....	27
Chapter 4: Materials and methods.....	29
4.1 Mice	29
4.2 Skeletal Preparations	29
4.3 Histology	29
References	32
Appendix A: Published articles and contributions	36
A.1 CCN2/Connective Tissue Growth Factor is essential for pericyte adhesion and endothelial basement membrane formation during angiogenesis.....	36

A.2 Hypoxia-inducible Factor (HIF)-1 α and CCN2 form a regulatory circuit in hypoxic nucleus pulposus cells	48
A.3 CCN2/CTGF is required for matrix organization and cellular survival during chondrogenesis	62

ACKNOWLEDGEMENTS

I would like to thank Dr. Karen Lyons, who granted me the opportunity to work as an undergraduate and Masters student in her lab. Her mentorship has helped me to become a better scientist, and her numerous letters of recommendation also facilitated the several scholarships and awards I received.

I would like to acknowledge that Andrea R. De-Young and Faith Hall-Glenn contributed to the work in Chapter 2 with preliminary findings that were further supported by my findings. Also, a very special thanks to Faith Hall-Glenn, who trained me as an undergraduate and passed on her wisdom to me. Furthermore, this work could not have been done without the advice and kindness of the other Lyons' lab members, namely Weiguang Wang, Diana Rigueur, and YooJin Lee.

Much gratitude goes to the Beckman Foundation and Diane and Henry H. Hilton Scholarship Fund whose financial support went to the funding of this work and of my growth as a scientist while at UCLA.

Finally, I would like to thank my very supportive family, friends, and boyfriend who have helped me balance my life and are always able to put a smile on my face.

CHAPTER 1: AN INTRODUCTION TO CCN1 AND CCN2

1.1 A background to the CCN family of proteins

Members of the CCN (CYR61/CTGF/NOV) family of proteins are termed “matricellular” because they are secreted into the extracellular matrix (ECM), but function as regulatory molecules rather than structural ones (Brigstock et al., 2003). The 6 members (CCN1-6) of this family are highly structurally conserved and rich in cysteine motifs, with an N-terminal secretory peptide and four distinct modules: the insulin-like growth factor binding protein (IGFBP) homology domain, the von Willebrand factor type C repeat (vWC), the thrombospondin type I repeat (TSP), and a carboxyl-terminal (CT) domain (Chen and Lau, 2009). In addition, between the vWC and TSP modules, a hinge region exists which is sensitive to proteolysis. This conserved protein structure with various domains facilitates interactions with growth factors, cytokines, and structural ECM components such as proteoglycans (Leask and Abraham, 2006). From what is known thus far, although many CCNs do have independent functions, their main functions are as signaling adaptors that modulate extracellular signals to intracellular changes largely via integrin binding (Lau and Lam, 1999). Many of the CCN family members are expressed in a variety of tissues and are involved in many developmental and pathological processes, although they have mostly been studied within the context of angiogenesis and skeletogenesis (Chen and Lau, 2009). In addition, most work in the field has focused on examining the first three family members identified, CCN1-3, of which CCN2 is the most well-studied (Leask and Abraham, 2006). However, much has yet to be elucidated regarding the functions of the CCN proteins, particularly within skeletogenesis.

1.2 Known roles of CCN1 and CCN2 during endochondral bone formation

Vertebrates contain two types of bones: membranous bones, which are primarily found in the skull, and endochondral bones, which include all of the long bones and vertebrae. As most bones in our body are endochondral bones, it is of interest to examine their development in order

to better understand the process and pathogenesis of chondrodysplasias. Endochondral bone formation, also called endochondral ossification, is a process by which a cartilaginous mold is utilized to create bone. Chondrocytes, the main cartilage cell type, comprise this cartilaginous mold (Kronenberg, 2003).

Ultimately, a process of chondrocyte proliferation and differentiation manifests as a stratified cell structure called the growth plate (Figure 1) (Kronenberg, 2003). As these chondrocytes proliferate and differentiate, they synthesize ECM molecules vital to the structural integrity of cartilage and imperative for proper bone formation. In the first step of long bone formation mesenchymal stem cell condensations differentiate into chondrocytes (Kronenberg, 2003). The cells at the border form the perichondrium (Kronenberg, 2003). Within the condensation, chondrocytes proliferate, and eventually exit the cell cycle and enlarge to become hypertrophic chondrocytes (Figure 1) (Kronenberg, 2003). The hypertrophic chondrocytes then undergo cell death, leaving behind an ECM that supports the ingrowth of osteoblasts, which invade and form trabecular bone (Figure 1) (Kronenberg, 2003).

All CCN proteins are expressed in the developing growth plate of long bones, implying potential roles in endochondral bone formation (Kawaki et al., 2008; Leask and Abraham, 2006). In the growth plate, multiple cell-cell, cell-matrix, and growth factor interactions occur to control chondrocyte differentiation. The first CCN that has been identified to be functionally important for skeletogenesis *in vivo* is CCN2, previously known as connective tissue growth factor (CTGF) (Ivkovic et al., 2003).

It had previously been shown that CCN2 could promote chondrocyte proliferation and differentiation *in vitro* (Nakanishi et al., 2000). However, its essential role in endochondral ossification *in vivo* was demonstrated by the perinatal lethality of a complete *Ccn2* null (*Ccn2*^{-/-}) mouse due to severe kinks in the ossified regions of mutant ribcages (Ivkovic et al., 2003). In order to distinguish whether these kinks, which were also apparent in the radius, ulna, tibia, and fibula, were a result of a defect in cartilage formation or in ossification, embryonic day (E) 14.5 embryo skeletons were examined (Ivkovic et al., 2003). At this earlier time point the defect was

apparent in the cartilage and not the bone, so it could be concluded that the absence of CCN2 was vital for proper ECM integrity of cartilage. In addition, while the overall lengths of the skeletons and individual ribs were the same length, the ratio of bone to cartilage was increased in the *Ccn2*^{-/-} mutant, indicating delayed ossification. Further histological examination of the *Ccn2*^{-/-} phenotype identified a characteristic expanded hypertrophic zone, apparent starting at E14.5 in growth plates indicating the significance of CCN2 for the later stages of chondrogenesis. Two possible explanations for the expanded hypertrophic zone were either cells were differentiating too soon from the proliferative zone (reduced proliferation) or cells were not being removed fast enough before ossification. It was shown through quantification of Proliferating Cell Nuclear Antigen (PCNA), a marker for cells in both G1 and S phases of the cell cycle, that proliferation was reduced in the proliferative zone starting at E14.5, although no difference in the reserve zone was seen at E16.5—a finding that will be different from the one discussed in Chapter 2. In addition, while apoptosis yielded no significant difference it was also discovered that an additional contributing factor to the expanded hypertrophic zone in the *Ccn2*^{-/-} mutant was a lack of vascularization and bone mineralization at the ossification front. In summary, CCN2 was shown to be essential to proper chondrocyte proliferation, differentiation, bone mineralization, and vascular invasion (Ivkovic et al., 2003).

Although CCN1, also known as cysteine rich 61 (Cyr61), has a very similar expression pattern to CCN2 in tibial growth plates and a similarly important role in angiogenesis, its role in endochondral ossification has not been explored beyond *in vitro* studies (Chen and Lau, 2009; Kawaki et al., 2008; O'Brien and Lau, 1992). The examination of CCN1 during endochondral bone formation was largely hampered because of the *Ccn1* null (*Ccn1*^{-/-}) mouse model being embryonic lethal, with no viable mutants surviving past E14.5 (Mo et al., 2002). However, it is known that *Ccn1* is expressed in cartilage elements and can stimulate cartilage formation *in vitro* (Mo et al., 2002; O'Brien and Lau, 1992). We hypothesize in Chapter 2 that CCN1 and CCN2 have overlapping functions during endochondral bone formation.

1.3 Similar and opposing roles of CCN1 and CCN2

From what is known regarding the CCN proteins, an interesting relationship has emerged between CCN1 and CCN2, which has revealed that they often work in similar tissues but on different cell types, while in other contexts they have the same functions. Here the similar and opposing roles of CCN1 and CCN2 will be discussed.

CCN1 and CCN2 were first identified as the only CCN products induced by cell proliferation and are both encoded by immediate-early genes (Lau and Nathans, 1987; Perbal, 2013; Ryseck et al., 1991). They have 45% amino acid sequence identity (Bradham et al., 1991; Chen et al., 2001; O'Brien and Lau, 1992) and have similar IRES capabilities (as with CCN4) in the 5'UTR (Huang et al., 2007). In addition, both CCN1 and CCN2 may play a role in cell cycle progression and are known to regulate cell migration, adhesion, proliferation, and differentiation although many of their functions are cell and tissue type dependent (Chen and Lau, 2009; Chen et al., 2001).

As discussed in section 1.2, both CCN1 and CCN2 promote chondrogenesis *in vitro* (Nakanishi et al., 2000; Wong et al., 1997). In addition, both are expressed in cartilaginous elements as early as E12.5 (Ivkovic et al., 2003; Kawaki et al., 2008; O'Brien and Lau, 1992). While all CCNs are expressed in osteoblasts, CCN1 and CCN2 have very similar patterns of expression both in osteoblasts and osteocytes (Kawaki et al., 2011). Both are also positively regulated during osteoblast proliferation and differentiation, although CCN2 was a more powerful regulator, and both are proposed to act during maturation and the early mineralization steps of osteogenesis (Kadota et al., 2004; Kawaki et al., 2011; Si et al., 2006).

The *in vivo* data of the complete *Ccn1* and *Ccn2* null mouse models indicate an obvious difference in their earliest roles within development: CCN1 is more vital for placental angiogenesis, and CCN2 is more vital for chondrogenesis although it plays a role in vascular invasion during endochondral ossification (Ivkovic et al., 2003; Mo et al., 2002). However, both CCN1 and CCN2 are essential for angiogenesis with some similarities and some differences (Chen and Lau, 2009). Both CCN1 and CCN2 are secreted by Human Umbilical Vein

Endothelial Cells (HUVECs) (Abe and Sato, 2001; Bradham et al., 1991). It has been further proposed that as heparin-binding proteins that strongly associate with the ECM, CCN1 and CCN2 may act similarly to promote the mitogenic activity of basic FGF (bFGF) on fibroblasts or HUVECS (Brigstock, 2002). In addition, CCN1 and CCN2 can induce angiogenesis by binding to the same integrin, $\alpha_v\beta_3$ (Lau, 2012). Both CCN1 and CCN2 are expressed in the heart: in the atria, ventricles, and outflow tract (Friedrichsen et al., 2003; Hall-Glenn and Lyons, 2011; Mo and Lau, 2006; Mo et al., 2002; Sawai et al., 2007; unpublished data).

Despite such similarities and the fact that both CCN1 and CCN2 are expressed in atrial cardiomyocytes of hearts, CCN1 expression remained within the cytoplasm and CCN2 remained in the perinuclear cytoplasm, highlighting the idea that they may both be expressed with different precise cellular and subcellular localizations in the same cell (Bonda et al., 2012). It was further found that CCN1 was upregulated but CCN2 remained constant with induced myocardial infarction (Bonda et al., 2012). This is consistent with the more prevalent role CCN1 plays in embryonic vascularization as *Ccn1*^{-/-} mice die early *in utero* due to severely impaired placental angiogenesis and faulty large vessel formation (Mo and Lau, 2006; Mo et al., 2002).

CCN1 has also been shown to promote angiogenesis in multiple contexts, including during tumor growth in gastric cells (Babic et al., 1998). CCN2 also exhibits proangiogenic activity *in vivo* and *in vitro* and is required for proliferation and migration of vascular endothelial cells and recruitment of pericytes (Babic et al., 1998; Hall-Glenn et al., 2012; Nishida et al., 2000). Distinct from *Ccn1* mutants where the large vessels are affected (Mo and Lau, 2006), vascular defects in *Ccn2* mutants are more prominent in microvasculature (Hall-Glenn et al., 2012). It is unclear whether CCN1 and CCN2 also exhibit overlapping functions in angiogenesis, but this seems likely.

Interestingly, while all 6 CCN transcripts are expressed in human skin *in vivo*, UV irradiation was able to stimulate mRNA expression of only CCN1 and CCN2 (Quan et al., 2009). This most likely has to do with the notion of CCN1 and CCN2 as proliferative factors and immediate early genes (Quan et al., 2009). In fibroblasts, CCN1 and CCN2 can also both

promote apoptotic cell death (Chen and Lau, 2009). Furthermore, it has been shown in human primary fibroblasts that both CCN1 and CCN2 can induce adhesive signaling and function in matrix remodeling (Chen et al., 2001). CCN1 and CCN2 are both expressed in epidermis, but CCN1 at low levels and CCN2 at high levels in melanocytes and the dermis (Rittié et al., 2011). While CCN1 is also vital for collagen homeostasis in fibroblasts (Quan et al., 2010), CCN2 seems to be the most prominent CCN protein involved in extracellular matrix formation during wound healing and regeneration (Shi-Wen et al., 2008; Sisco et al., 2008). Interestingly, while CCN2 promotes scarring and fibrosis in diseases such as scleroderma as well as in various organs including the liver, kidneys, and lungs (Chen and Lau, 2009; Igarashi et al., 1996), CCN1 seems to have the opposite effect, preventing excessive fibrosis in cutaneous wound healing (Jun and Lau, 2010).

While CCN2 has been highly studied for its role in many fibrotic diseases, CCN1 was studied for its role in increased tumorigenicity due to increased vascularization (Babic et al., 1998). In some cancers, both CCN1 and CCN2 are similarly regulated, including glioma (Goodwin et al., 2010; Yin et al., 2010), pancreatic (Dornhöfer et al., 2006; Haque et al., 2011), colon (Ladwa et al., 2011), and lung cancers (Chen et al., 2007; Jun and Lau, 2011). Conversely, in other cancers the roles of CCN1 and CCN2 are inverse or independent. For example, in the borderline tumors and ovarian carcinomas, both CCN1 and CCN2 are expressed but with inverse expression of CCN1 in high grade and CCN2 in low grade (Bartel et al., 2012; Nguyen et al., 2006). In addition, CCN2 is independently associated with cancers such as melanomas, musculoskeletal tumors, and leukemia (Jun and Lau, 2011; Sha and Leask, 2011) whereas CCN1 is independently associated with such cancers such as endometrial cancer (Jun and Lau, 2011; Watari et al., 2009).

In conclusion, it is evident that although CCN1 and CCN2 may both be expressed similarly in a tissue, their similar or disparate functions depend largely on the tissue—a notion further supported by the analysis in Chapter 2. Much more work needs to be done to understand

how CCN1 and CCN2 interact with each other to regulate the physiological events that were listed above. In addition, the roles highlighted above as well as the expression of all six CCNs in highly ECM-rich tissues such as the skin, cartilage, and bone exemplify their importance as ECM regulators (Kawaki et al., 2008, 2011; Quan et al., 2009). The vital roles of these proteins for embryonic development, inflammation, and fibrosis have made them potentially very interesting pharmacological targets, some of which are already undergoing clinical trials (Jun and Lau, 2011).

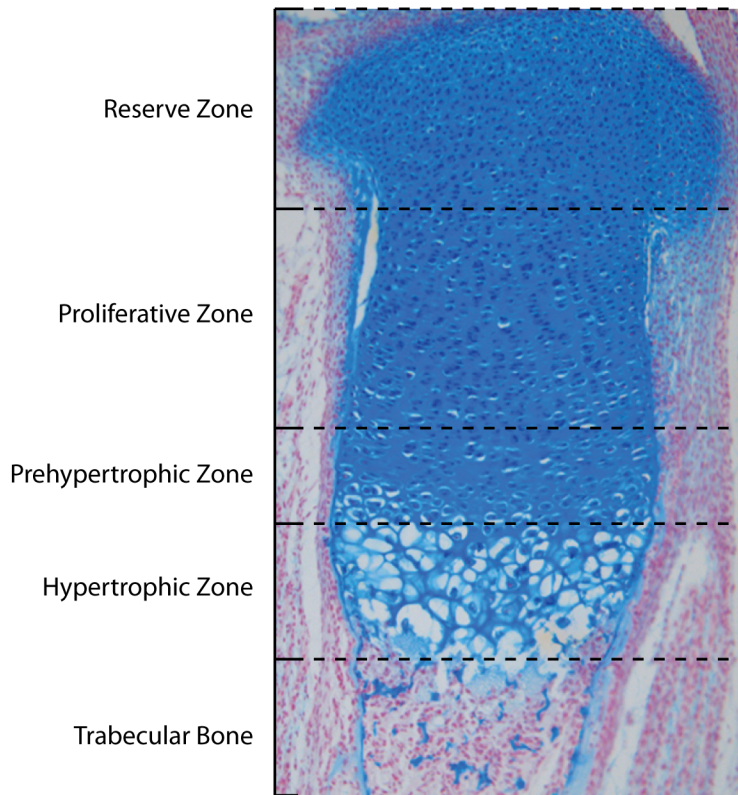


Figure 1. A tibial growth plate. An embryonic day (E) 18.5 wild type mouse tibial growth plate is stained with Alcian Blue (cartilage) and Nuclear Fast Red (nuclei). In the reserve zone slowly proliferating chondrocytes reside, which will eventually give rise to the proliferative zone. In the proliferative zone chondrocytes are more rapidly dividing, forming structured columnar stacks of cells. In the prehypertrophic zone proliferative cells prepare for hypertrophy. In the hypertrophic zone, chondrocytes enlarge and undergo apoptosis at the junction where the cartilage meets the trabecular bone. Trabecular bone is then made from the matrix of chondrocytes.

CHAPTER 2: A SKELETAL ANALYSIS OF CCN1 AND CCN2 IN *COL2A1* EXPRESSING CELLS

2.1 Rationale and hypothesis

Despite the similar roles of *Ccn1* and *Ccn2* in angiogenesis, whether they have similar roles in skeletogenesis has yet to be examined in detail, although it is apparent that CCN2 plays a vital role (Ivkovic et al., 2003; Mo et al., 2002). CCN1 and CCN2 have similar protein expression within tibial growth plates (Figure 1A,B). Due to their similar expression patterns within the growth plate (Figure 1A,B) and essential roles in angiogenesis (Chen and Lau, 2009), we hypothesize that CCN1 and CCN2 have overlapping functions during endochondral ossification. To examine our hypothesis, we are employing cartilage-specific deletions of *Ccn1* and/or *Ccn2* with the Cre-LoxP system (Sauer, 1998). These genes are deleted from chondrocytes under the direction of Cre recombinase that is expressed under the control of the *Col2a1* promoter (Ovchinnikov et al., 2000). In order to obtain mutant phenotypes, *Ccn1*^{fx/fx}, *Ccn2*^{fx/fx}, or *Ccn1*^{fx/fx};*Ccn2*^{fx/fx} mice (Figure 1E) were mated to *Col2a1-Cre*^{Tg/+} mice. These respectively produced *Ccn1*^{fx/+};*Col2a1-Cre*^{Tg/+}, *Ccn2*^{fx/+};*Col2a1-Cre*^{Tg/+}, and *Ccn1*^{fx/+};*Ccn2*^{fx/+};*Col2a1-Cre*^{Tg/+} mice, which when mated to the same genotype produced the following mutants: *Ccn1*^{fx/fx};*Col2a1-Cre*^{Tg/+} or *Ccn1*^{CKO}, *Ccn2*^{fx/fx};*Col2a1-Cre*^{Tg/+} or *Ccn2*^{CKO} and *Ccn1*^{fx/fx}*Ccn2*^{fx/+};*Col2a1-Cre*^{Tg/+} mice or *Ccn1*^{CKO};*Ccn2*^{CKO} or double mutant. The conditional null efficiently ablates CCN1 and/or CCN2 expression from cartilage as shown by the absence of immunofluorescent staining (Figure 1C,D). Genotypes were verified with polymerase chain reaction (PCR) and agarose gel electrophoresis (Figure 1F). We initially predicted a more severe phenotype for *Ccn1*^{CKO};*Ccn2*^{CKO} double mutants compared to either single mutant strain, which would be indicative of overlapping roles during endochondral ossification.

2.2 *Ccn1/Ccn2* double mutants have more severe axial skeleton defects

After obtaining mutant phenotypes, skeletal preparations were done in order to examine overall skeletal phenotypes (Figure 2). Although all the mutants were lethal at birth, the *Ccn1* mutants have apparently normal skeletal phenotypes at the level of overall morphology, whereas the *Ccn2* mutants have a more severe phenotype that phenocopies that of the *Ccn2*^{-/-} mouse (Figure 2A) (Ivkovic et al., 2003). The *Ccn1*^{CKO};*Ccn2*^{CKO} double mutants resemble *Ccn2*^{CKO} mice, but display a more severe rib phenotype, discussed in greater detail below (Figure 2A).

When examining the lateral side of the cranium, it appears that while *Ccn1*^{CKO} mutants have a cranium similar to wild type littermates, the *Ccn2*^{CKO} and *Ccn1*^{CKO};*Ccn2*^{CKO} mutants have domed skulls and malformed mandibles (Figure 2A). Because the *Ccn1*^{CKO};*Ccn2*^{CKO} domed skull phenotype is similar to that of *Ccn2*^{CKO} mice, and this phenotype is not seen in *Ccn1*^{CKO} mice, it appears that *Ccn2* has a more significant role in cranial skeletal formation than does *Ccn1* (Figure 2A). Similarly, the palatal shelves were not elevated and the ethmoid bones were defective in only the *Ccn2*^{CKO} and *Ccn1*^{CKO};*Ccn2*^{CKO} mutants, although further histology would need to be done to confirm this phenotype (Figure 2C).

On the other hand, the phenotypic analysis did reveal a role for *Ccn1* in chondrogenesis. The domed skull defect is generally a secondary consequence of a malformed cranial base. While the *Ccn1*^{CKO} mutant has a cranial base very similar to wild type, there is still an evident defect, as the foramen magnum is broader in the *Ccn1*^{CKO} mutant as well as in the *Ccn2*^{CKO} and *Ccn1*^{CKO};*Ccn2*^{CKO} mutants (Figure 2C). Consistent within all three mutants is also a shorter cranial base, which is significantly shorter in the *Ccn1*^{CKO};*Ccn2*^{CKO} mutant than in either of the single mutant strains (Figure 2C). Moreover, the mandibles appear shortened as a result of kinks in the mandibles, which are worse in the *Ccn1*^{CKO};*Ccn2*^{CKO} double mutant than in *Ccn2*^{CKO} mice (data not shown). In addition, both the single mutants and double mutants have wider first cervical vertebrae, or atlases, compared to wild type littermates (Figure 2B). This is consistent with an ECM defect in the vertebrae, such that as the neural tube grows, the vertebrae expand and become thinner since the cartilaginous matrix is not strong enough to counteract the force of the expanding neural tube.

Next, in examining the ribcage it appears that the *Ccn1*^{CKO} mutant has a normal sternum (Figure 2D). The *Ccn2*^{CKO} mutant occasionally exhibits sternal misalignment (seen in 1/3 samples), consistent with the *Ccn2*^{-/-} mice (Ivkovic et al., 2003). The ribs of the *Ccn1*^{CKO} mutant are also apparently normal, whereas the characteristic kinking seen in the ossified regions in *Ccn2*^{-/-} mice within a subset of ribs (Ivkovic et al., 2003) is once again apparent in the *Ccn2*^{CKO} mutant (Figure 2E). The characteristic *Ccn2*^{-/-} phenotype (Ivkovic et al., 2003) is also seen in the *Ccn1*^{CKO};*Ccn2*^{CKO} double mutant (Figure 2E). However, in the *Ccn1*^{CKO};*Ccn2*^{CKO} mutants, the rib phenotype is more severe, as more kinking is also seen in more posterior ribs (Figure 2E). Another novel phenotype is apparent in the *Ccn1*^{CKO};*Ccn2*^{CKO} when also examining the vertebral columns (Figure 2F), where kinks are seen that are not present in either single mutant strain. Thus, this initial analysis indicates some overlapping functions for *Ccn1* and *Ccn2* in formation of axial elements.

However, when examining the appendicular skeleton as exemplified by the hindlimbs (Figure 2G), the *Ccn1*^{CKO} mutant once again has a normal phenotype and the *Ccn2*^{CKO} mutant has the characteristic kinks as seen previously (Ivkovic et al., 2003). The *Ccn1*^{CKO};*Ccn2*^{CKO} mutant hindlimb (Figure 2G) does not have a more severe phenotype than either single mutants, but phenocopies the *Ccn2*^{CKO} mutant phenotype. This indicates that in the appendicular skeleton, CCN2 is epistatic to CCN1. Therefore, CCN1 and CCN2 may have more similar (overlapping) roles within the axial skeleton as compared to the appendicular skeleton.

2.3 CCN1 and CCN2 are vital for proper growth plate formation

The absence of a more severe phenotype in appendicular elements in *Ccn1*^{CKO};*Ccn2*^{CKO} was somewhat unexpected based on the fact that both CCN1 and CCN2 can stimulate chondrogenesis *in vitro* (Nakanishi et al., 2000; O'Brien and Lau, 1992) and are co-expressed in appendicular cartilage (Figure 1A,B). Therefore, a histological analysis was performed to search for more subtle alterations. In a histological examination of tibial growth plates at E16.5, no reproducible alterations in intensity of Safranin-O staining were apparent (Figure 3). The

Ccn1^{CKO} mutant (Figure 3B) has a larger reserve zone yet normal a proliferative and hypertrophic zone compared to wild type mice (Figure 3A), although this must be confirmed and quantified through analysis of additional mice. The *Ccn2*^{CKO} mutant (Figure 3C) has a smaller reserve zone than in wild type littermates, which was not reported for *Ccn2*^{-/-} mice (Ivkovic et al., 2003), but similarly to the *Ccn2*^{-/-} mouse model it has a smaller proliferative and larger hypertrophic zone compared to wild type littermates (Figure 3A). The *Ccn1*^{CKO};*Ccn2*^{CKO} mutant (Figure 3D) also has a smaller reserve zone and proliferative zone, as well as a larger proliferative zone compared to wild type littermates (Figure 3A)—very similar to the *Ccn2*^{CKO} mutant. However, the longer hypertrophic zone of the *Ccn1*^{CKO};*Ccn2*^{CKO} mutant compared to that of *Ccn2*^{CKO} mice (Figure 3D,P) may indicate similar roles for CCN1 and CCN2 in clearance of hypertrophic chondrocytes.

Examination of the reserve (Figure 3E-H) and hypertrophic (Figure 3M-P) zones revealed no apparent defects, but this needs to be investigated using differentiation markers. When examining the proliferative zones at a higher magnification (Figures 3I-L), the *Ccn1*^{CKO} mutant proliferative zone (Figure 3J) is organized and has an appearance similar to that of wild type littermates (Figure 3I). The *Ccn2*^{CKO} mutant (Figure 3K) has a disrupted and hypocellular proliferative zone. In addition, the *Ccn2*^{CKO} mutant's smaller proliferative zone and larger hypertrophic zone confirms the previous report of the complete null (Ivkovic et al., 2003). Unexpectedly, the *Ccn1*^{CKO};*Ccn2*^{CKO} mutant has a surprisingly normal proliferative zone compared to wild type (Figure 3I). Thus, the increased length of the hypertrophic zone in double mutants compared to single mutants provides evidence that *Ccn1* and *Ccn2* may have overlapping functions in hypertrophic chondrocytes. On the other hand, the finding that double mutants have a less severe phenotype in the proliferative zone than do *Ccn2*^{CKO} mice may be an indication that CCN1 and CCN2 may have some distinct, and possibly opposing, functions in regulating chondrocyte proliferation.

2.4 CCN1 and CCN2 are not essential for apoptosis at the chondro-osseous junction

As discussed above, the hypertrophic zone appears enlarged in double mutants compared to the corresponding single mutant strains. One possible explanation for this would be a reduction in the extent of chondrocyte apoptosis at the chondro-osseous junction. In order to examine whether the double mutant had a defect in chondrocyte clearance, apoptosis was examined in E16.5 tibial growth plates (Figure 4). Apoptosis was quantified using a TUNEL assay kit on 3 independent sets of mutants compared to wild type littermates (Figure 4A-D). The quantification of percent TUNEL and DAPI double positive cells yielded no significant difference in apoptosis at the chondro-osseous junction (Figure 4E). This confirms the similar result previously reported for the *Ccn2*^{-/-} mutant, with no significant difference in apoptosis (Ivkovic et al., 2003). However, a novel phenotype was discovered: a significant increase in apoptosis was found in the perichondrial border of all *Ccn1*^{CKO};*Ccn2*^{CKO} mutants (Figure 4D-E). A trend toward an increase in apoptosis within the hypertrophic zone and in the perichondrial border was seen in the *Ccn2*^{CKO} mutants, although it was not statistically significant (Figure 4E). Thus it appears that apoptosis is not affected in the absence of CCN1 and CCN2 within the chondro-osseous junction, although CCN1 and CCN2 may have an overlapping function in cell survival within the perichondrium.

2.5 CCN1 and CCN2 may work conversely to maintain proper proliferation in the reserve zone

Since *Ccn2*^{-/-} mice exhibit impaired proliferation within the proliferative zone (Ivkovic et al., 2003), next we examined whether this phenotype is recapitulated in *Ccn2*^{CKO} mice, and whether the absence of *Ccn1* also affected proliferation. Proliferation was quantified using immunofluorescence for phosphorylated-HistoneH3 (pHistoneH3), a sensitive proliferation marker for cells in mitosis—marking the end of Prophase (Figure 5A-D). Quantification of pHistoneH3 and DAPI double positive cells divided by total DAPI were done on 3 independent sets of mutants with wild type littermates (Figure 5A-D). The reserve zone generally has very few proliferating cells. It appears that with the absence of *Ccn1* there is a trend for increased proliferation although it is not statistically significant relative to wild type (Figure 5E). The

increase in proliferation within the reserve zone for the *Ccn1*^{CKO} mutants is, however, statistically significant compared to the other two mutants (Figure 5E). The absence of *Ccn2* results in a previously unreported and statistically significant decrease in proliferation within the reserve zone (Figure 5E). The *Ccn1*^{CKO};*Ccn2*^{CKO} mutant has a similar decrease in proliferation as compared to the *Ccn2*^{CKO} mutant, indicating once again that CCN2 is epistatic to CCN1 within the tibia (Figure 5E).

A similar trend is seen within the proliferative zone, which has more proliferative cells, compared to that seen in the reserve zone. The *Ccn1*^{CKO} mutant exhibits a similar proliferation rate to wild type (Figure 5E). The *Ccn2*^{CKO} mutant has a significant decrease in proliferation in the proliferative zone (Figure 5E). The *Ccn1*^{CKO};*Ccn2*^{CKO} mutant interestingly takes an intermediate phenotype between the single mutants (Figure 5E). For both the *Ccn2*^{CKO} and *Ccn1*^{CKO};*Ccn2*^{CKO} mutants their reduced proliferation within the proliferative zone can potentially be explained by a lack of entry of proliferating progenitor cells from the reserve zone to supply cells to the proliferative zone. It is conceivable that the trend of increased proliferation within the reserve zone in *Ccn1*^{CKO} mutants reflects an increased rate of entry of cells from this zone into the proliferative zone. The concept that there is increased proliferation in the reserve zone in *Ccn1*^{CKO} mutants is consistent with the apparently increased length of the of reserve zone in these mice (Figure 3). If so, this would counteract the decreased rate of entry seen in *Ccn2*^{CKO} mutants. It may be that under normal circumstances, CCN2 promotes proliferation and CCN1 inhibits proliferation within the reserve zone. Analysis of additional mutants of each genotype will be required to test this hypothesis.

2.6 Discussion

The evidence shown here suggests that although *Ccn1* and *Ccn2* may have some overlapping functions, they may also have discrete functions that have yet to be further explored within endochondral ossification. So far we have been able to indicate that loss of either *Ccn1* or *Ccn2* in *Col2a1*-expressing cells leads to lethality. For the *Ccn1* mutant, it is not clear whether this lethality is due to a defect in chondrogenesis, since the cleared skeletal preparations and histological analysis did not reveal any obvious defects (Figure 2A). Another possibility is that the lethality of *Ccn1* mutant mice is due to a cardiovascular valve defect, as *Ccn1* is essential for cardiovascular development (Mo and Lau, 2006), and *Col2a1* is expressed in heart valves. Moreover, we have shown that *Ccn2* mutant mice phenocopy the skeletal defects in *Ccn2*^{-/-} mice (Ivkovic et al., 2003), demonstrating that the role of CCN2 in cartilage is direct. The lethality of the *Ccn2* mutant mice could possibly be attributed to kinked ribcages (Figure 2A) as seen with the *Ccn2*^{-/-} mouse (Ivkovic et al., 2003). For the *Ccn1/Ccn2* or double mutant the lethality may be due to a combination of cardiovascular and skeletal defects, but this cannot be definitely claimed without further investigation.

The skeletal phenotype of the *Ccn1*^{CKO};*Ccn2*^{CKO} mutant was not as we had predicted. Although certain regions appeared to have a more severe phenotype than both single mutants, consistent with our original hypothesis of overlapping functions, other regions appeared to have a phenotype similar to the *Ccn2*^{CKO} mutant. Furthermore, we observed an unexpected apparent correction of the growth plate proliferative defect seen in *Ccn2*^{CKO} mice in double mutants, which exhibited a less severe impairment in proliferation within the proliferative zone.

More severe double mutant phenotypes were evident within the expanded atlases (Figure 2B), shorter cranial bases (Figure 2C), broader foramen magna (Figure 2C), kinked xiphoid processes (Figure 2D), and severe kyphosis in vertebral columns (Figure 2F). Phenotypes that were apparent in the *Ccn1*^{CKO};*Ccn2*^{CKO} mutant that were more similar to the *Ccn2*^{CKO} mutant included kinking in the ossified regions of the ribcage (Figure 2E) and kinking in the hindlimbs (Figure 2G). Such phenotypic differences highlight the tissue specificity of CCN1 and CCN2

function, and how in certain skeletal elements they may work together and in others they may work sequentially or separately. It may be that in the tissues with a more *Ccn2*^{CKO} mutant phenotype in the *Ccn1*^{CKO};*Ccn2*^{CKO} mutant that despite such similar protein expression patterns, CCN2 functions epistatically to CCN1. These skeletal phenotypic differences highlight the importance of CCN1 and CCN2 working together in the axial skeleton (Figure A-D) and not so much in the appendicular skeleton (Figure 2G).

In addition it appears that CCN1 and CCN2 are vital to proper growth plate morphogenesis as evident from the histological analysis (Figure 3). Due to prior reports that both CCN1 and CCN2 promote chondrogenesis (Nakanishi et al., 2000; Nishida et al., 2007; O'Brien and Lau, 1992) it is surprising that no consistent decrease in Safranin-O is evident in the three mutants. However, a larger sample size would be required to definitively make this conclusion (Figure 3). The differences in proliferative zone organization were quite profound (Figure 3I-L). The intermediate phenotype of the *Ccn1*^{CKO};*Ccn2*^{CKO} mutant proliferative zone stratification (Figure 3L) compared to the *Ccn1*^{CKO} (Figure 3J) and *Ccn2*^{CKO} mutants (Figure 3K) is further validated by the intermediate proliferation rate between the two single mutants (Figure 5). In addition, the smaller reserve and proliferative zones in *Ccn2*^{CKO} (Figure 3C) and *Ccn1*^{CKO};*Ccn2*^{CKO} mutants (Figure 3D) and larger reserve and equal proliferative zones in the *Ccn1*^{CKO} mutant further are consistent with the proliferation quantification (Figure 5). The increased hypertrophic zone in the *Ccn1*^{CKO};*Ccn2*^{CKO} mutants compared to wild type and all the single mutants (Figure 3D) could potentially indicate overlapping functions of CCN1 and CCN2 in terminal differentiation of tibial growth plates.

Next in examination of survival defects, no apparent alterations in apoptosis were evident in the chondro-osseous junction of all three mutants, although we report a new perichondrial defect (Figure 4E). The apoptosis data indicate that CCN1 and CCN2 may coordinate proper cell survival in the perichondrium (Figure 5D,E). This phenotype represents a very interesting potential question to address in future studies.

The proliferation quantification (Figure 5E) confirms the histology shown here (Figure 3).

While the decreased proliferation in the *Ccn2*^{CKO} mutant proliferative zone (Figure 5E) has previously been shown to be partially responsible for the increased hypertrophic zone in the *Ccn2*^{-/-} (Ivkovic et al., 2003), the increased hypertrophic zone in the *Ccn1*^{CKO};*Ccn2*^{CKO} mutant cannot be fully explained by a decrease in proliferation since the proliferation rate it is at an intermediate level. Other mechanisms must compensate for the loss of *Ccn1* in the proliferative zone when both *Ccn1* and *Ccn2* are missing—such mechanisms may be the other CCNs, whose functions have yet to be explored within developing bone. Also, the quantification of proliferation introduces a new mechanism by which CCN1 and CCN2 may coordinate chondrocytes in the reserve zone (Figure 5E). We hypothesize that CCN1 normally inhibits proliferation and CCN2 promotes proliferation in the reserve zone: that CCN1 and CCN2 may act sequentially upon proliferation in the reserve zone with CCN2 acting first. This proposed mechanism highlights the idea that many of the CCNs act in concert perhaps sometimes simultaneously or sequentially (Perbal, 2013).

The aforementioned data have suggested that although CCN1 and CCN2 may have some overlapping functions particularly within the axial skeleton, they may also have some discrete functions. It may be that they act at different times during chondrogenesis or antagonistically or synergistically depending on the region. Perhaps CCN1 and CCN2 act antagonistically by conversely regulating downstream signaling pathways or being oppositely regulated by ECM components. Also, it seems that CCN2 plays a distinctly more important role in skeletal development than does CCN1. This has been evident for the roles of the CCNs within bone as CCN2 has a stronger ability to promote osteoblastogenesis and induce osteoblast gene marker expression in bone than does CCN1 (Kawaki et al., 2011).

By examining the functions of the matricellular proteins CCN1 and CCN2, we were able to further explore the basic science of endochondral ossification. Moreover, this facilitated clarification of the roles of CCN1 and CCN2 within pathological contexts, especially within the skeletal system. We have also been able to show that in some contexts during endochondral bone formation CCN2 is epistatic to CCN1. Defects in endochondral ossification cause many

developmental disorders, such as lethal chondrodysplasias and dwarfisms. Thus this study contributes to knowledge concerning the purpose of CCN family members in the developmental process of bone formation.

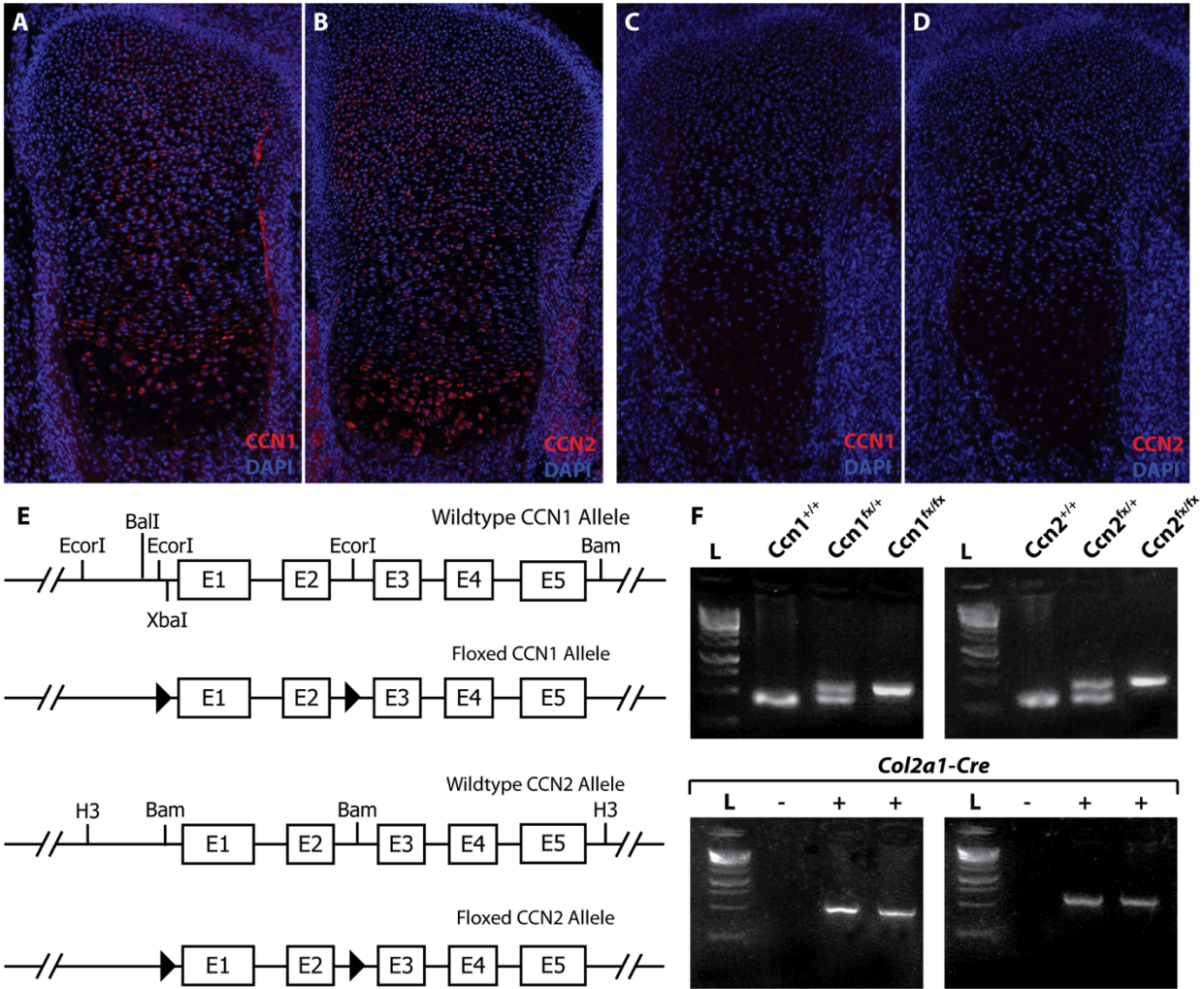


Figure 1. CCN1 and CCN2 have overlapping expression in tibial growth plates.

Immunofluorescent/protein expression of CCN1 (A) and CCN2 (B) in E16.5 wild type femoral growth plates showing their similar expression patterns. Immunofluorescent staining of CCN1 (C) and CCN2 (D) in E16.5 *Ccn1^{CKO};Ccn2^{CKO}* mutant tibial growth plates showing the absence of the proteins. (E) The *Ccn1* and *Ccn2* genes each contain 5 exons (E1-5), the first two which are “floxed” by two LoxP sites (arrowheads). Cre recombinase under control of Collagen II (*Col2a1-Cre*), the major collagen expressed in chondrocytes, excises the “floxed” locus, leaving behind a non-functional allele. (F) A representative agarose gel of a PCR reaction to identify mutant genotypes. (L = ladder)

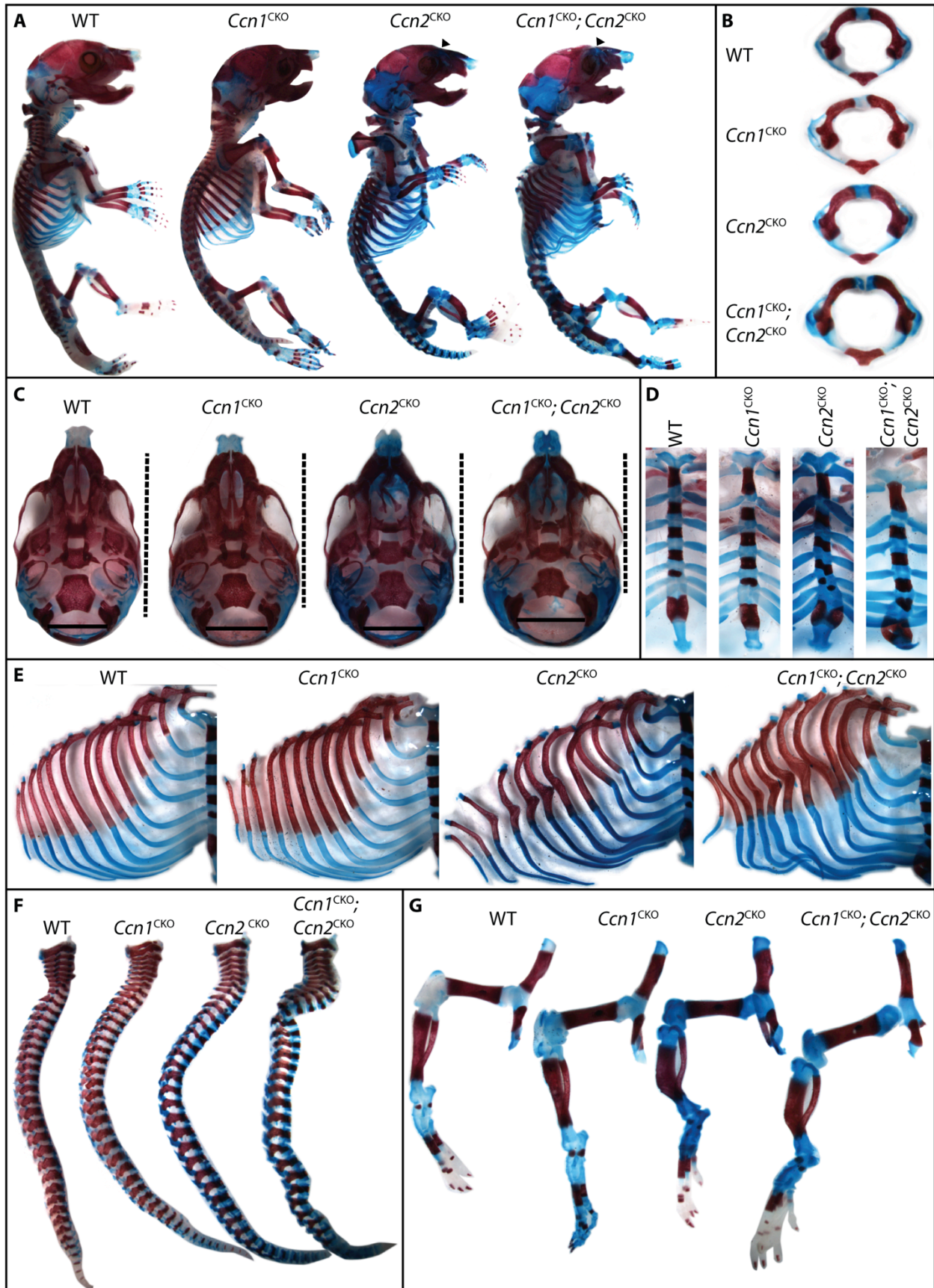


Figure 2. CCN1 and CCN2 have more similar phenotypes in the axial skeleton. Alcian Blue (cartilage)/Alizarin Red (bone) skeletal preparations of postnatal day (P)0 mice. (A) Despite no visible defects compared to wild type, *Ccn1*^{CKO} mutants die at birth, perhaps due to tracheal defects. *Ccn2*^{CKO} mutants die at birth and phenocopy the *Ccn2*^{-/-} mouse. Arrowheads point to domed skulls in the *Ccn2*^{CKO} and *Ccn1*^{CKO};*Ccn2*^{CKO} mutants. At an initial glance the double mutant has a more severe rib phenotype than both the *Ccn1* and *Ccn2* single mutants. (B) First cervical atlases are broadened in all three of the mutants as compared to wild type. (C) Cranial bases of wild type and mutant P0 mice. Solid lines indicate broader openings of the cranial base and the dashed lines to the right indicate the lengths of the skull bases, which are shorter in the mutants. (D) Sterna of wild type and mutant mice. Occasionally *Ccn2*^{CKO} sterna exhibit sternal misalignment (1/3). *Ccn1*^{CKO};*Ccn2*^{CKO} sterna are kinked, especially the xiphoid process which curls upwards. (E) Ribcages of *Ccn1*^{CKO} mutants are normal, while *Ccn2*^{CKO} mutant ribcages have kinks resembling those in *Ccn2*^{-/-} mice. *Ccn1*^{CKO};*Ccn2*^{CKO} ribcages exhibit a more severe phenotype within the rib cartilage. (F) Isolated vertebral columns demonstrate that there is a more severe phenotype in the *Ccn1*^{CKO};*Ccn2*^{CKO} mutant, which exhibits multiple kinks not seen in either single mutant strain. (G) Hindlimbs show that there is no phenotype in the *Ccn1*^{CKO} mutants, while the distinctive *Ccn2*^{CKO} tibial kinking is apparent in the *Ccn1*^{CKO};*Ccn2*^{CKO} mutant although it is not exacerbated. The data indicates that CCN1 and CCN2 seem to have more similar roles within the axial skeleton than in the appendicular skeleton. (n=3)

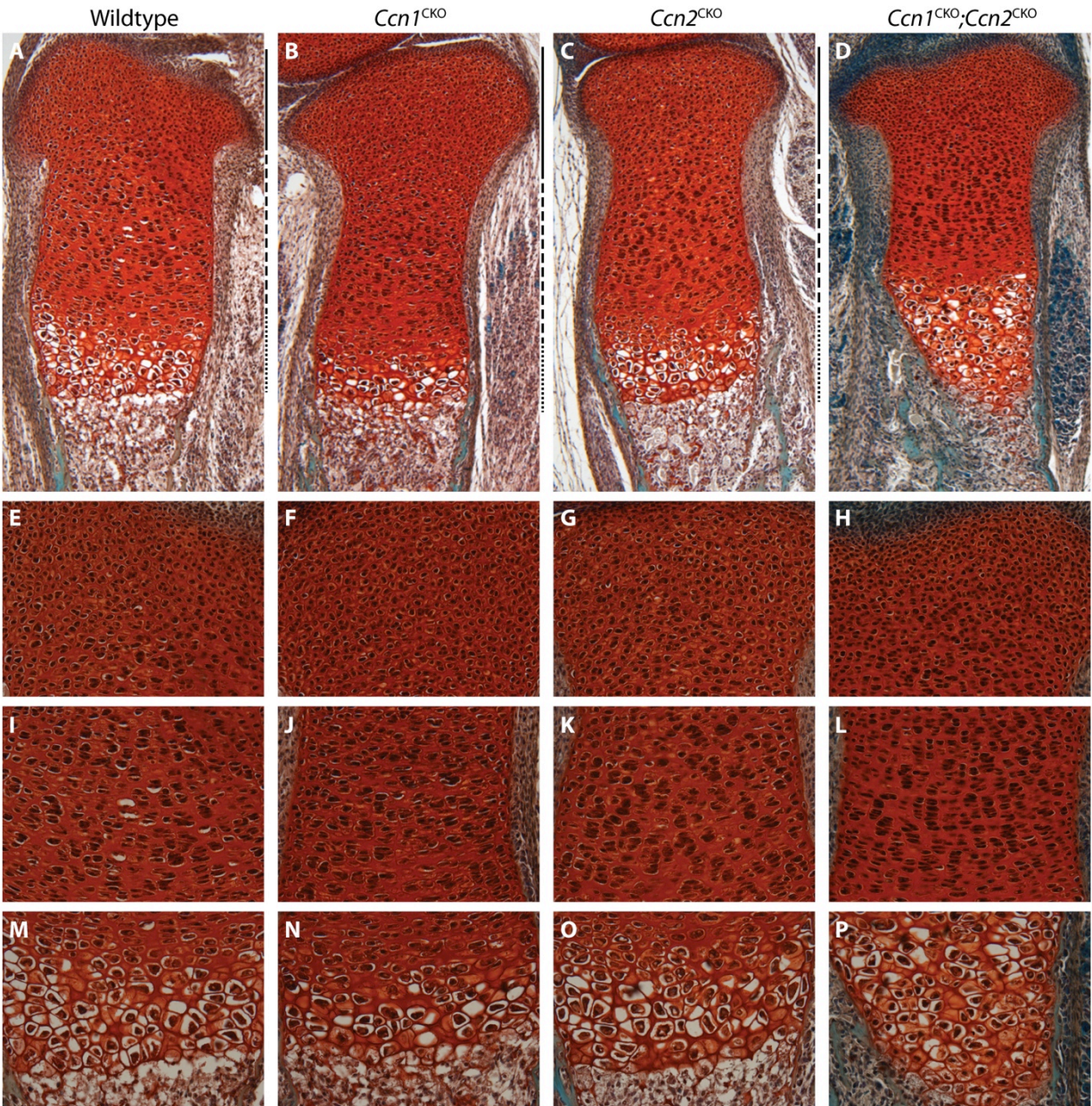


Figure 3. *Ccn1* and/or *Ccn2* mutants display growth plate defects. Safranin-O (proteoglycan)/Nuclear Fast Green (nuclei) stain of E16.5 proximal tibial growth plates. (A) Wild type, (B) *Ccn1*^{CKO} mutant, (C) *Ccn2*^{CKO} mutant, and (D) *Ccn1*^{CKO};*Ccn2*^{CKO} mutant growth plates at 10x magnification. To the right of respective images (A-D), the solid line refers to the length of the reserve zone, the dashed line refers to the length of the proliferative zone, and the dotted line refers to the length of the hypertrophic zone. The *Ccn1*^{CKO} mutant (B) has a larger reserve and similar proliferative and hypertrophic zones compared to wild type (A). The

Ccn2^{CKO} mutant (C) has a smaller reserve and proliferative zone but a larger hypertrophic zone compared to wild type (A). The *Ccn1*^{CKO};*Ccn2*^{CKO} mutant (D) has a smaller reserve and proliferative zone but a larger hypertrophic zone compared to wild type as well (A). (E) Wild type, (F) *Ccn1*^{CKO} mutant, (G) *Ccn2*^{CKO} mutant, and (H) *Ccn1*^{CKO};*Ccn2*^{CKO} mutant reserve zones at 40x magnification. (I) Wild type, (J) *Ccn1*^{CKO} mutant, (K) *Ccn2*^{CKO} mutant, and (L) *Ccn1*^{CKO};*Ccn2*^{CKO} mutant proliferative zones at 40x magnification. (M) Wild type, (N) *Ccn1*^{CKO} mutant, (O) *Ccn2*^{CKO} mutant, and (P) *Ccn1*^{CKO};*Ccn2*^{CKO} mutant hypertrophic zones at 40x magnification. (n=2)

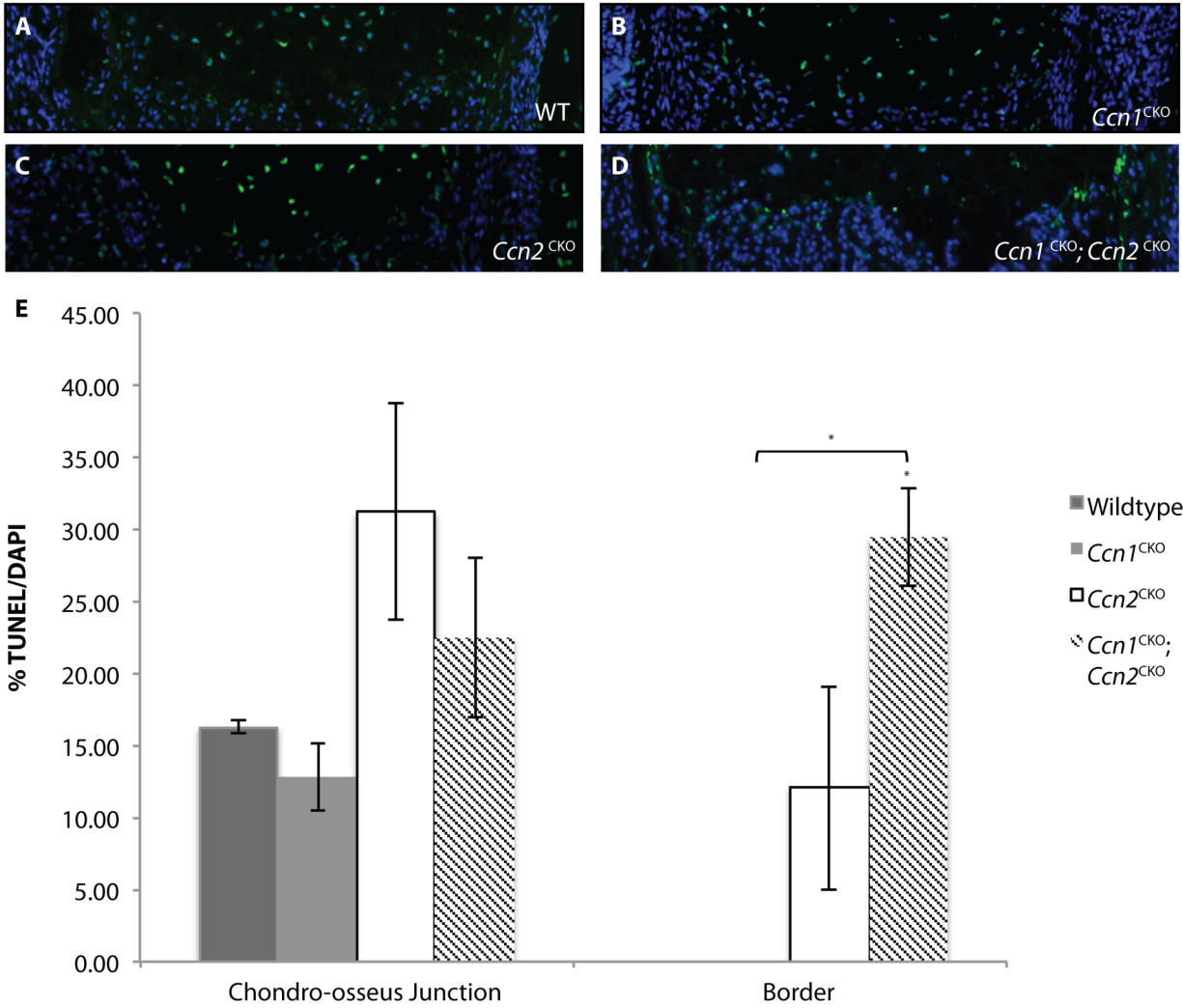


Figure 4. Apoptosis in E16.5 tibial growth plates is increased in the perichondrial border of double mutants. Representative images of TUNEL quantifications for the wild type (A), *Ccn1*^{CKO} (B), *Ccn2*^{CKO} (C), and *Ccn1*^{CKO};*Ccn2*^{CKO} (D). (E) Quantification of TUNEL/DAPI double positive cells divided by total DAPI cells to indicate apoptotic cells for the chondro-osseus junction and the perichondrial border. A trend is apparent for apoptosis in the chondro-osseus junction although significance was not calculated using the student's t-test. In the perichondrial border, however, there was a new novel phenotype and significant increase in apoptosis for the *Ccn1*^{CKO};*Ccn2*^{CKO} mutant. (n=3; * indicates p<0.05)

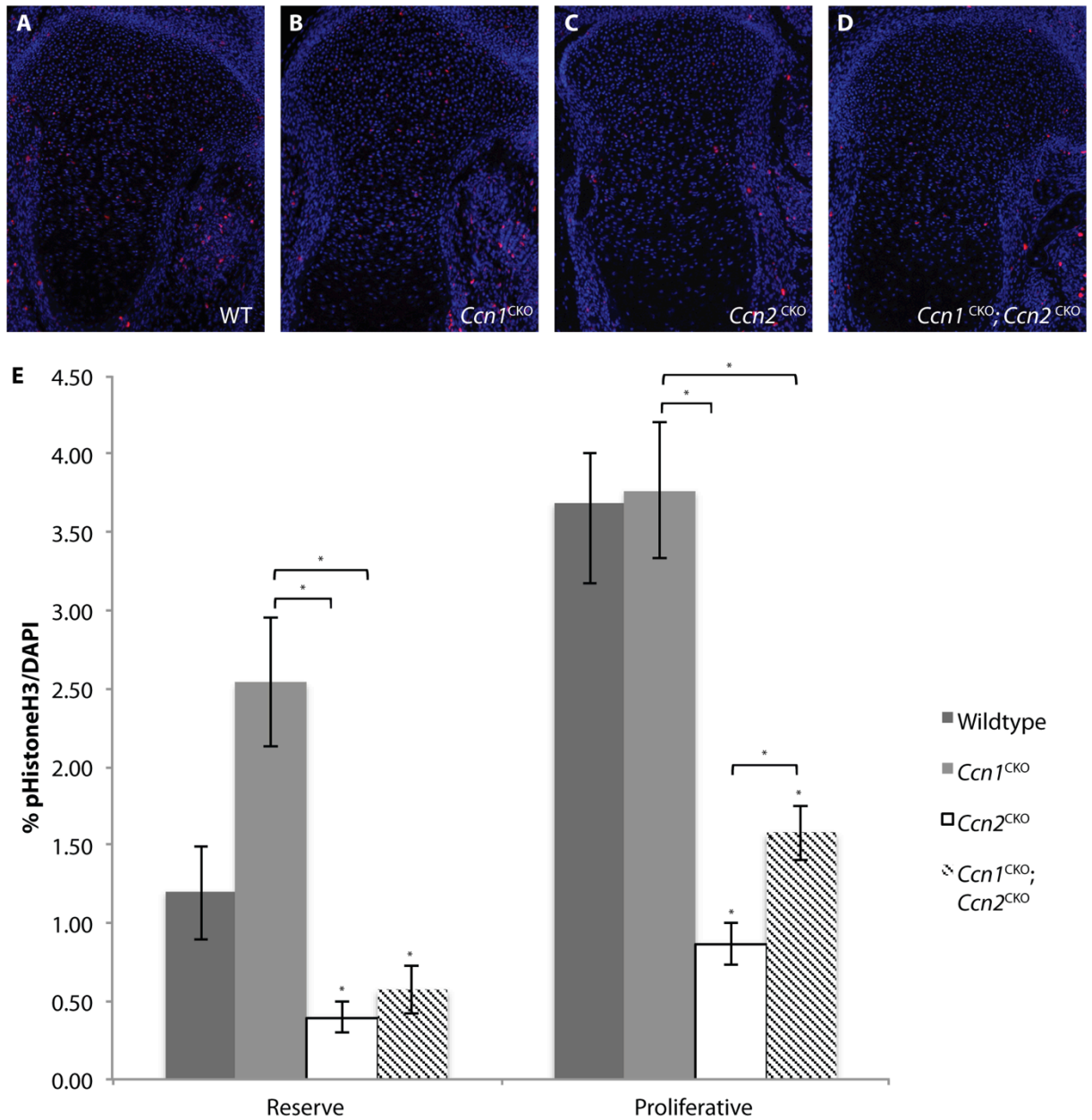


Figure 5. CCN1 and CCN2 may act conversely in regulating proliferation in the tibial growth plates of E16.5 mice. Representative images of phospho-histoneH3 (pHistoneH3) and DAPI used for quantifications for wild type (A), *Ccn1*^{CKO} (B), *Ccn2*^{CKO} (C), and *Ccn1*^{CKO}; *Ccn2*^{CKO} (D) mice. (E) Quantification of pHistoneH3 and DAPI double positive cells divided by DAPI cells for the reserve and proliferative zones. Within the reserve zone, a normally slowly proliferating region, it appears that the absence of CCN1 allows for an increase

in proliferation, although this increase was not significant with our sample size. The absence of CCN2 in the reserve zone results in a decrease in proliferation that is significant, a phenotype that is epistatic in the *Ccn1*^{CKO};*Ccn2*^{CKO} mutant. It is proposed that while CCN1 may normally serve to limit proliferation in the reserve zone, CCN2 may normally promote proliferation. The phenotype in the reserve zone is once again reflected in the proliferative zone with significant decreases in proliferation for the *Ccn2*^{CKO} and *Ccn1*^{CKO};*Ccn2*^{CKO} mutants. (n = 3; * indicates p<0.05)

CHAPTER 3: REMAINING QUESTIONS AND FUTURE DIRECTIONS

So far we have shown that CCN1 and CCN2 may have some overlapping functions in maintaining proper axial skeletal development but some distinct functions in the appendicular skeleton. In addition, CCN1 and CCN2 may regulate chondrocyte proliferation within the reserve zone antagonistically or sequentially.

One of the largest underlying questions is clarifying the role of CCN1 and CCN2 in the axial skeleton. This could be done by examining different time points and doing the same apoptosis and proliferation assays on axial elements including the vertebrae and the cranial base. Furthermore, more markers for differentiation should be used to see if the same defects persist in the *Ccn1*^{CKO};*Ccn2*^{CKO} mutant as seen in the *Ccn2*^{-/-} (Ivkovic et al., 2003): VEGF, MMP13, *Ihh*, Col X, PECAM, and MMP8. Expression of such markers should be quantified using qRT-PCR as well as visualized using immunofluorescence. It would also be interesting to see how mineralization was affected in the *Ccn1*^{CKO} and *Ccn1*^{CKO};*Ccn2*^{CKO} mutants using a von kossa stain. Finally, analysis of mice lacking *Ccn1* and/or *Ccn2* at earlier stages of chondrogenesis, using *Prx1-Cre* to drive excision in limb bud mesenchyme is in progress to test whether or not *Ccn1* and *Ccn2* exhibit overlapping or distinct functions during condensation and commitment to chondrogenesis.

Understanding how CCN1 and CCN2 may work conversely to maintain proper proliferation in the reserve zone's growth plate is a new idea that needs further investigation. *In vivo* experiments such as BrdU pulse chase in wild type and *Col2a1*-ablated mutants would be vital to understanding this. In addition, doing FACS analysis of cell cycle markers isolated from micro-dissected growth plate regions would give further insight into exactly what CCN1 and CCN2 are doing to maintain proliferation. These experiments could be continued *in vitro* with isolation of primary chondrocytes from the sterna of *Ccn1*^{fx/fx}, *Ccn2*^{fx/fx}, or *Ccn1*^{fx/fx};*Ccn2*^{fx/fx}

mice and infection with Adeno-Cre or Adeno-GFP (as a control). With these chondrocytes, *in vitro* proliferation could be tested using a micromass assays.

In addition, the novel phenotype found here in the perichondrium is a potential avenue of study. Further analysis would consist of increased replicates, different time points (both younger and older), and co-staining with different cell markers. It is imperative to find out which cells are undergoing apoptosis within the perichondrial border—so colocalization studies with TUNEL and markers for chondrocytes or osteoblasts would be essential (Kronenberg, 2007).

The implication of the overlapping functions between the two family members CCN1 and CCN2 brings us to the question of the other CCN family members. The results shown here indicate the potential functional redundancy of CCN1 and CCN2 during endochondral bone formation, possibly explaining the unexpectedly mild skeletal phenotype of the *Ccn1*^{CKO} mutant (Figure 2A). In addition, the unexpectedly mild phenotype also seen in the *Ccn1*^{CKO};*Ccn2*^{CKO} mutant may be explained by functional redundancy with the other CCNs (CCN3-6). It has been shown that CCN2 acts antagonistically on CCN3 expression, with increased expression of CCN3 in CCN2-depleted chondrocytes (Kawaki et al., 2008), so we would expect increased CCN3 in the *Ccn1*^{CKO};*Ccn2*^{CKO} mutant as well. However it would be interesting to see if this increase in CCN3, or other CCNs, was augmented in the *Ccn1*^{CKO};*Ccn2*^{CKO} mutant compared to the *Ccn1*^{CKO} mutant. Such expression could be studied using qRT-PCR with cells *in vitro* and *in vivo*, in situ hybridization, and immunofluorescence. From expression patterns of the other CCNs, then their potential functions within endochondral bone formation may become clearer.

CHAPTER 4: MATERIALS AND METHODS

4.1 Mice

Ccn1^{fx/fx} mice were a generous gift from Dr. Lester Lau (University of Illinois). *Ccn2*^{fx/fx} were made by Dr. Karen Lyons, and *Ccn1*^{fx/fx}*Ccn2*^{fx/fx} mice were made by mating *Ccn1*^{fx/fx} and *Ccn2*^{fx/fx} mice together. *Col2a1-Cre*^{Tg/+} mice are those from (Ovchinnikov et al., 2000). All mice were treated and maintained according to IACUC standards under approved protocols.

4.2 Skeletal Preparations

Dissected embryos were placed in 95% ethanol (Decon Laboratories) for 1 day. Then the embryos were transferred to a staining solution for 5 days: 1/20 Alcian blue 8GX (Sigma) in 70% ethanol, 1/20 0.1 Alizarin Red S (Sigma) in 95% ethanol, 1/20 glacial acetic acid (Fisher Scientific), and 17/20 70% ethanol. The embryos were left in 2% aqueous potassium hydroxide (KOH, Fisher Scientific) for 1 day in 4 °C, then left in 1% KOH for 2 days at room temperature. Next, embryos were transferred to a 1:1 solution of 0.5% KOH and glycerol (Fisher Scientific) for 4 days at room temperature and were stored in a 1:1 solution of ethanol and glycerol. Alcian Blue stains proteoglycans such as aggrecan (cartilage), while Alizarin Red stains mineral (bone). Pictures of skeletal preparations were taken with a Leica MZ 16F Bright Field microscope and captured with QCapture through Q imaging color 12 BIT scope.

4.3 Histology

Dissected tibial growth plates were left overnight in 4% paraformaldehyde (PFA, Sigma-Aldrich). Specimens were dehydrated in increasing concentrations of ethanol. The specimens were transferred to xylene (Fisher Scientific), then changed to a 1:1 xylene-paraffin (McCormick) solution overnight. The paraffin was changed two times and the tissues were embedded. Paraffin sections (7 µm) were cut using a Leica RM 2615 microtome.

For the Safranin-O and Nuclear Fast Green stain, sections were first deparaffinized and rehydrated: 4 washes for 2 minutes in xylene and 2 washes for 2 minutes in 100% ethanol, 95%

ethanol, and 70% ethanol. Next slides were stained with Gill's Hematoxylin (Sigma Aldrich) for 10 minutes, then washed for 5 minutes in running tap. Then slides were stained in 1% Fast Green (Sigma) in double deionized water for 10 minutes and rinsed in 1% glacial acetic acid for less than 10 seconds. Slides were stained with 0.1% Safranin O (Sigma) in double deionized water for 5 minutes then dehydrated using the reverse ethanol gradient to xylene. The slides were subsequently mounted with coverslips using Permount (Fisher Scientific)

For CCN1 and CCN2 immunofluorescence, sections were deparaffinized and rehydrated as mentioned above. Next, antigen retrieval was done by incubating samples for 30 minutes in 1 mg/mL hyaluronidase (Sigma) in double deionized water at 37 °C followed by washing (each wash from now on will be three times 5 minutes) in 1X PBS/0.05% Tween-20 (ACROS). The sections were blocked for 30 minutes in TNB buffer (PerkinElmer Tyramide kit) at room temperature, and then incubated with the primary antibody (CCN1/Cyr61 H-78 rabbit 1:50 dilution or CCN2/Ctgf L-20 goat 1:100 dilution; both from Santa Cruz) made in TNB buffer overnight at 4 °C. The next day samples were washed three times and incubated in biotinylated secondary antibody (VECTOR Biotinylated Rabbit and Goat IgG (H&L)) in a 1:500 dilution in TNB buffer at room temperature for 30 minutes and washed three times. Next they were treated with streptavidin AlexaFluor 594 conjugated (Invitrogen) in a 1:250 dilution made in TNB for 30 minutes at room temperature and washed three times. They were then incubated with DAPI in a 1:500 dilution in PBS for 5 minutes and washed three times. Slides were mounted with ProLong Gold antifade reagent (Invitrogen).

For TUNEL assays, the Roche In Situ Cell Death Detection Kit Fluorescein was used according to the provided protocol with slight modifications within a humidified chamber. Slides were deparaffinized and rehydrated. Next they were incubated in 20 µg/mL of Proteinase K (Roche) for 10 minutes at 37 °C and washed two times for 5 minutes with PBS. Next 50 µL of the enzyme solution was mixed with 450 µL of the label solution, pipetted up and down to mix, and incubated on the samples in the dark for 1 hour at 37 °C. They were then washed two times with PBS, and incubated with DAPI and mount as mentioned above.

For phosphorylated-Serine10 Histone H3 (pHistoneH3) the Tyramide Signal Amplification kit (Invitrogen; kits 21 and 25) were used. After deparaffinization and dehydration, antigen retrieval was done at 95 °C first with the tyramide antigen retrieval solution (10 mM Tris from Fisher Scientific, 1 mM EDTA from Fisher Scientific, 0.05% Tween-20) for 15 minutes then in a 10 mM sodium citrate (Sigma) solution (in PBS, pH 6.0) for 15 minutes. Endogenous peroxidases were quenched with 1.5 mL 30% hydrogen peroxide (Fisher Scientific) in 50 mL methanol (Fisher Scientific). Samples were washed in PBS and blocked in Tyramide Blocking Buffer (Tyramide BB: 10 mL 1x PBS, 100 mg blocking reagent from kit, 1% triton-X from Sigma) for 1 hour at room temperature. Then the primary antibody (p-HistoneH3 antibody: 1/500, Cell Signaling, rabbit anti mouse) made in Tyramide BB was incubated overnight at 4 °C. The next day the samples were washed (each wash was two times 5 minutes each) in PBS-Tween and incubated with biotinylated rabbit antibody (VECTOR) at room temperature for 30 minutes. After washing with PBS-Tween, they were incubated for 30 minutes in HRP (kit) solution made in Tyramide BB. Next they were washed again in PBS-Tween and solution “E1” was made: 1 µL of hydrogen peroxide (kit) in 200 µL of Component E (kit). Next solution “E2” was made: 1/100 dilution of E1 as well as Tyramide XX (kit) in Component E. Samples were incubated with E2 for 7.5 minutes and wash in PBS-Tween. Then ABC Elite (VECTASTAIN ABC Kit Elite PK 6100 standard) was incubated for 30 minutes at room temperature. Next samples were incubated in the fluorophore solution for 7.5 minutes: 1/100 dilution of the AlexaFluor 594 (kit) as well as E1 in Component E. After washing in PBS, exogenous peroxidases were quenched with 0.02 N HCl in PBS, and washed in PBS. DAPI was added in a 1/500 dilution for 5 minutes, then the samples were mounted.

All histological stains were examined using the Olympus BX60 light microscope, using appropriate filters and UV light (Chiu Technical Corporation Mercury 100-W) when needed. Pictures were imaged with QCapture Pro.

REFERENCES

- Abe, M., and Sato, Y. (2001). cDNA microarray analysis of the gene expression profile of VEGF-activated human umbilical vein endothelial cells. *Angiogenesis* 4, 289–298.
- Babic, A.M., Kireeva, M.L., Kolesnikova, T. V, and Lau, L.F. (1998). CYR61, a product of a growth factor-inducible immediate early gene, promotes angiogenesis and tumor growth. *Proceedings of the National Academy of Sciences of the United States of America* 95, 6355–6360.
- Bartel, F., Balschun, K., Gradhand, E., Strauss, H.G., Dittmer, J., and Hauptmann, S. (2012). Inverse expression of cysteine-rich 61 (Cyr61/CCN1) and connective tissue growth factor (CTGF/CCN2) in borderline tumors and carcinomas of the ovary. *International Journal of Gynecological Pathology : Official Journal of the International Society of Gynecological Pathologists* 31, 405–415.
- Bonda, T.A., Kamiński, K.A., Dziemidowicz, M., Litvinovich, S., Kozuch, M., Hirnle, T., Dmitruk, I., Chyczewski, L., and Winnicka, M.M. (2012). Atrial expression of the CCN1 and CCN2 proteins in chronic heart failure. *Folia Histochemica Et Cytobiologica / Polish Academy of Sciences, Polish Histochemical and Cytochemical Society* 50, 99–103.
- Bradham, D.M., Igarashi, A., Potter, R.L., and Grotendorst, G.R. (1991). Connective tissue growth factor: a cysteine-rich mitogen secreted by human vascular endothelial cells is related to the SRC-induced immediate early gene product CEF-10. *The Journal of Cell Biology* 114, 1285–1294.
- Brigstock, D.R. (2002). Regulation of angiogenesis and endothelial cell function by connective tissue growth factor (CTGF) and cysteine-rich 61 (CYR61). *Angiogenesis* 5, 153–165.
- Brigstock, D.R., Goldschmeding, R., Katsube, K., Lam, S.C.-T., Lau, L.F., Lyons, K., Naus, C., Perbal, B., Riser, B., Takigawa, M., et al. (2003). Proposal for a unified CCN nomenclature. *Molecular Pathology : MP* 56, 127–128.
- Chen, C.-C., and Lau, L.F. (2009). Functions and mechanisms of action of CCN matricellular proteins. *The International Journal of Biochemistry & Cell Biology* 41, 771–783.
- Chen, C.C., Chen, N., and Lau, L.F. (2001). The angiogenic factors Cyr61 and connective tissue growth factor induce adhesive signaling in primary human skin fibroblasts. *The Journal of Biological Chemistry* 276, 10443–10452.
- Chen, P.-P., Li, W.-J., Wang, Y., Zhao, S., Li, D.-Y., Feng, L.-Y., Shi, X.-L., Koeffler, H.P., Tong, X.-J., and Xie, D. (2007). Expression of Cyr61, CTGF, and WISP-1 correlates with clinical features of lung cancer. *PloS One* 2, e534.
- Dornhöfer, N., Spong, S., Bennewith, K., Salim, A., Klaus, S., Kambham, N., Wong, C., Kaper, F., Sutphin, P., Nacamuli, R., et al. (2006). Connective tissue growth factor-specific monoclonal antibody therapy inhibits pancreatic tumor growth and metastasis. *Cancer Research* 66, 5816–5827.
- Friedrichsen, S., Heuer, H., Christ, S., Winckler, M., Brauer, D., Bauer, K., and Raivich, G. (2003). CTGF expression during mouse embryonic development. *Cell and Tissue Research* 312, 175–188.
- Goodwin, C.R., Lal, B., Zhou, X., Ho, S., Xia, S., Taeger, A., Murray, J., and Latterra, J. (2010). Cyr61 mediates hepatocyte growth factor-dependent tumor cell growth, migration, and Akt activation. *Cancer Research* 70, 2932–2941.

Hall-Glenn, F., and Lyons, K.M. (2011). Roles for CCN2 in normal physiological processes. *Cellular and Molecular Life Sciences : CMLS* 68, 3209–3217.

Hall-Glenn, F., De Young, R.A., Huang, B.-L., Van Handel, B., Hofmann, J.J., Chen, T.T., Choi, A., Ong, J.R., Benya, P.D., Mikkola, H., et al. (2012). CCN2/connective tissue growth factor is essential for pericyte adhesion and endothelial basement membrane formation during angiogenesis. *PloS One* 7, e30562.

Haque, I., Mehta, S., Majumder, M., Dhar, K., De, A., McGregor, D., Van Veldhuizen, P.J., Banerjee, S.K., and Banerjee, S. (2011). Cyr61/CCN1 signaling is critical for epithelial-mesenchymal transition and stemness and promotes pancreatic carcinogenesis. *Molecular Cancer* 10, 8.

Huang, B.-L., Dornbach, L.M., and Lyons, K.M. (2007). The 5' untranslated regions (UTRs) of CCN1, CCN2, and CCN4 exhibit cryptic promoter activity. *Journal of Cell Communication and Signaling* 1, 17–32.

Igarashi, A., Nashiro, K., Kikuchi, K., Sato, S., Ihn, H., Fujimoto, M., Grotendorst, G.R., and Takehara, K. (1996). Connective tissue growth factor gene expression in tissue sections from localized scleroderma, keloid, and other fibrotic skin disorders. *The Journal of Investigative Dermatology* 106, 729–733.

Ivkovic, S., Yoon, B.S., Popoff, S.N., Safadi, F.F., Libuda, D.E., Stephenson, R.C., Daluiski, A., and Lyons, K.M. (2003). Connective tissue growth factor coordinates chondrogenesis and angiogenesis during skeletal development. *Development (Cambridge, England)* 130, 2779–2791.

Jun, J.-I., and Lau, L.F. (2010). The matricellular protein CCN1 induces fibroblast senescence and restricts fibrosis in cutaneous wound healing. *Nature Cell Biology* 12, 676–685.

Jun, J.-I., and Lau, L.F. (2011). Taking aim at the extracellular matrix: CCN proteins as emerging therapeutic targets. *Nature Reviews. Drug Discovery* 10, 945–963.

Kadota, H., Nakanishi, T., Asaumi, K., Yamaai, T., Nakata, E., Mitani, S., Aoki, K., Aiga, A., Inoue, H., and Takigawa, M. (2004). Expression of connective tissue growth factor/hypertrophic chondrocyte-specific gene product 24 (CTGF/Hcs24/CCN2) during distraction osteogenesis. *Journal of Bone and Mineral Metabolism* 22, 293–302.

Kawaki, H., Kubota, S., Suzuki, A., Lazar, N., Yamada, T., Matsumura, T., Ohgawara, T., Maeda, T., Perbal, B., Lyons, K.M., et al. (2008). Cooperative regulation of chondrocyte differentiation by CCN2 and CCN3 shown by a comprehensive analysis of the CCN family proteins in cartilage. *Journal of Bone and Mineral Research : the Official Journal of the American Society for Bone and Mineral Research* 23, 1751–1764.

Kawaki, H., Kubota, S., Suzuki, A., Suzuki, M., Kohsaka, K., Hoshi, K., Fujii, T., Lazar, N., Ohgawara, T., Maeda, T., et al. (2011). Differential roles of CCN family proteins during osteoblast differentiation: Involvement of Smad and MAPK signaling pathways. *Bone* 49, 975–989.

Kronenberg, H.M. (2003). Developmental regulation of the growth plate. *Nature* 423, 332–336.

Kronenberg, H.M. (2007). The role of the perichondrium in fetal bone development. *Annals of the New York Academy of Sciences* 1116, 59–64.

Ladwa, R., Pringle, H., Kumar, R., and West, K. (2011). Expression of CTGF and Cyr61 in colorectal cancer. *Journal of Clinical Pathology* 64, 58–64.

Lau, L.F. (2012). CCN1 and CCN2: blood brothers in angiogenic action. *Journal of Cell Communication and Signaling* 6, 121–123.

- Lau, L.F., and Lam, S.C. (1999). The CCN family of angiogenic regulators: the integrin connection. *Experimental Cell Research* 248, 44–57.
- Lau, L.F., and Nathans, D. (1987). Expression of a set of growth-related immediate early genes in BALB/c 3T3 cells: coordinate regulation with c-fos or c-myc. *Proceedings of the National Academy of Sciences of the United States of America* 84, 1182–1186.
- Leask, A., and Abraham, D.J. (2006). All in the CCN family: essential matricellular signaling modulators emerge from the bunker. *Journal of Cell Science* 119, 4803–4810.
- Mo, F.-E., and Lau, L.F. (2006). The matricellular protein CCN1 is essential for cardiac development. *Circulation Research* 99, 961–969.
- Mo, F.-E., Muntean, A.G., Chen, C.-C., Stolz, D.B., Watkins, S.C., and Lau, L.F. (2002). CYR61 (CCN1) is essential for placental development and vascular integrity. *Molecular and Cellular Biology* 22, 8709–8720.
- Nakanishi, T., Nishida, T., Shimo, T., Kobayashi, K., Kubo, T., Tamatani, T., Tezuka, K., and Takigawa, M. (2000). Effects of CTGF/Hcs24, a product of a hypertrophic chondrocyte-specific gene, on the proliferation and differentiation of chondrocytes in culture. *Endocrinology* 141, 264–273.
- Nguyen, N., Kuliopulos, A., Graham, R.A., and Covic, L. (2006). Tumor-derived Cyr61(CCNI) promotes stromal matrix metalloproteinase-1 production and protease-activated receptor 1-dependent migration of breast cancer cells. *Cancer Research* 66, 2658–2665.
- Nishida, T., Nakanishi, T., Asano, M., Shimo, T., and Takigawa, M. (2000). Effects of CTGF/Hcs24, a hypertrophic chondrocyte-specific gene product, on the proliferation and differentiation of osteoblastic cells in vitro. *Journal of Cellular Physiology* 184, 197–206.
- Nishida, T., Kawaki, H., Baxter, R.M., Deyoung, R.A., Takigawa, M., and Lyons, K.M. (2007). CCN2 (Connective Tissue Growth Factor) is essential for extracellular matrix production and integrin signaling in chondrocytes. *Journal of Cell Communication and Signaling* 1, 45–58.
- O'Brien, T.P., and Lau, L.F. (1992). Expression of the growth factor-inducible immediate early gene *cyr61* correlates with chondrogenesis during mouse embryonic development. *Cell Growth & Differentiation: the Molecular Biology Journal of the American Association for Cancer Research* 3, 645–654.
- Ovchinnikov, D.A., Deng, J.M., Ogunrinu, G., and Behringer, R.R. (2000). Col2a1-directed expression of Cre recombinase in differentiating chondrocytes in transgenic mice. *Genesis (New York, N.Y. : 2000)* 26, 145–146.
- Perbal, B. (2013). CCN proteins: A centralized communication network. *Journal of Cell Communication and Signaling*.
- Quan, T., Shin, S., Qin, Z., and Fisher, G.J. (2009). Expression of CCN family of genes in human skin in vivo and alterations by solar-simulated ultraviolet irradiation. *Journal of Cell Communication and Signaling* 3, 19–23.
- Quan, T., Qin, Z., Xu, Y., He, T., Kang, S., Voorhees, J.J., and Fisher, G.J. (2010). Ultraviolet irradiation induces CYR61/CCN1, a mediator of collagen homeostasis, through activation of transcription factor AP-1 in human skin fibroblasts. *The Journal of Investigative Dermatology* 130, 1697–1706.

- Rittié, L., Perbal, B., Castellot, J.J., Orringer, J.S., Voorhees, J.J., and Fisher, G.J. (2011). Spatial-temporal modulation of CCN proteins during wound healing in human skin in vivo. *Journal of Cell Communication and Signaling* 5, 69–80.
- Ryseck, R.P., Macdonald-Bravo, H., Mattéi, M.G., and Bravo, R. (1991). Structure, mapping, and expression of fisp-12, a growth factor-inducible gene encoding a secreted cysteine-rich protein. *Cell Growth & Differentiation : the Molecular Biology Journal of the American Association for Cancer Research* 2, 225–233.
- Sauer, B. (1998). Inducible gene targeting in mice using the Cre/lox system. *Methods (San Diego, Calif.)* 14, 381–392.
- Sawai, K., Mukoyama, M., Mori, K., Kasahara, M., Koshikawa, M., Yokoi, H., Yoshioka, T., Ogawa, Y., Sugawara, A., Nishiyama, H., et al. (2007). Expression of CCN1 (CYR61) in developing, normal, and diseased human kidney. *American Journal of Physiology. Renal Physiology* 293, F1363–72.
- Sha, W., and Leask, A. (2011). CCN2 expression and localization in melanoma cells. *Journal of Cell Communication and Signaling* 5, 219–226.
- Shi-Wen, X., Leask, A., and Abraham, D. (2008). Regulation and function of connective tissue growth factor/CCN2 in tissue repair, scarring and fibrosis. *Cytokine & Growth Factor Reviews* 19, 133–144.
- Si, W., Kang, Q., Luu, H.H., Park, J.K., Luo, Q., Song, W.-X., Jiang, W., Luo, X., Li, X., Yin, H., et al. (2006). CCN1/Cyr61 is regulated by the canonical Wnt signal and plays an important role in Wnt3A-induced osteoblast differentiation of mesenchymal stem cells. *Molecular and Cellular Biology* 26, 2955–2964.
- Sisco, M., Kryger, Z.B., O’Shaughnessy, K.D., Kim, P.S., Schultz, G.S., Ding, X.-Z., Roy, N.K., Dean, N.M., and Mustoe, T.A. (2008). Antisense inhibition of connective tissue growth factor (CTGF/CCN2) mRNA limits hypertrophic scarring without affecting wound healing in vivo. *Wound Repair and Regeneration : Official Publication of the Wound Healing Society [and] the European Tissue Repair Society* 16, 661–673.
- Watari, H., Xiong, Y., Hassan, M.K., and Sakuragi, N. (2009). Cyr61, a member of ccn (connective tissue growth factor/cysteine-rich 61/nephroblastoma overexpressed) family, predicts survival of patients with endometrial cancer of endometrioid subtype. *Gynecologic Oncology* 112, 229–234.
- Wong, M., Kireeva, M.L., Kolesnikova, T. V, and Lau, L.F. (1997). Cyr61, product of a growth factor-inducible immediate-early gene, regulates chondrogenesis in mouse limb bud mesenchymal cells. *Developmental Biology* 192, 492–508.
- Yin, D., Chen, W., O’Kelly, J., Lu, D., Ham, M., Doan, N.B., Xie, D., Wang, C., Vadgama, J., Said, J.W., et al. (2010). Connective tissue growth factor associated with oncogenic activities and drug resistance in glioblastoma multiforme. *International Journal of Cancer. Journal International Du Cancer* 127, 2257–2267.

APPENDIX A: PUBLISHED ARTICLES AND CONTRIBUTIONS

A.1 CCN2/Connective Tissue Growth Factor is essential for pericyte adhesion and endothelial basement membrane formation during angiogenesis

I collected the data in Figure 1C and 1E and also helped in optimizing several immunofluorescent stains.

CCN2/Connective Tissue Growth Factor Is Essential for Pericyte Adhesion and Endothelial Basement Membrane Formation during Angiogenesis

Faith Hall-Glenn¹[✉], R. Andrea De Young²^{✉a}, Bau-Lin Huang³^{✉b}, Ben van Handel¹, Jennifer J. Hofmann^{1,4}^{✉c}, Tom T. Chen¹^{✉d}, Aaron Choi², Jessica R. Ong¹, Paul D. Benya², Hanna Mikkola¹, M. Luisa Iruela-Arispe^{1,4,5}, Karen M. Lyons^{1,2,4,5}*

1 Department of Molecular, Cell and Developmental Biology, University of California Los Angeles, Los Angeles, California, United States of America, **2** Department of Orthopaedic Surgery, University of California Los Angeles, Los Angeles, California, United States of America, **3** Department of Oral Biology, University of California Los Angeles, Los Angeles, California, United States of America, **4** Molecular Biology Institute, University of California Los Angeles, Los Angeles, California, United States of America, **5** Jonsson Comprehensive Cancer Center, University of California Los Angeles, Los Angeles, California, United States of America

Abstract

CCN2/Connective Tissue Growth Factor (CTGF) is a matricellular protein that regulates cell adhesion, migration, and survival. CCN2 is best known for its ability to promote fibrosis by mediating the ability of transforming growth factor β (TGF β) to induce excess extracellular matrix production. In addition to its role in pathological processes, CCN2 is required for chondrogenesis. CCN2 is also highly expressed during development in endothelial cells, suggesting a role in angiogenesis. The potential role of CCN2 in angiogenesis is unclear, however, as both pro- and anti-angiogenic effects have been reported. Here, through analysis of *Ccn2*-deficient mice, we show that CCN2 is required for stable association and retention of pericytes by endothelial cells. PDGF signaling and the establishment of the endothelial basement membrane are required for pericytes recruitment and retention. CCN2 induced PDGF-B expression in endothelial cells, and potentiated PDGF-B-mediated Akt signaling in mural (vascular smooth muscle/pericyte) cells. In addition, CCN2 induced the production of endothelial basement membrane components *in vitro*, and was required for their expression *in vivo*. Overall, these results highlight CCN2 as an essential mediator of vascular remodeling by regulating endothelial-pericyte interactions. Although most studies of CCN2 function have focused on effects of CCN2 overexpression on the interstitial extracellular matrix, the results presented here show that CCN2 is required for the normal production of vascular basement membranes.

Citation: Hall-Glenn F, De Young RA, Huang B-L, van Handel B, Hofmann JJ, et al. (2012) CCN2/Connective Tissue Growth Factor Is Essential for Pericyte Adhesion and Endothelial Basement Membrane Formation during Angiogenesis. PLoS ONE 7(2): e30562. doi:10.1371/journal.pone.0030562

Editor: Costanza Emanuelli, University of Bristol, United Kingdom

Received: October 3, 2011; **Accepted:** December 19, 2011; **Published:** February 20, 2012

This is an open-access article, free of all copyright, and may be freely reproduced, distributed, transmitted, modified, built upon, or otherwise used by anyone for any lawful purpose. The work is made available under the Creative Commons CC0 public domain dedication.

Funding: This work was supported by NIH AR052686, Scleroderma Foundation, and the Jonsson Comprehensive Cancer Center, UCLA (KML), UCLA Vascular Biology Training Grant HL069766 and Ruth L. Kirschstein National Research Service Award T32HL69766 (FHG), and NIH HL097766 (HM). The funders had no role in study design, data collection and analysis, decision to publish, or preparation of the manuscript.

Competing Interests: The authors have declared that no competing interests exist.

* E-mail: klyons@mednet.ucla.edu

^a Current address: Amgen, Thousand Oaks, California, United States of America

^b Current address: Center for Cancer Research, National Cancer Institute, Frederick, Maryland, United States of America

^c Current address: Karolinska Institutet, Stockholm, Sweden

^d Current address: South San Francisco, California, United States of America

✉ These authors contributed equally to this work.

Introduction

CCN2, also known as connective tissue growth factor, is a member of the CCN (CCN1-6) family of matricellular proteins. CCN family members are cysteine-rich and contain an N-terminal secretory peptide, followed by four multi-functional domains that interact with a diverse array of binding partners [1,2]. Proteins that interact with CCN2 through recognition of these domains include integrins, low-density lipoprotein receptor-related proteins (LRPs), growth factors, and extracellular matrix (ECM) components. The first domain shares homology to insulin-like growth factor binding proteins (IGFBPs), but has very low affinity for IGF [3]. The second domain encodes a von Willebrand type C (VWC) repeat. This motif mediates CCN2 interactions with growth

factors such as bone morphogenetic proteins (BMPs) and transforming growth factor β (TGF β) [4]. The third domain is a type-1 thrombospondin (TSP) repeat, known to mediate the ability of CCN2 to bind to ECM proteins, matrix metalloproteinases (MMPs) and integrin $\alpha 6 \beta 1$ [5,6]. The final C-terminal (CT) motif contains a cysteine knot similar to those present in many growth factors, including members of the TGF β superfamily, platelet derived growth factor (PDGF), and nerve growth factor (NGF). This motif mediates interactions with integrins $\alpha v \beta 3$, $\alpha 5 \beta 1$, and $\alpha 6 \beta 1$ [7–13].

CCN2 was originally isolated from human umbilical vein endothelial cells (HUVECs) [14]. *In situ* hybridization and immunohistochemical studies demonstrated that CCN2 is expressed predominantly in endothelial cells in embryonic and adult

vasculature [15–18]. The physiological role of CCN2 in angiogenesis is unclear, however, as it appears to have both pro- and anti-angiogenic activities *in vitro*. For example, CCN2 induces corneal angiogenesis, and anti-CCN2 antibodies block angiogenesis in the chick chorioallantoic membrane assay [19,20]. On the other hand, anti-angiogenic activities have been reported; although *Ccn2* expression is induced by VEGF [21], CCN2 binds to and sequesters VEGF in an inactive form [5], and combined administration of CCN2 and VEGF inhibits VEGF-induced angiogenesis [22]. The role of CCN2 in angiogenesis *in vivo* is unknown.

The majority of studies have focused on the role of CCN2 as a stimulator of excess ECM production in the context of pathological fibrosis [23]. CCN2 is overexpressed in all fibrotic conditions described to date, and depending on the tissue involved, induces collagen type I deposition and increased susceptibility to injury [24]. Conversely, the loss of CCN2 in fibroblasts results in decreased collagen deposition and resistance to chemically induced skin fibrosis [25,26]. In addition to its role as a mediator of fibrosis, CCN2 is required for ECM production in cartilage [27]. *Ccn2* knockout mice survive in Mendelian ratios throughout gestation, but die within minutes of birth. They exhibit severe chondrodysplasia as a result of decreased collagen type II and aggrecan expression by chondrocytes *in vivo* and *in vitro* [27,28]. CCN2 regulates cell survival, adhesion, migration, and ECM production in multiple cell types by regulating integrin expression and activation [13]. In *Ccn2* mutant chondrocytes, integrin $\alpha 5\beta 1$ expression and downstream focal adhesion kinase (FAK) and extracellular signal-related kinase (ERK1/2) signaling are decreased, indicating that CCN2 regulates ECM production through integrins [28].

In endothelial cells, CCN2 mediates adhesion, migration and survival through binding to integrin $\alpha v\beta 3$ [7]. CCN2 is also a ligand for $\alpha 5\beta 1$ and $\alpha 6\beta 1$ [13], and these integrins are required for endothelial basement membrane formation and vessel stabilization *in vitro* [29]. Taken together, these studies implicate CCN2 as an important regulator of cellular adhesion and ECM production during angiogenesis, but do not address its role *in vivo*. As CCN2 is the major mediator of excess ECM production during fibrosis, and has also been implicated in tumor angiogenesis [30], it is important to understand its function in normal tissues. Therefore, the function of CCN2 in angiogenesis was investigated through analysis of *Ccn2* mutant mice.

Results

CCN2 is expressed in the developing vasculature

Using transgenic mice in which lacZ expression is driven by the 4 kb proximal *Ccn2* promoter [31], CCN2 expression was seen throughout the vasculature and microvasculature at E16.5 (Figure 1A). Expression was observed in large vessels, arterioles and capillaries at all stages examined (E13.5–P0). CCN2 was detected as early as E13.5 in developing dermal microvasculature (Figure 1B), where lacZ is present in large and small caliber vessels (Figure 1A,B). Similar results were seen using bacterial artificial chromosome (BAC) transgenic mice expressing enhanced green fluorescent protein (EGFP) under the control of the *Ccn2* locus (CCN2-EGFP) [32]. This analysis revealed *Ccn2* expression in endothelium of arterial and venous elements, and in capillaries. In large arteries, CCN2-EGFP was expressed in both endothelial and vascular smooth muscle cells (vSMCs) (Figure 1C,E). CCN2 was also expressed in developing capillary networks (Figure 1D). Endothelial-specific expression in microvasculature was also shown by immunostaining for CCN2 (Figure 1F–H). Specificity

of the antibody was confirmed by the absence of staining sections from *Ccn2* mutants (Figure 1H). Punctate intracellular staining was observed, most likely within the Golgi and in secretory vesicles, as reported previously [33]. Cell-associated expression was also seen on the abluminal surface of the endothelium (Figure 1G). Co-immunostaining with the endothelial-specific marker PECAM (CD31) revealed CCN2 expression in endothelial cells and in mural cells (Figure S1A). Thus, *Ccn2* is expressed in both endothelial and mural cells in blood vessels and capillaries during development.

Ccn2 mutant mice exhibit vascular defects

Ccn2 mutant mice exhibit perinatal lethality due to a severe chondrodysplasia [27]. CCN2 expression in developing blood vessels raised the possibility of an additional role in vascular development. *Ccn2*^{-/-} embryos were examined to investigate this possibility. No overt differences between *Ccn2* mutants and WT littermates were apparent during the initial formation of the vasculature from E9.5–E13.5 (data not shown). Moreover, placentas were normal in appearance, weight, and vascularity throughout development (Figure S1B,C, and data not shown). However, beginning at E14.5, minor enlargement of vessels was observed in mutants (Figure S1D,E), which became more pronounced at later stages (Figure 2A,B). Local edema was seen in E18.5 mutant dermis (Figure 2C,D). Immunofluorescence analysis of the vSMC marker smooth muscle actin (SMA) and PECAM (CD-31) did not reveal obvious evidence that SMC coverage of large vessels was affected in mutants (Figure S1F–I). However, comparison of hematoxylin and eosin-stained sections of the aorta at thoracic and lumbar levels from E16.5 embryos showed defects in the organization of the tunica media (Fig. 2E–H). In WT embryos, SMCs had a spindle-like morphology and were circumferentially oriented around the vessel lumen in distinct layers (Figure 2E,G). In mutants, SMCs failed to adopt this spindle-like morphology, were more heterogeneous in size, and were not organized into distinct layers (Figure 2F,H). The large vessel phenotype will be reported in more detail elsewhere. Here we focus on the microvascular phenotype.

Morphological examination (Figure S1J,K) revealed that arterial-venous identity appeared to be maintained in mutants (see also Figure S1H,I). Ephrin B2 (expressed on arterial elements) and EphB4 (preferentially expressed on veins) staining demonstrated no defects in arterial-venous identity (Figure S1L,M, and data not shown). However, inspection of E18.5 dermal microvasculature revealed evidence of defective remodeling in *Ccn2* mutants. Consistent with a defect in remodeling, vessel density was increased in *Ccn2* mutants (Figure 2I–L and Figure S2A–C). Moreover, mutant capillaries had multiple protrusions along their surfaces (Figure 2M,N). Electron microscopy revealed numerous luminal and abluminal protrusions in mutant capillaries, consistent with the confocal analysis (Figure 2O,P).

CCN2 mutants exhibit defects in vascular remodeling

PCNA labeling and TUNEL analyses were performed to assess whether defects in proliferation and/or survival might contribute to the microvascular abnormalities in *Ccn2* mutants. No differences were detected in mutants in comparison to WT littermates (Figure S2D–G). During vascular remodeling, immature vascular beds become less dense, arterioles become smaller in diameter than venules, and pericytes form stable associations with endothelial tubes [34]. Angiopoetin 1 (Ang1) is required for stabilizing endothelial-pericyte interactions and is expressed primarily by mural cells [35]. *Ang1* mRNA levels were diminished in *Ccn2*^{-/-} skin (Figure S2H). No differences were detected in levels of

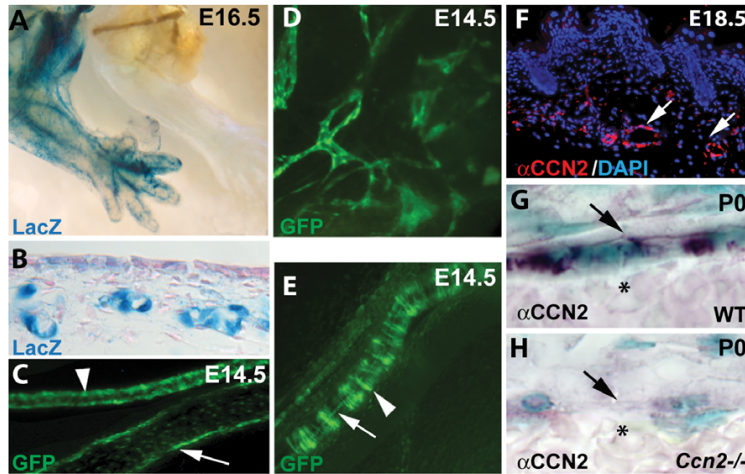


Figure 1. Expression of *Ccn2* in developing vasculature. (A) β -galactosidase activity in *Ccn2-lacZ* transgenic mice reveals *Ccn2* promoter activity throughout the vasculature in E16.5 embryos. (B) *Ccn2-lacZ* expression in dermal microvessels at E13.5. (C–E) EGFP fluorescence in CCN2-EGFP BAC transgenic mice demonstrates CCN2 expression in the endothelium of arterial elements (C and E), venous elements (C), and developing capillary networks (D). Arrowheads in (C) and (E) demarcate arterial element. Arrow in (C) identifies endothelial cells of a venous element. Arrowhead in (E) highlights EGFP expression in mural cells in the arterial element. Arrow in (E) highlights expression in endothelial cells in the arterial element. (F) Immunofluorescence and (G,H) immunohistochemical staining with an α CCN2 antibody on paraffin sections through dermis, demonstrating CCN2 expression in endothelial cells. Arrows in (F) highlight endothelial cells in E18.5 microvasculature. Specificity of the α CCN2 antibody is demonstrated by the absence of reactivity in the *Ccn2*^{-/-} section (H). Arrows in (G) and (H) demarcate abluminal surface of the endothelium. Asterisks in (G) and (H) identify blood cells within the vessels. α CCN2 staining in (G) shows punctate intracellular expression, presumably with the Golgi, in addition to the surface expression marked by the arrow.
doi:10.1371/journal.pone.0030562.g001

expression of *Tie2*, the endothelial-specific receptor for Ang1 (data not shown). However, levels of the mRNA encoding the bio-active VEGF isoform 164 were elevated in mutants (Figure S2J). Versican is the principal chondroitin sulfate proteoglycan in blood vessels and exists in at least four isoforms, V0, V1, V2, and V3 [36]. Embryonic endothelial cells express more V0 than other isoforms, and V0 expression declines during vascular maturation [37]. No differences were seen in levels of versican *V1* in *Ccn2* mutants and WT littermates (Figure S2J); however, *Ccn2* mutants exhibited increased levels of *V0* (Figure S2K). Therefore, the loss of *Ccn2* leads to diminished expression of vessel maturation marker *Ang1* and elevated expression of markers of immature vasculature, indicative of a potential defect in vascular remodeling.

The vascular phenotype in *Ccn2* mutants bears some resemblance to mice lacking platelet-derived growth factor-B (PDGF-B) or its receptor, PDGFR β [38,39]. In particular, defective pericyte recruitment is seen in these mice. Therefore, we examined pericyte recruitment in *Ccn2* mutants. Pericytes, which express NG2 and desmin, become associated with small diameter vessels during vessel maturation [40]. Consistent with the gene expression analysis described above, confocal analysis of desmin expression revealed incomplete coverage of microvessels by pericytes in the dermis of *Ccn2* mutants at E16.5 and E18.5 (Figure 3A–C; data not shown). Similar results were seen for NG2 expression in the lung liver, and brain microvasculature (Figure 3D–F, and data not shown). Thus, the loss of CCN2 affects the microvasculature in multiple tissues. Flow cytometric analysis of lung, liver, and brain samples from E16.5 embryos for cells negative for the endothelial cell marker PECAM, but expressing the pericyte markers NG2 and PDGFR β [41] revealed normal numbers of endothelial cells and pericytes in *Ccn2* mutants (Figure S3, and data not shown). This suggests that the reduced pericyte coverage in *Ccn2* mutants is

not caused by a decrease in pericyte number or migration, but possibly by defects in the ability of pericytes to make stable associations and elongate along endothelial cells in *Ccn2* mutant mice.

Confocal analysis of E16.5 dermal and lung microvasculature co-stained with NG2, desmin, and PECAM supports this possibility. NG2 staining demonstrated that pericytes associated with WT vessels were in close contact with the capillary endothelium and appeared elongated along the endothelial surface (Figure 3G). In contrast, pericytes associated with capillaries in mutants were more rounded and exhibited less elongation (Figure 3H). Immunostaining with desmin also suggested a defect in pericyte association with endothelial cells in mutants. In WT capillaries, pericytes were elongated and covered the surface of endothelial tubes (Figure 3I,J and Figure S4A,B). In contrast, pericytes on mutant capillaries were rarely elongated, and vessel coverage was incomplete (Figure 3K,L and Figure S4C,D). Taken together, these findings indicate that the ability of pericytes to form stable associations with microvascular endothelium is defective in *Ccn2* mutants.

CCN2 potentiates PDGF signaling in vascular cells

PDGF-B, produced by endothelial cells, and its receptor, PDGFR β expressed in pericytes, are required for pericyte recruitment to nascent vessels [38]. CCN2 was originally identified as a protein that competes with PDGF-B for binding to NIH 3T3 cells, leading to the suggestion that CCN2 binds to PDGF receptors [42]. However, subsequent studies using a C-terminal isoform of CCN2 showed no interaction between CCN2 and PDGF receptors [43]. We tested whether full-length CCN2 interacts with PDGF-B or its receptor through co-immunoprecipitation and found no evidence for a direct physical interaction

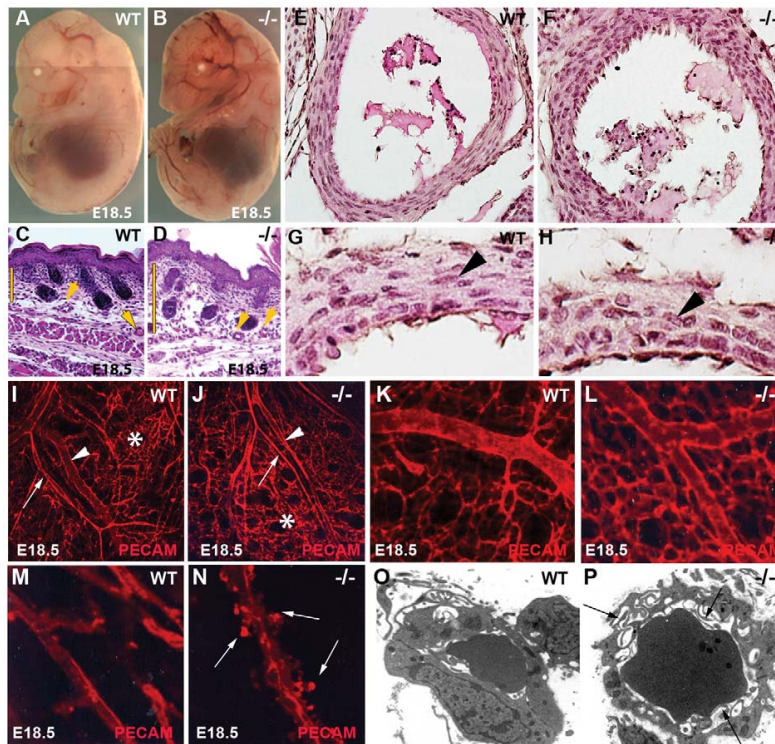


Figure 2. Vascular abnormalities in *Ccn2* mutant embryos. (A) E18.5 WT and (B) *Ccn2*^{-/-} littermate, showing vessel dilation throughout the mutant embryo. (C, D) H&E-stained paraffin sections through the lumbar dorsal dermis of (C) E18.5 WT and (D) *Ccn2*^{-/-} littermate. Arrowheads point to vessels. Bars highlight the enlarged distance between the hypodermal and epidermal layers in the mutant, indicative of local edema. (E, F) Hematoxylin and eosin-stained sections through E16.5 WT (E) and *Ccn2*^{-/-} (F) descending aorta at thoracic level. Smooth muscle cells in the tunica media are spindle-shaped and arranged in layers in the WT embryo, but are more cuboidal and disorganized in the *Ccn2*^{-/-} littermate. (G, H) Higher magnification images through aorta at lumbar level in E16.5 (G) WT and (H) *Ccn2*^{-/-} littermate showing spindle-shaped smooth muscle cells (arrowheads) in WT that have a cuboidal shape in the mutant. (I, J) Confocal images of PECAM-stained dorsal dermal vasculature in (I) WT and (J) *Ccn2*^{-/-} littermates. Arrows demarcate arterial elements; arrowheads demarcate venous elements; asterisks identify capillary beds. (K, L) Higher magnification confocal images of (K) WT and (L) *Ccn2*^{-/-} dorsal dermal capillary beds, showing increased capillary density in the mutant. (M, N) High magnification confocal image of (M) WT and (N) *Ccn2*^{-/-} dorsal dermal capillaries, showing numerous abluminal protrusions (arrows in (N)) on the mutant capillary. (O, P) Electron micrographs of newborn (P0) (O) WT and (P) *Ccn2*^{-/-} dermal capillaries, showing abluminal and luminal (arrows in (P)) protrusions.

doi:10.1371/journal.pone.0030562.g002

(Figure S5, Methods S1). These findings suggest that CCN2 does not influence PDGF signaling by interacting directly with PDGF-B or PDGFR β .

Next, we investigated whether CCN2 could induce PDGF-B expression in endothelial cells. Recombinant CCN2 (rCCN2) induced PDGF-B protein expression in human umbilical vein endothelial cells (HUVECs) at 1 and 4 hours of stimulation (Figure 4A). This was confirmed using HUVECs transfected with a CCN2-GFP adenovirus (adCCN2GFP). AdCCN2GFP-transfected cells induced PDGF-B protein expression at all time points tested, and the level of PDGF-B induction correlated with levels of CCN2 expression (Figure 4B). Given that CCN2 induces PDGF-B expression in endothelial cells, the potential effects of CCN2 on PDGF signaling pathways in mural cells, which express PDGFR β , were investigated. CCN2 on its own did not activate Stat3, ERK1/2, or AKT, whereas PDGF activated all of these pathways. Furthermore, CCN2 had no effect on PDGF-B-induced ERK1/2 or Stat3 activation, but Akt activation was elevated and prolonged upon treatment with PDGF and CCN2 (Figure 4C). Thus CCN2

can potentiate PDGF signaling between endothelial cells and mural cells.

Components of the endothelial basement membrane are compromised in *Ccn2* mutants

Decreased expression of PDGF-B and reduced PDGF signaling are unlikely to be the entire basis for the *Ccn2* mutant phenotype because endothelial-specific loss of PDGF-B is compatible with survival, and mice having as much as a 90% decrease in pericyte number survive as adults [44]. The basement membrane is essential for coordinating key signaling events that stabilize the vasculature during angiogenesis [45]. The expression of fibronectin (FN) by endothelial cells is an early event in vascular basement membrane formation [46]. The provisional fibronectin matrix provides organizational signals to endothelial cells, and establishes a framework for the incorporation of permanent basement membrane components such as collagen type IV [29,46,47]. Defects in basement membrane formation lead to severe defects in angiogenesis [48–51]. Because overexpression of CCN2 leads to

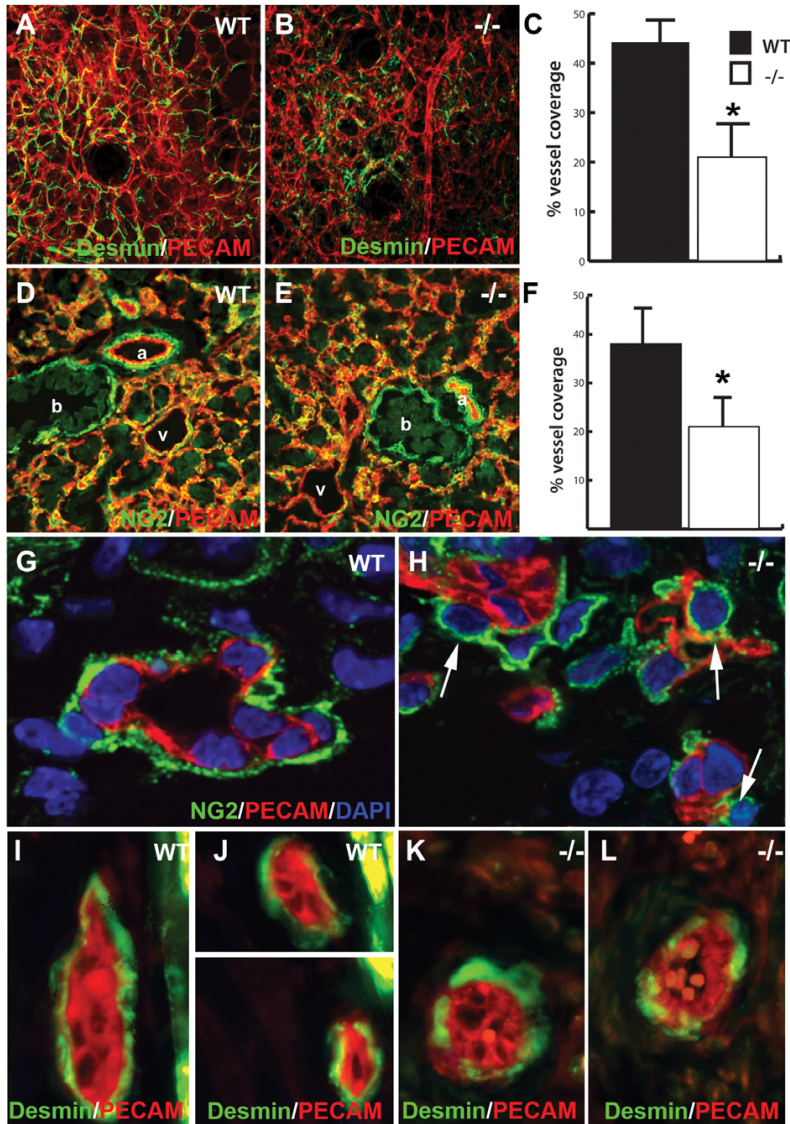


Figure 3. Defective endothelial-pericyte interactions in *Ccn2* mutants. (A, B) Co-immunofluorescence staining for desmin and PECAM in E18.5 dermis from (A) WT and (B) *Ccn2*^{-/-} mice analyzed by confocal microscopy. (C) Quantification of vessel coverage by pericytes in E18.5 dermis; asterisk, $p < 0.05$. (D, E) Co-immunofluorescence staining for NG2 and PECAM in E16.5 lung from (D) WT and (E) *Ccn2*^{-/-} mice analyzed by confocal microscopy. (F) Quantification of vessel coverage by pericytes in E16.5 lung; asterisk, $p < 0.05$. (G, H) Confocal analysis of NG2 and PECAM immunostaining in (G) WT and (H) *Ccn2*^{-/-} E16.5 dermis. Pericytes are elongated around the microvessel in (G), whereas in mutants (H), pericytes (arrows) are associated with the endothelium, but are rounder, and fewer of them have elongated along the endothelial surface. (I-L) Confocal sections through E16.5 dermis analyzed for desmin (green) and PECAM (red) immunofluorescence. (I, J) WT desmin positive pericytes appear elongated and cover most of the surface of the microvessels. (K, L) *Ccn2*^{-/-} desmin-positive pericytes have a rounder appearance and show less extensive coverage of the surface of the endothelium.
doi:10.1371/journal.pone.0030562.g003

thickening of glomerular and retinal capillary basement membranes in diabetic mice [52,53], we investigated whether CCN2 is required for the formation of endothelial basement membranes during development.

Electron microscopy provided evidence for defects in microvascular endothelial basement membrane assembly in *Ccn2* mutants. In WT microvessels, the interstitial matrix was compact

and localized near the surface of the plasma membrane (Figure 5A). It was more diffuse in mutants (Figure 5B). Therefore, expression of FN and Col4 α 2 was investigated through confocal analysis. FN expression and association with vessels is significantly decreased in E16.5 *Ccn2* mutant skin and lung vasculature (Figure 5C-F, and data not shown). Collagen type IV expression was also diminished and discontinuous in vascular basement

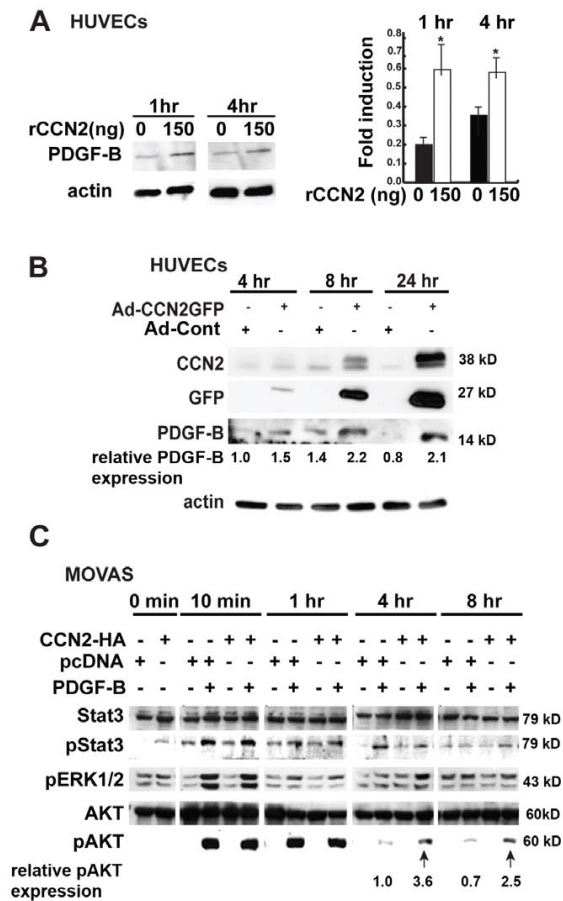


Figure 4. CCN2 potentiates PDGF-B signaling. (A) rCCN2 induces PDGF-B expression in HUVEC cells. Right panel, representative Western blot. Left panel, Quantification of relative expression levels of PDGF-B in cells treated with or without rCCN2 from three separate experiments. *, $p < 0.02$. (B) Adenovirally expressed CCN2 induces PDGF-B expression in HUVECs compared to transfection with an empty adenoviral control. The extent of PDGF-B induction correlated with levels of CCN2 expression. As reported previously, a higher molecular weight isoform of CCN2, presumably a result of post-translational modification [1], is detected 4 and 8 hours post-infection. Relative level of PDGF-B expression was assessed using ImageJ software. The experiment was repeated three times, with similar results each time. The induction of PDGF-B in the presence of CCN2 was statistically significant for each time point; $p < 0.05$. A representative Western blot is shown. (C) Effects of rPDGF-B, and/or pcDNA3-CCN2-HA expression on activation of PDGF pathways in MOVAS cells. PDGF-B stimulated activation of Stat3, ERK, and Akt, whereas CCN2-HA on its own had no effect. However, combined treatment with PDGF-B and CCN2-HA led to prolonged Akt activation (arrows). Relative levels of pAKT expression were assessed using ImageJ software. All experiments were performed in triplicate and repeated three times, with similar results each time. The increase in pAKT levels in the presence of CCN2 was statistically significant at each time point; $p < 0.05$. A representative Western blot is shown. doi:10.1371/journal.pone.0030562.g004

membranes in mutants (Figure 5G–J). Western blot analysis of Ad-CCN2GFP-transfected cells demonstrated that CCN2 induced expression of FN in HUVECs compared to empty vector-transfected controls (Figures 5K and S6). CCN2 had no apparent effect on Col4 α 2 expression (Figures 5K and S6).

Discussion

Endothelial cells proliferate and migrate toward the sources of angiogenic signals during development. Upon removal of the angiogenic trigger, a switch to a maturation phase occurs, involving cessation of cell proliferation and migration, followed by the recruitment of mural cells to the vessels, and deposition of the basement membrane. Although the importance of the basement membrane in vascular maturation is widely accepted, the roles of specific ECM components have been difficult to ascertain, especially *in vivo* [45]. Here we show that the matricellular protein CCN2 is a crucial regulator of vascular remodeling.

The results reported here suggest that CCN2 is required for pericyte recruitment in part by potentiating PDGF signaling. We have shown that CCN2 induces expression of PDGF-B in endothelial cells. In turn, CCN2 is induced in pericytes in response to serum or TGF β [54]. Thus, PDGF and CCN2 appear to be components of a positive feedback loop that operates between endothelial cells and pericytes.

In addition to regulating levels of PDGF-B expression, CCN2 potentiates Akt activation by PDGF-B in vSMCs. Our findings extend previous studies [42] that indicate CCN2 does not interact directly with PDGF-B or PDGFR β in vascular cells. Thus, CCN2 most likely potentiates the ability of PDGF-B to activate PDGFR β in mural cells through indirect mechanisms. One of the most plausible of these involves interactions between CCN2 and integrin α v β 3. This integrin is expressed in endothelial cells and pericytes [55,56]. CCN2 binds to integrin α v β 3 to promote endothelial cell migration and proliferation [9]. Moreover, α v β 3 associates with and potentiates signaling through PDGFR β [55]. Although our *in vivo* studies cannot address the physiological consequences of altered Akt signaling to the *Ccn2*^{-/-} vascular phenotype, the *Ccn2*^{-/-} phenotype is consistent with the possibility that reduced activation of Akt makes a contribution; *Akt1*^{-/-} vasculature is characterized by an incomplete basement membrane [57].

As discussed above, reduced PDGF signaling alone cannot explain the severity of the *Ccn2*^{-/-} endothelial phenotype. Rather, the data indicate an essential role for CCN2 in formation of the vascular provisional ECM and basement membrane. The relationship between CCN2 and FN expression and function is likely to be complex. CCN2 binds to FN and FN receptors (integrins α 4, α 5 and β 1) [12,58,59]. Moreover, loss of CCN2 leads to defective adhesion and spreading of cells on FN, suggesting that these physical interactions are essential for certain cell types, at least *in vitro* [28,59]. Other studies have shown that CCN2 is required for FN protein and mRNA expression in pathological processes *in vivo* [60,61]. Studies employing siRNA knockdown approaches demonstrate that CCN2 induces FN expression in various cell types [25,62]. The studies reported here show that CCN2 induces FN expression in endothelial cells, and that CCN2 is required for normal levels of FN expression during development *in vivo*. While we have focused here on the role of CCN2 as a mediator of FN production by vascular cells, decreased FN synthesis was also seen in fibroblasts in *Ccn2*^{-/-} dermis (Figure 5E,F). These data are consistent with previous studies showing that CCN2 is required for FN synthesis in fibroblasts *in vitro* [61]. Additional studies employing tissue-specific CCN2 knockouts will be required to determine whether the defect in FN synthesis in dermal fibroblasts has physiological consequences.

The reduced deposition of collagen IV in *Ccn2* mutants reveals that CCN2 is an essential regulator of vascular basement membrane formation. The underlying mechanisms by which

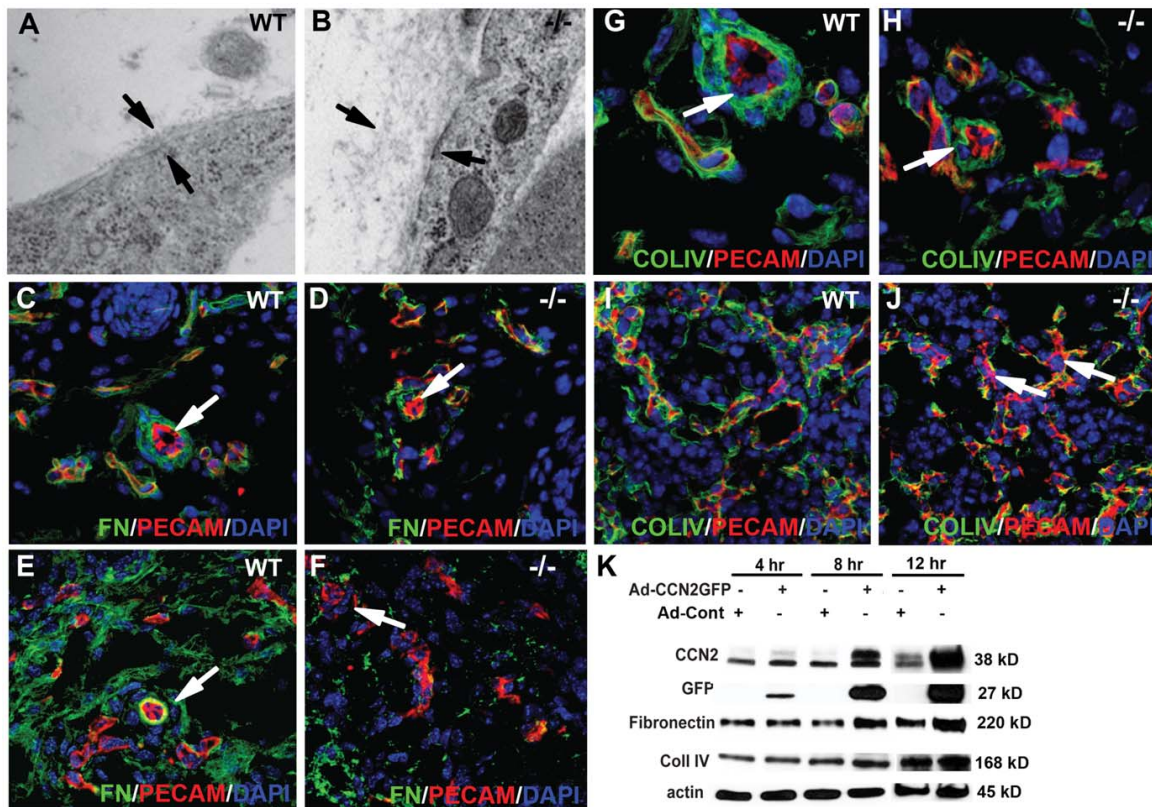


Figure 5. Endothelial basement membrane defects in *Ccn2* mutants. Electron microscopical images of endothelial basement membranes in dermal capillaries of E16.5 (A) WT and (B) *Ccn2*^{-/-} littermates. Arrows demarcate the plasma membrane (bottom arrow) and top of the interstitial matrix (top arrow). (C,D) Confocal images of dermis of E16.5 WT (C) and *Ccn2*^{-/-} (D) mice analyzed by immunofluorescence for fibronectin (FN) and PECAM. Arrows identify an arteriole. The arteriole in (C) is surrounded by several layers of FN. The arteriole in (D) is incompletely invested with FN. (E,F) Lower magnification confocal images through (E) WT and (F) *Ccn2*^{-/-} E16.5 dermis, illustrating less fibronectin throughout the dermis in mutants. (G,H) Confocal images of dermis of E16.5 (G) WT and (H) *Ccn2*^{-/-} mice analyzed by immunofluorescence for ColIV (Col4 α 2) and PECAM. Arrows identify an arteriole. ColIV coverage of the mutant vasculature is incomplete. (I,J) Confocal images of lungs of E16.5 (I) WT and (J) *Ccn2*^{-/-} mice analyzed by immunofluorescence for ColIV and PECAM. Most of the vascular elements in the WT lung are surrounded by ColIV. Coverage is incomplete in the *Ccn2* mutant lung. Arrows in (J) identify vessels lacking coverage by ColIV. (K) CCN2 induces expression of FN and ColIV in HUVECs. HUVECs were infected with Ad-CCN2-GFP or Ad-control. Lysates were collected at the indicated time points post-infection. Levels of FN are elevated 8 hours after infection, concomitant with accumulation of CCN2. There appeared to be an increase in FN levels at 12 hours in the presence of CCN2 in the blot shown, but this was not seen in every experiment and the result did not reach statistical significance at this time point. Similarly, there was a trend towards increased expression of Col IV at 12 hr, but this increase did not reach statistical significance ($p = 0.065$). The experiment was repeated three times. A representative blot is shown. Quantification of levels of FN and Col IV are shown in Figure S6. doi:10.1371/journal.pone.0030562.g005

CCN2 mediates basement membrane formation are unknown. Our studies indicate that CCN2 does not directly regulate levels of expression of *Col4 α 2*. Therefore, the loss of collagen IV expression in vascular basement membranes may be a secondary consequence of altered FN synthesis and folding. As discussed above, CCN2 directly interacts with FN and its receptors. Increased expression of matrix metalloproteinases (MMPs) that target type IV collagen might also contribute to reduced type IV collagen deposition in endothelial basement membranes. Additional *in vivo* studies will be required to evaluate these possibilities. A growing body of literature implicates CCN2 in abnormal basement membrane thickening in pathological processes. Glomerular basement membrane thickening is prevented in diabetic *Ccn2*^{+/-} mice compared to WT littermates [52]. Moreover, one of the most prominent features in transgenic mice overexpressing CCN2 from the type I collagen promoter is a thickening of endothelial

basement membranes [63]. Taken together with the data reported here, CCN2 appears to be a critical mediator of basement membrane formation. CCN2 is required for normal elaboration of the basement membrane during developmental angiogenesis, but CCN2 overexpression leads to basement membrane thickening in multiple fibrotic processes.

The formation of mature endothelial basement membranes involves both pericytes and endothelial cells. While we have focused here on effects of CCN2 in endothelial cells *in vivo*, it is very conceivable that primary defects in both endothelial cells and pericytes in *Ccn2*^{-/-} mice contribute to the basement membrane defects seen in these mutants. It is likely that CCN2 has direct effects on ECM production in pericytes, as CCN2 promotes ECM production and fibroblast activation *in vitro* [64]. Moreover, our preliminary analysis reveals that in addition to the microvasculature, large vessels are impacted by loss of CCN2. This finding

raises the possibility that CCN2 plays a direct role in SMCs in addition to pericytes. It is noteworthy that the related matricellular protein CCN1 (Cyr61) is expressed in major vessels, and *Ccn1*^{-/-} mice die early in embryogenesis as a result of defects in large vessel integrity [65]. Although vascular basement membranes have not been investigated in *Ccn1*^{-/-} mice, the defects in vessel integrity raise the possibility that CCN1 and CCN2 will exhibit functional redundancy in vascular elements. It will thus be of interest in future studies to investigate vascular cell recruitment and basement membrane assembly in *Ccn1* and *Ccn1/Ccn2* mutants.

Finally, the use of tissue-specific *Ccn2* knockouts and co-culture experiments will be required to understand the physiological relevance of CCN2 produced by endothelial and mural cells in large vessels.

Methods

Ethics Statement

All the experiments related to mice were performed in accordance with National Institutes of Health guidelines for care and use of animals, and also approved by the UCLA Institutional Animal Care and Use Committee (IACUC), protocol #95-018.

Transgenic Mice

***Ccn2*^{-/-} mice.** The generation of *Ccn2*^{-/-} mice was described previously [27]. As previously described, *Ccn2*^{+/-} mice appear indistinguishable from WT littermates, and are viable and fertile [27]. *Ccn2*^{-/-} embryos and neonates were obtained by intercrossing *Ccn2*^{+/-} mice. The 4 kb proximal promoter LacZ mice were generated and genotyped as previously described [31]. CCN2-eGFP mice were ordered from the Mutant Mouse Resource Center (MMRC, UC Davis) [32]. All mice were treated and euthanized in accordance with the UCLA Institutional Animal Care and Use Committee (ARC # 1995-018-52A), and the Association of Assessment and Accreditation of Laboratory Animal Care International (AAALAC) guidelines.

Histochemical and Immunofluorescent Staining. Freshly isolated embryos were fixed and embedded in paraffin wax as described previously [27]. 5 μm sections were stained with hematoxylin and eosin using standard protocols. LacZ staining was performed as described [66]. Immunofluorescence was performed as described previously [27]. Briefly, paraffin, sections were boiled for 15 min in citrate buffer. Sections were blocked with 5% goat or donkey serum for 1 hour and incubated with primary antibody overnight at 4°C, followed by incubation with secondary antibody for 1 hour at room temperature, then with fluorophore for 30 minutes at room temperature. The following antibodies were used: PECAM (1:500; MEC 13.3, BD Biosciences), CCN2 (1:500; L-20 Santa Cruz Biotechnology), NG2 (1:100; Abcam), Collagen IV (1:500; Abcam and Santa Cruz Biotech), Desmin (1:1000; Abcam), anti-Smooth Muscle Actin-FITC (1:500; Sigma), Col4α2 (1:1,000; Abcam) and Fibronectin (1:1,000; Santa Cruz Biotech). Secondary antibodies were conjugated with Alexa-Fluor-555 and Alexa-Fluor-488 (Invitrogen). Sections were counterstained with DAPI (Vectashield). Immunofluorescence was visualized on a Leica TCS-SP Confocal Microscope. For TUNEL staining, the fluorescein In Situ Cell Death Detection Kit (Roche) was used according to manufacturer's protocol. PCNA staining was performed on paraffin sections as described previously [27] using an anti-PCNA antibody (Zymed) and, vessels were identified by PECAM immunofluorescence. The percentage of TUNEL- or PCNA-positive endothelial cells (PECAM-positive) was quantified

on digital photomicrographs processed with Photoshop software (Adobe), using Image-Pro software. Pericyte coverage of microvasculature was quantified as described [67]. Capillary density was quantified as the area of PECAM1-positive cells on anti-PECAM1 immunostained images as described [68]. Ten images each for WT and *Ccn2*^{-/-} mice, obtained from 5 independent pairs of littermates, were analyzed. Statistical analysis was performed using Student's *t* test. A *p* value of less than 0.05 was considered statistically significant.

Confocal Microscopy. Confocal laser scanning microscopy was performed at the CNSI Advanced Light Microscopy/Spectroscopy Shared Resource Facility at UCLA, supported with funding from NIH-NCRR grant (CJX1-443835-WS-29646) and NSF grant (CHE-0722519). Representative images are shown.

Real-time quantitative polymerase chain reaction. RNA was isolated using TRIZOL (Invitrogen) according to the manufacturer's protocol. Synthesis of cDNA was performed with Superscript III (Invitrogen). Semi-quantitative PCR was performed with 20 ng reverse-transcribed RNA. Amplifications were performed for 30 cycles, followed by a 5 min extension at 72°C. Reaction products were gel electrophoresed and quantified using Image Quant software (Molecular Dynamics). Primers for the genes investigated by semi-quantitative RT-PCR were: VegfA and C: VEGFACF 5'-GAA GTC CCA TGA AGT GAT CAA G-3', VEGF164 5'-CAA GGC TCA CAG TGA TTT TCT GGC-3'; ANG1: ANG1F 5'-CAT TCT TCG CTG CCA TTC TG, ANGR 5'-GCA CAT TGC CCA TGT TGA ATC-3'; PECAM: PECAMF 5'-GAG CCC AAT CAC GTT TCA GTT T-3', PECAMR 5'-TCC TTC CTG CTT CTT GCT AGC T-3'; Versican0: V₀F 5'-TTC ACA GAA CGC CAC CCT TGA GTC C-3', V₀R 5'-CTA GCT TCT GCA GCT GGC CGG GTC C-3'; Versican1-3: V1F 5'-GCA GCT TGG AGA AAT GGC TTT GAC C-3', V₁R 5'-CGA GTA GTT GTG GGT GAT TCC GTG G-3'; PDGFBF 5'-GATCCGCTCCCTTGTGATGATC-3', PDGFBR 5'-GTCTCACACTTGCATGCCAG-3'; PDGFRbetaF 5'-AATGTCTCCAGCACCTTCGT-3', PDGFRbetaR 5'-AGC-GGATGTGGTAAGGCATA-3' [69]; GAPDH, GapdhF 5'-GCA GTG GCA AAG TGG AGA TT-3'; Gapdhr 5'-AGT GGA TGC AGG GAT GAT GT. cDNA was amplified using Sybr Green I PCR Master Mix (Applied Biosystems). Amplicons were generated and analyzed with the ABI 7000 Real-time PCR system (Applied Biosystems). Data were normalized to the levels of *Gapdh*. Triplicate assays were run and analyses were repeated three times. Specificity was tested by measurement of T_m-values and by gel electrophoresis of the amplicons. Data are represented as the means of relative levels of expression+the S.E. of the mean, and statistical analysis was performed with Student's *t* test. A *p* value of less than 0.05 was considered statistically significant.

Flow Cytometry. FACS analysis was performed as previously described [70]. Brain, liver and lung samples were harvested from E16.5 CCN2 wild type and mutant embryos. Single cell suspensions were created by serial syringe digestion in 0.2% Collagenase (Sigma *Clostridium histolyticum* C2674-6), 0.05% Dispase (Invitrogen 17105-041), 0.0075% DnaseI (Sigma D4513), 0.02% Penicillin Streptomycin (GIBCO-Invitrogen 15140148) in 1× PBS/10%Fetal Bovine Serum (GIBCO-Invitrogen 10437-028). Cell suspensions were incubated with the following primary antibodies: CD45-APC Cy7 (1:200;Abcam); NG2 (1:200; Abcam); CD31-PE (1:200; Abcam); PDGFRβ-APC (1:50; Invitrogen). A secondary goat anti-rabbit conjugated antibody 488 (Invitrogen) was used for the unconjugated NG2 antibody. FITC, APC, APC-Cy7, PE control beads (Invitrogen) and 488 secondary alone were used as controls to correct for background fluorescence and gate parameters. FACS sorting was performed using the LSRII FACS

analyzer and cell counts were plotting by FlowJo analysis (TreeStar).

Transmission Electron Microscopy. Ultrastructural analysis was performed on dermal microvasculature by the University of California, Los Angeles, Electron Microscopy Core Facility. 10 images were taken from each E18.5 embryo. Four *Ccn2*^{-/-} and four WT littermates were examined. Representative images are shown.

Cell lines and treatments. Human umbilical vein endothelial cells (HUVECs a gift from Dr. Jau-Nian Chen) were maintained in HUVEC culture media (Sigma) as described previously [71]. HUVECs were maintained in 0.5% serum for 12 hr prior to treatment with recombinant protein. Cells were treated with 150 ng/ml recombinant (r) CCN2 (Peptide) and/or 150 ng/ml rPDGF-B (Peptide), using serum free treated cells as control. Mouse vascular smooth muscle (MOVAS) (ATTC) cells were cultured in DMEM, 10% FBS. MOVAS cells were washed with Hepes buffered saline (HBS) containing 5 mM MgCl₂ (HBS+Mg), and treated with or without 150 ng/ml rPDGF-B in DMEM, 0.5% FBS for the indicated times. In other experiments, MOVAS cells were transiently transfected with pcDNA3-CCN2-HA [72] using Lipofectamine (Invitrogen), and treated with 150 ng/ml rPDGF-B 24 hrs later for the indicated time periods. Each experiment was performed in triplicate and repeated at least twice. HUVECs were also transfected with CCN2-GFP adenovirus and adenoviral control vectors at a multiplicity of infection (MOI) of 200 (a kind gift of Dr. Fayed Safadi).

Western blot analysis. Cells were lysed with RIPA buffer with 1× protease (Complete Mini Roche) and 1× phosphatase inhibitors (Cocktail 2, Sigma). Lysates were separated by 6–12% SDS-PAGE and transferred to nitrocellulose membrane (0.45 μm; BioRad). Membranes were incubated with antibodies against CCN2 (L-20; 1:2,000, Santa Cruz Biotechnology), PDGF-B (1:2000, Cell Signaling), PDGFR β (1:2,000 Cell Signaling), STAT3 (1:1,000, Cell Signaling), pSTAT3 (1:2,000, Cell Signaling), total AKT (1:2,000, Cell Signaling), phospho-AKT (1:2,000, Cell Signaling), phospho-ERK1/2 (1:2,000, Cell Signaling), Collagen type IV (1:2,000; Abcam), Fibronectin (1:2,000; Santa Cruz Biotech) and actin (1:5,000, Sigma). Antibody-antigen complexes were detected with HRP-conjugated secondary goat and rabbit antibodies (Bio-Rad). Western blots were performed in triplicate and normalized to actin. Quantification was performed using ImageJ. Statistical analysis was performed using the Student's t-Test, and a p-value less than 0.05 was considered significant. Representative western blots are shown.

Supporting Information

Methods S1 Methods for co-immunoprecipitation and western blot analysis (Figure S5). (DOCX)

Figure S1 Expression of CCN2 in vasculature and vascular defects in *Ccn2* mutants. (A) Confocal image of dermal microvasculature immunostained for CCN2 (green) and PECAM (red). Yellow indicates co-expression in endothelial cells. The staining is punctate, as reported previously [30]. Associated mural cells expressing CCN2 (green) are indicated by arrows. Endothelium demonstrating CCN2 expression is indicated by arrowheads. (B,C) Confocal images of fetal placenta from E16.5 WT (B) and *Ccn2*^{-/-} (C) littermates immunostained for NG2 (green) and PECAM (red) and counterstained with DAPI showing no obvious changes in vascular organization. (D) E14.5 WT and (E) *Ccn2*^{-/-} littermate. Arrows highlight dilation of cerebral vessels in the mutant. Dilated vessels are apparent in the mutant.

(F–I) Confocal images of immunofluorescence staining for αSMA (green) and PECAM (red) in dorsal dermis of newborn (P0) WT (F,H) and *Ccn2*^{-/-} (G,I) littermates. Arrows in (F–I) indicate arteries; arrowheads demarcate veins. (J,K) Confocal images of immunofluorescence staining for αSMA (green) and PECAM (red) in dorsal dermis of newborn (P0) WT (J) and *Ccn2*^{-/-} (K) littermates showing paired arterioles (arrows) and venules (arrowheads). (L,M) Confocal images of immunofluorescence staining for EphB4 (green) and PECAM (red) of E16.5 WT (L) and *Ccn2*^{-/-} littermate (M) dorsal dermal microvasculature. (TIF)

Figure S2 Altered gene expression in *Ccn2* mutants. (A) Quantification of microvessel density. (B,C) Additional representative confocal images of PECAM-immunostained dorsal dermal microvasculature from WT (B) and *Ccn2*^{-/-} (C) E18.5 littermates showing increased vessel density in mutants. (D) Representative image of paraffin section through E16.5 dorsal dermis analyzed by αPECAM and αPCNA co-immunofluorescence and counterstained with DAPI, used to assess endothelial cell proliferation. Image from WT dermis is shown. Arrows point to PCNA-positive endothelial cells. (E) Quantification of PCNA-positive cells revealed no differences in proliferation in WT versus mutant vessels. (F) Representative images of paraffin section through E16.5 dorsal dermis analyzed by immunostaining for PECAM and TUNEL-positive endothelial cells and counterstained with DAPI. Image from WT dermis is shown. (G) Quantification of TUNEL-positive endothelial cells revealed no evidence for altered levels of cell death in *Ccn2* mutant vasculature. (H–K) Quantitative RT-PCR analysis of relative levels of expression of (H) *Ang1*, (I) *Vegf164*, (J) *Vesican1*, and (K) *Vesican0* mRNA in WT and *Ccn2*^{-/-} E16.5 vasculature. *, p<0.05. (TIF)

Figure S3 FACS analysis of pericyte or endothelial cell number in *Ccn2* mutants. (A, C) FACS analysis of (A) WT and (C) *Ccn2*^{-/-} skin samples analyzed for expression of PDGFRβ. (B, D) FACS analysis of (B) WT and (D) *Ccn2*^{-/-} skin samples analyzed for expression of NG2. (E) Quantification of percentages of PDGFRβ, NG2, and PECAM-expressing cells revealed no differences. (TIF)

Figure S4 Defective pericyte association with endothelium in *Ccn2* mutants. Paraffin sections through E16.5 dermis immunostained with desmin (red) and counterstained with DAPI. (A,B) WT desmin positive pericytes appear elongated and cover most of the surface of the microvessels. (C,D) *Ccn2*^{-/-} desmin-positive pericytes have a rounder appearance and desmin staining has a less uniform appearance. (TIF)

Figure S5 No physical interaction between CCN2 and PDGF-B or PDGFRβ. (A) No physical interactions between CCN2 and PDGF-B. MOVAS cells were infected with a lentiviral vector encoding CCN-HA (M-CCN2 cells). Non-crosslinked or DSP-crosslinked lysates (see Supplementary Materials and Methods) were immunoprecipitated with αHA antibody. Western blots of the immunoprecipitates were probed with αCCN2 and αPDGFB antibodies. First lane in each panel shows rCCN2 and rPDGFB standards. TXsol and TX insol, triton X-soluble and -insoluble pellets, respectively. (B) No direct interactions between CCN2 and PDGFRβ. M-CCN2 cells were treated with or without PDGF-B, followed by immunoprecipitation with αHA antibody. Western blots of the immunoprecipitates were probed with αPDGFRβ (PDGFR) or αphospho (Y751) PDGFRβ antibody. (TIF)

Figure S6 CCN2 induces fibronectin expression in endothelial cells. Quantification of relative levels of expression of fibronectin (FN) and Col IV in endothelial cells in the presence or absence of CCN2. See legend to Figure 5 for experimental details. Induction of FN was seen by 8 hrs. There was a trend towards increased FN at 12 hrs ($p < 0.06$), but this did not reach statistical significance. *, $p < 0.05$. There was no significant increase in Col IV levels at any time point. (TIF)

References

- Brigstock DR (2003) The CCN family: a new stimulus package. *J Endocrinol* 178: 169–175.
- Bork P (1993) The modular architecture of a new family of growth regulators related to connective tissue growth factor. *FEBS Lett* 327: 125–130.
- Vorwerk P, Hohmann B, Oh Y, Rosenfeld RG, Shymko RM (2002) Binding properties of insulin-like growth factor binding protein-3 (IGFBP-3), IGFBP-3 N- and C-terminal fragments, and structurally related proteins mac25 and connective tissue growth factor measured using a biosensor. *Endocrinology* 143: 1677–1685.
- Abreu JG, Ketpura NI, Reversade B, De Robertis EM (2002) Connective-tissue growth factor (CTGF) modulates cell signalling by BMP and TGF-beta. *Nat Cell Biol* 4: 599–604.
- Hashimoto G, Inoki I, Fujii Y, Aoki T, Ikeda E, et al. (2002) Matrix metalloproteinases cleave connective tissue growth factor and reactivate angiogenic activity of vascular endothelial growth factor 165. *J Biol Chem* 277: 36288–36295.
- Heng EC, Huang Y, Black SA, Jr., Trackman PC (2006) CCN2, connective tissue growth factor, stimulates collagen deposition by gingival fibroblasts via module 3 and alpha6- and beta1 integrins. *J Cell Biochem* 98: 409–420.
- Babic AM, Chen CC, Lau LF (1999) Fisp12/mouse connective tissue growth factor mediates endothelial cell adhesion and migration through integrin alpha5beta3, promotes endothelial cell survival, and induces angiogenesis in vivo. *Mol Cell Biol* 19: 2958–2966.
- Gao R, Brigstock DR (2004) Connective tissue growth factor (CCN2) induces adhesion of rat activated hepatic stellate cells by binding of its C-terminal domain to integrin alpha(v)beta3 and heparan sulfate proteoglycan. *J Biol Chem* 279: 8848–8855.
- Chen CC, Chen N, Lau LF (2001) The angiogenic factors Cyr61 and connective tissue growth factor induce adhesive signaling in primary human skin fibroblasts. *J Biol Chem* 276: 10443–10452.
- Gao R, Brigstock DR (2005) Connective tissue growth factor (CCN2) in rat pancreatic stellate cell function: integrin alpha5beta1 as a novel CCN2 receptor. *Gastroenterology* 129: 1019–1030.
- Gao R, Brigstock DR (2006) A novel integrin alpha5beta1 binding domain in module 4 of connective tissue growth factor (CCN2/CTGF) promotes adhesion and migration of activated pancreatic stellate cells. *Gut* 55: 856–862.
- Hoshijima M, Hattori T, Inoue M, Araki D, Hanagata H, et al. (2006) CT domain of CCN2/CTGF directly interacts with fibronectin and enhances cell adhesion of chondrocytes through integrin alpha5beta1. *FEBS Lett* 580: 1376–1382.
- Chen CC, Lau LF (2009) Functions and mechanisms of action of CCN matricellular proteins. *Int J Biochem Cell Biol* 41: 771–783.
- Bradham DM, Igarashi A, Potter RL, Grotendorst GR (1991) Connective tissue growth factor: a cysteine-rich mitogen secreted by human vascular endothelial cells is related to the SRC-induced immediate early gene product CEF-10. *J Cell Biol* 114: 1285–1294.
- Friedrichsen S, Heuer H, Christ S, Winckler M, Brauer D, et al. (2003) CTGF expression during mouse embryonic development. *Cell Tissue Res* 312: 175–188.
- Friedrichsen S, Heuer H, Christ S, Cuthill D, Bauer K, et al. (2005) Gene expression of connective tissue growth factor in adult mouse. *Growth Factors* 23: 43–53.
- Surveyor GA, Brigstock DR (1999) Immunohistochemical localization of connective tissue growth factor (CTGF) in the mouse embryo between days 7.5 and 14.5 of gestation. *Growth Factors* 17: 115–124.
- Kireeva ML, Latinkic BV, Kolesnikova TV, Chen CC, Yang GP, et al. (1997) Cyr61 and Fisp12 are both ECM-associated signaling molecules: activities, metabolism, and localization during development. *Exp Cell Res* 233: 63–77.
- Babic AM, Chen C-C, Lau L (1999) Fisp12/Mouse Connective Tissue Growth Factor mediates endothelial cell adhesion and migration through integrin alpha5beta3, promotes endothelial cell survival, and induces angiogenesis in vivo. *Mol Cell Biol* 19: 2958–2966.
- Shimo T, Nakanishi T, Nishida T, Asano M, Kanyama M, et al. (1999) Connective tissue growth factor induces the proliferation, migration, and tube formation of vascular endothelial cells in vitro, and angiogenesis in vivo. *J Biochem* 126: 137–145.
- Suzuma K, Naruse K, Suzuma I, Takahara N, Ueki K, et al. (2000) Vascular endothelial growth factor induces expression of connective tissue growth factor

Acknowledgments

We thank Bonnie Lee and Kevin Mouillesseaux for technical assistance.

Author Contributions

Conceived and designed the experiments: KML MLI-A HM. Performed the experiments: FH-G RAD B-LH BvH JJH TTC JRO AC PDB. Analyzed the data: FH-G MLI-A HM PDB KML. Contributed reagents/materials/analysis tools: PDB HM MLI-A. Wrote the paper: FH-G KML.

- via KDR, Flt1, and phosphatidylinositol 3-kinase-akt-dependent pathways in retinal vascular cells. *J Biol Chem* 275: 40725–40731.
- Inoki I, Shiomi T, Hashimoto G, Enomoto H, Nakamura H, et al. (2002) Connective tissue growth factor binds vascular endothelial growth factor (VEGF) and inhibits VEGF-induced angiogenesis. *FASEB J* 16: 219–221.
- Shi-Wen X, Leask A, Abraham D (2008) Regulation and function of connective tissue growth factor/CCN2 in tissue repair, scarring and fibrosis. *Cytokine Growth Factor Rev* 19: 133–144.
- Brigstock DR (2010) Connective tissue growth factor (CCN2, CTGF) and organ fibrosis: lessons from transgenic animals. *J Cell Commun Signal* 4: 1–4.
- Shi-Wen X, Stanton LA, Kennedy L, Pala D, Chen Y, et al. (2006) CCN2 is necessary for adhesive responses to transforming growth factor-beta1 in embryonic fibroblasts. *J Biol Chem* 281: 10715–10726.
- Liu S, Shi-wen X, Abraham DJ, Leask A (2011) CCN2 is required for bleomycin-induced skin fibrosis in mice. *Arthritis Rheum* 63: 239–246.
- Ivkovic S, Yoon BS, Popoff SN, Safadi FF, Libuda DE, et al. (2003) Connective tissue growth factor coordinates chondrogenesis and angiogenesis during skeletal development. *Development* 130: 2779–2791.
- Nishida T, Kawaki H, Baxter RM, Deyoung RA, Takigawa M, et al. (2007) CCN2 (Connective Tissue Growth Factor) is essential for extracellular matrix production and integrin signaling in chondrocytes. *J Cell Commun Signal* 1: 45–58.
- Stratman AN, Malotte KM, Mahan RD, Davis MJ, Davis GE (2009) Pericyte recruitment during vasculogenic tube assembly stimulates endothelial basement membrane matrix formation. *Blood* 114: 5091–5101.
- Shimo T, Nakanishi T, Nishida T, Asano M, Sasaki A, et al. (2001) Involvement of CTGF, a hypertrophic chondrocyte-specific gene product, in tumor angiogenesis. *Oncology* 61: 315–322.
- Huang BL, Brugger SM, Lyons KM (2010) Stage-specific control of connective tissue growth factor (CTGF/CCN2) expression in chondrocytes by Sox9 and beta-catenin. *J Biol Chem* 285: 27702–27712.
- Gong S, Zheng C, Doughty ML, Losos K, Ditzkovsky N, et al. (2003) A gene expression atlas of the central nervous system based on bacterial artificial chromosomes. *Nature* 425: 917–925.
- Chen Y, Segarini P, Raoufi F, Bradham D, Leask A (2001) Connective tissue growth factor is secreted through the Golgi and is degraded in the endosome. *Exp Cell Res* 271: 109–117.
- Gaengel K, Genove G, Armulik A, Betsholtz C (2009) Endothelial-mural cell signaling in vascular development and angiogenesis. *Arterioscler Thromb Vasc Biol* 29: 630–638.
- Suri C, Jones PF, Patan S, Bartunkova S, Maisonpierre PC, et al. (1996) Requisite role of angiopoietin-1, a ligand for the TIE2 receptor, during embryonic angiogenesis. *Cell* 87: 1171–1180.
- Wight TN (2008) Arterial remodeling in vascular disease: a key role for hyaluronan and versican. *Front Biosci* 13: 4933–4937.
- Cattaruzza S, Schiappacassi M, Ljungberg-Rose A, Spessotto P, Perissinotto D, et al. (2002) Distribution of PG-M/versican variants in human tissues and de novo expression of isoform V3 upon endothelial cell activation, migration, and neoangiogenesis in vitro. *J Biol Chem* 277: 47626–47635.
- Lindahl P, Johansson BR, Leveen P, Betsholtz C (1997) Pericyte loss and microaneurysm formation in PDGF-B-deficient mice. *Science* 277: 242–245.
- Hellstrom M, Kalen M, Lindahl P, Abramsson A, Betsholtz C (1999) Role of PDGF-B and PDGFR-beta in recruitment of vascular smooth muscle cells and pericytes during embryonic blood vessel formation in the mouse. *Development* 126: 3047–3055.
- Diaz-Flores L, Gutierrez R, Madrid JF, Varela H, Valladares F, et al. (2009) Pericytes. Morphofunction, interactions and pathology in a quiescent and activated mesenchymal cell niche. *Histol Histopathol* 24: 909–969.
- Crisan M, Yap S, Castella L, Chen CW, Corselli M, et al. (2008) A perivascular origin for mesenchymal stem cells in multiple human organs. *Cell Stem Cell* 3: 301–313.
- Bradham DM, Igarashi A, Potter RL, Grotendorst GR (1991) Connective Tissue Growth Factor: a cysteine-rich mitogen secreted by human vascular endothelial cells is related to the SRC-induced immediate early gene product CEF-10. *J Cell Biol* 114: 1285–1294.
- Steffen CL, Ball-Mirth DK, Harding PA, Bhattacharyya N, Pillai S, et al. (1998) Characterization of cell-associated and soluble forms of connective tissue growth

- factor (CTGF) produced by fibroblast cells in vitro. *Growth Factors* 15: 199–213.
44. Bjarnegard M, Enge M, Norlin J, Gustafsdottir S, Fredriksson S, et al. (2004) Endothelium-specific ablation of PDGFB leads to pericyte loss and glomerular, cardiac and placental abnormalities. *Development* 131: 1847–1857.
 45. Davis GE, Senger DR (2005) Endothelial extracellular matrix: biosynthesis, remodeling, and functions during vascular morphogenesis and neovessel stabilization. *Circ Res* 97: 1093–1107.
 46. Risau W, Lemmon V (1988) Changes in the vascular extracellular matrix during embryonic vasculogenesis and angiogenesis. *Dev Biol* 125: 441–450.
 47. Jain RK (2003) Molecular regulation of vessel maturation. *Nat Med* 9: 685–693.
 48. Simon-Assmann P, Orend G, Mammadova-Bach E, Spenle C, Lefebvre O (2011) Role of laminins in physiological and pathological angiogenesis. *Int J Dev Biol* 55: 455–465.
 49. Astrof S, Hynes RO (2009) Fibronectins in vascular morphogenesis. *Angiogenesis* 12: 165–175.
 50. Poschl E, Schlotzer-Schrehardt U, Brachvogel B, Saito K, Ninomiya Y, et al. (2004) Collagen IV is essential for basement membrane stability but dispensable for initiation of its assembly during early development. *Development* 131: 1619–1628.
 51. Favor J, Gloeckner CJ, Janik D, Klempt M, Neuhauser-Klaus A, et al. (2007) Type IV procollagen missense mutations associated with defects of the eye, vascular stability, the brain, kidney function and embryonic or postnatal viability in the mouse, *Mus musculus*: an extension of the Col4a1 allelic series and the identification of the first two Col4a2 mutant alleles. *Genetics* 175: 725–736.
 52. Nguyen TQ, Roestenberg P, van Nieuwenhoven FA, Bovenschen N, Li Z, et al. (2008) CTGF inhibits BMP-7 signaling in diabetic nephropathy. *J Am Soc Nephrol* 19: 2098–2107.
 53. Kuiper EJ, van Zijderveld R, Roestenberg P, Lyons KM, Goldschmeding R, et al. (2008) Connective tissue growth factor is necessary for retinal capillary basal lamina thickening in diabetic mice. *J Histochem Cytochem* 56: 785–792.
 54. Kale S, Hanai J, Chan B, Karihaloo A, Grotendorst G, et al. (2005) Microarray analysis of in vitro pericyte differentiation reveals an angiogenic program of gene expression. *FASEB J* 19: 270–271.
 55. Schmeller M, Vuori K, Ruoslahti E (1997) Alphavbeta3 integrin associates with activated insulin and PDGFbeta receptors and potentiates the biological activity of PDGF. *EMBO J* 16: 5600–5607.
 56. Jones PL, Crack J, Rabinovitch M (1997) Regulation of tenascin-C, a vascular smooth muscle cell survival factor that interacts with the alpha v beta 3 integrin to promote epidermal growth factor receptor phosphorylation and growth. *J Cell Biol* 139: 279–293.
 57. Chen J, Somanath PR, Razorenova O, Chen WS, Hay N, et al. (2005) Akt1 regulates pathological angiogenesis, vascular maturation and permeability in vivo. *Nat Med* 11: 1188–1196.
 58. Yoshida K, Munakata H (2007) Connective tissue growth factor binds to fibronectin through the type I repeat modules and enhances the affinity of fibronectin to fibrin. *Biochim Biophys Acta* 1770: 672–680.
 59. Chen Y, Abraham DJ, Shi-Wen X, Pearson JD, Black CM, et al. (2004) CCN2 (connective tissue growth factor) promotes fibroblast adhesion to fibronectin. *Mol Biol Cell* 15: 5635–5646.
 60. Yokoi H, Mukoyama M, Sugawara A, Mori K, Nagae T, et al. (2002) Role of connective tissue growth factor in fibronectin expression and tubulointerstitial fibrosis. *Am J Physiol Renal Physiol* 282: F933–942.
 61. Guha M, Xu ZG, Tung D, Lanting L, Natarajan R (2007) Specific down-regulation of connective tissue growth factor attenuates progression of nephropathy in mouse models of type 1 and type 2 diabetes. *FASEB J* 21: 3355–3368.
 62. Arnott JA, Nuglozeh E, Rico MC, Arango-Hisijara I, Odgren PR, et al. (2007) Connective tissue growth factor (CTGF/CCN2) is a downstream mediator for TGF-beta1-induced extracellular matrix production in osteoblasts. *J Cell Physiol* 210: 843–852.
 63. Sonnylal S, Shi-Wen X, Leoni P, Naff K, Van Pelt CS, et al. (2010) Selective expression of connective tissue growth factor in fibroblasts in vivo promotes systemic tissue fibrosis. *Arthritis Rheum* 62: 1523–1532.
 64. Brigstock DR (2002) Regulation of angiogenesis and endothelial cell function by connective tissue growth factor (CTGF) and cysteine-rich 61 (CYR61). *Angiogenesis* 5: 153–165.
 65. Mo FE, Muntean AG, Chen CC, Stolz DB, Watkins SC, et al. (2002) CYR61 (CCN1) is essential for placental development and vascular integrity. *Mol Cell Biol* 22: 8709–8720.
 66. Brugger SM, Merrill AE, Torres-Vazquez J, Wu N, Ting MC, et al. (2004) A phylogenetically conserved cis-regulatory module in the *Msx2* promoter is sufficient for BMP-dependent transcription in murine and *Drosophila* embryos. *Development* 131: 5153–5165.
 67. Daneman R, Zhou L, Kebede AA, Barres BA (2010) Pericytes are required for blood-brain barrier integrity during embryogenesis. *Nature* 468: 562–566.
 68. Matsui T, Kanai-Azuma M, Hara K, Matoba S, Hiramatsu R, et al. (2006) Redundant roles of Sox17 and Sox18 in postnatal angiogenesis in mice. *J Cell Sci* 119: 3513–3526.
 69. Basciani S, Mariani S, Arizzi M, Ullisse S, Rucci N, et al. (2002) Expression of platelet-derived growth factor-A (PDGF-A), PDGF-B, and PDGF receptor-alpha and -beta during human testicular development and disease. *J Clin Endocrinol Metab* 87: 2310–2319.
 70. Van Handel B, Prasad SL, Hassanzadeh-Kiabi N, Huang A, Magnusson M, et al. (2010) The first trimester human placenta is a site for terminal maturation of primitive erythroid cells. *Blood* 116: 3321–3330.
 71. Choi J, Mouillesseaux K, Wang Z, Fiji HD, Kinderman SS, et al. (2011) Apolipoprotein B targets the HMG-CoA reductase pathway and differentially regulates arteriovenous angiogenesis. *Development* 138: 1173–1181.
 72. Chien W, O'Kelly J, Lu D, Leiter A, Sohn J, et al. (2011) Expression of connective tissue growth factor (CTGF/CCN2) in breast cancer cells is associated with increased migration and angiogenesis. *Int J Oncol* 38: 1741–1747.

A.2 Hypoxia-inducible Factor (HIF)-1 α and CCN2 form a regulatory circuit in hypoxic nucleus pulposus cells

I collected the data for Figure 9G and 9H as well as helped replicate some of the other histology data in Figure 9.

Hypoxia-inducible Factor (HIF)-1 α and CCN2 Form a Regulatory Circuit in Hypoxic Nucleus Pulposus Cells

CCN2 SUPPRESSES HIF-1 α LEVEL AND TRANSCRIPTIONAL ACTIVITY*

Received for publication, December 26, 2012, and in revised form, March 20, 2013. Published, JBC Papers in Press, March 24, 2013, DOI 10.1074/jbc.M112.448860

Cassie M. Tran^{†1}, Nobuyuki Fujita^{‡5}, Bau-Lin Huang^{¶2}, Jessica R. Ong[¶], Karen M. Lyons[¶], Irving M. Shapiro[‡], and Makarand V. Risbud^{‡3}

From the [†]Department of Orthopaedic Surgery and Graduate Program in Cell and Developmental Biology, Thomas Jefferson University, Philadelphia, Pennsylvania 19107, the [‡]Department of Orthopaedic Surgery, Keio University School of Medicine, Tokyo, Japan 108-8345, and the [¶]Departments of Molecular, Cell and Developmental Biology, and Orthopaedic Surgery, University of California, Los Angeles, Los Angeles, California 90024

Background: The relationship between connective tissue growth factor (CCN2) and hypoxia-inducible factor (HIF)-1 in hypoxic nucleus pulposus is unknown.

Results: HIF-1 α suppresses CCN2 expression, whereas CCN2 represses basal HIF-1 α levels and transcriptional activity.

Conclusion: In nucleus pulposus, HIF-1 α and CCN2 form a negative regulatory circuit.

Significance: Tight control of CCN2 and HIF-1 activities may play a role in disc homeostasis.

The objective of the study was to investigate if hypoxia-inducible factor (HIF)-1 α and connective tissue growth factor (CCN2) form a regulatory network in hypoxic nucleus pulposus (NP) cells. A decrease in CCN2 expression and proximal promoter activity was observed in NP cells after hypoxic culture. Analysis of both human and mouse CCN2 promoters using the JASPAR core database revealed the presence of putative hypoxia response elements. Transfection experiments showed that both promoter activities and CCN2 expression decreases in hypoxia in a HIF-1 α -dependent fashion. Interestingly, deletion analysis and mutation of the hypoxia responsive elements individually or in combination resulted in no change in promoter activity in response to hypoxia or in response to HIF-1 α , suggesting an indirect mode of regulation. Notably, silencing of endogenous CCN2 increased HIF-1 α levels and its target gene expression, suggesting a role for CCN2 in controlling basal HIF-1 α levels. On the other hand, treatment of cells with rCCN2 resulted in a decrease in the ability of HIF-1 α transactivating domain to recruit co-activators and diminished target gene expression. Last, knockdown of CCN2 in NP cells results in a significant decrease in GAG synthesis and expression of *AGGRECAN* and *COLLAGEN II*. Immunohistochemical staining of intervertebral discs of Ccn2 null embryos shows a decrease in aggrecan. These findings reveal a negative feedback loop between CCN2 and HIF-1 α in NP cells and demonstrate a role for CCN2 in maintaining matrix homeostasis in this tissue.

The intervertebral disc is a unique tissue that separates adjoining vertebrae and helps to accommodate biomechanical

forces on the spine. Cartilagenous end plates form its superior and inferior boundaries, whereas between these end plates a ligamentous annulus fibrosus circumferentially surrounds the proteoglycan-rich nucleus pulposus. Nutrients and oxygen reach the nucleus pulposus through diffusion from blood vessels that infiltrate only the outer annulus and end plate cartilage, resulting in the characteristically hypoxic microenvironment (1–3).

Nucleus pulposus cells have adapted to survive in this hypoxic niche through robust expression of hypoxia inducible factor (HIF-1 α),⁴ a transcription factor responsive to local oxygen tension (4). HIF is a basic helix-loop-helix transcription factor comprising a constitutively expressed β subunit and an α subunit that undergoes degradation by both oxygen-dependent and -independent pathways (5, 6). When stabilized, the α subunit dimerizes with the β subunit and binds to hypoxia response elements (HREs) in the promoter of target genes. In the disc, HIF-1 α is critical for maintenance of nucleus pulposus cell survival, glycolytic metabolism, and functional activities including proteoglycan matrix synthesis (7–11).

Connective tissue growth factor (CCN2/CTGF) is a member of the CCN family of proteins that plays an important role in chondrogenesis and angiogenesis, where it regulates cell proliferation and migration, as well as extracellular matrix production (12–18). Signaling through integrins and other cell surface receptors, CCN proteins function to modulate growth factor activity in response to a plethora of stimuli, including oxygen tension and mechanical force (16, 17, 19–24). Mice null for Ccn2 die immediately after birth due to severe skeletal and cartilage dysplasia, indicating its importance in development (13). In a pathological context, hypoxia induces CCN2 expression in a number of cell types, including fibroblasts and lung and pancreatic adenocarcinoma, where it is associated with

* This work was supported, in whole or in part, by National Institutes of Health Grants AR050087 and AR055655 (to M. R.) and AR052686 (to K. M. L.).

¹ Supported by National Institute on Aging Grant F31AG038125.

² Present address: Cancer and Developmental Biology Laboratory, National Cancer Institute, Frederick, MD.

³ To whom correspondence should be addressed: 1025 Walnut St., Suite 511 College Bldg., Thomas Jefferson University, Philadelphia, PA 19107. Tel.: 215-955-1063; Fax: 215-955-9159; E-mail: makarand.risbud@jefferson.edu.

⁴ The abbreviations used are: HIF-1 α , hypoxia inducible factor-1 α ; CCN2, connective tissue growth factor; HRE, hypoxia response element; DMOG, dimethyl oxalylglycine; TAD, transactivation domain.

Cross-talk between HIF-1 α and CCN2 in the Nucleus Pulposus

enhanced fibrosis and tumor growth (22, 25–28). On the other hand, in a tubular epithelial cell line, CCN2 expression is shown to decrease with hypoxia, underlying the cell type specificity of CCN2 regulation and function in response to hypoxia (30). In contrast, little information is available on the role of CCN2 in regulating HIF-1 α expression (24, 31).

In the context of the disc, CCN2 has been shown to stimulate extracellular matrix production by nucleus pulposus cells (32). However, little is known about the regulation of CCN in the nucleus pulposus under normal and pathological conditions. CCN2 may play a role in the development of the notochord in zebrafish, the embryonic anlagen of the intervertebral disc (33), but a similar effect on the notochord is not seen in mice lacking CCN2 (13). We have observed increasing levels of CCN2 in the degenerate nucleus pulposus and have identified TGF- β as an important regulator of its expression. However, it is yet to be determined if CCN2 expression is controlled by hypoxia in the disc (23). Resolution of this question is important because CCN2 is a major target and regulator of hypoxic pathways in many pathological conditions. Thus, the objective of this investigation is to determine whether CCN2 expression in nucleus pulposus cells is regulated by hypoxia and HIF-1 α and if CCN2, in turn, regulates HIF-1 α . Results of the study show that in nucleus pulposus cells hypoxia decreases CCN2 expression through HIF-1 α and that CCN2 suppresses HIF-1 α activity.

MATERIALS AND METHODS

Plasmids and Reagents—Human CCN2 promoter plasmids were obtained from Dr. George Yang, Stanford University, and the mouse Ccn2 promoter plasmids were as described previously (34). Expression plasmids were provided by Dr. Celeste Simon, University of Pennsylvania (pCA-HIF-2 α with a triple mutation (P405A/P530A/N851A)) and Dr. Eric Huang, National Cancer Research Institute, Bethesda (pARNT). siHIF-1 α (PBS/pU6-HIF1 α) (number 21103) developed by Dr. Connie Cepko, HA-HIF1 α P402A/P564A-pcDNA3 (number 18955) by William Kaelin, HRE-Luc (number 26731) by Navdeep Chandeland, and psPAX2 (number 12260) and pMD2.G (number 12259) by Didier Trono were obtained from Addgene. Lentiviral shHIF-1 α that co-expresses YFP was a gift Dr. Andree Yeremian, University of Lleida, Spain, and pre-validated pLKO.1Sh-CCN2 (TRC#0000061951) was purchased from Sigma. For transactivation studies of HIF-1, the binary Gal4 reporter plasmids (N+C TAD, amino acids 530–826; N-TAD, amino acids 530–778; and C-TAD, amino acids 740–826) were provided by Dr. Nianli Sang. Backbone plasmid pM (Clontech) contains no transactivation domain (TAD) but expresses the Gal4DBD. pFR-Luc (Stratagene) reporter contains the yeast Gal4-binding site upstream of a minimal promoter and the firefly luciferase gene. pRL-TK (Promega) containing the *Renilla reniformis* luciferase gene was used as an internal transfection control. The amount of transfected plasmid, the pre-transfection period after seeding, and the post-transfection period before harvesting have been previously optimized for rat nucleus pulposus cells using pSV β -galactosidase plasmid (Promega) (7).

Isolation of Nucleus Pulposus Cells and Treatments of Cells—Rat nucleus pulposus cells were isolated using a method

reported earlier by Risbud *et al.* (7). Nucleus pulposus cells were maintained in Dulbecco's modified Eagle's medium (DMEM) and 10% fetal bovine serum (FBS) supplemented with antibiotics. Cells were cultured in a Hypoxia Work Station (Invivo2 300, Ruskin, UK) with a mixture of 1% O₂, 5% CO₂, and 94% N₂ for 8 to 24 h. In some experiments, cells were treated with CCN2 (100 ng/ml, Prospec, Israel), TGF- β 1 (10 ng/ml, Peptrotech, NJ), or 1 mM dimethyl oxalylglycine (DMOG).

Real Time RT-PCR Analysis—Total RNA was extracted from nucleus pulposus cells using RNeasy mini columns (Qiagen). Before elution from the column, RNA was treated with RNase-free DNase I (Qiagen). The purified, DNA-free RNA was converted to cDNA using Superscript III Reverse Transcriptase (Invitrogen). Template cDNA and gene-specific primers were added to the SYBR Green master mixture (Applied Biosystems) and mRNA expression was quantified using the Step One Plus Real-time PCR System (Applied Biosystems). *Hprt1* and β -*ACTIN* were used to normalize gene expression. Melting curves were analyzed to verify the specificity of the RT-PCR and the absence of primer dimer formation. Each sample was analyzed in duplicate and included a template-free control. All primers used were synthesized by Integrated DNA Technologies, Inc. (Coralville, IA).

Western Blotting—Cells were placed on ice immediately following treatment and washed with ice-cold Hanks' balanced salt solution. All wash buffers and final re-suspension buffer included 1 \times protease inhibitor mixture (Roche Applied Science), NaF (5 mM), and Na₃VO₄ (200 μ M). Total cell proteins were resolved on 8–12% SDS-polyacrylamide gels and transferred by electroblotting to polyvinylidene difluoride membranes (Bio-Rad). The membranes were blocked with 5% nonfat dry milk in TBST (50 mM Tris, pH 7.6, 150 mM NaCl, 0.1% Tween 20) and incubated overnight at 4 °C in 3% nonfat dry milk in TBST with the anti-CCN2 (1:900, Santa Cruz), anti-HIF-1 α (1:1000, R&D Systems), or anti- β -tubulin antibody (1:2000, Developmental Studies Hybridoma Bank). Immunolabeling was detected using the ECL reagent (Amersham Biosciences).

Immunofluorescence Microscopy—Cells were plated in flat bottom 96-well plates (4 \times 10³/well) and cultured in hypoxia for 4–24 h. After incubation, cells were fixed with 4% paraformaldehyde, permeabilized with 0.2% Triton X-100 in PBS for 10 min, blocked with phosphate buffered saline containing 5% FBS, and incubated with antibodies against CCN2 (1:200) (Abcam) at 4 °C overnight. As a negative control, cells were reacted with isotype IgG under similar conditions. After washing, the cells were incubated with Alexa Fluor-488-conjugated anti-mouse secondary antibody (Invitrogen), at a dilution of 1:50 for 45 min at room temperature. Cells were imaged using a laser scanning confocal microscope (Olympus Fluoview, Japan).

Transfections and Dual Luciferase Assay—Cells were transferred to 24-well plates at a density of 4 \times 10⁴ cells/well 1 day before transfection. To measure the effect of hypoxia, cells were transfected with 500 ng of CCN2 reporter plasmids and 500 ng of pRL-TK plasmid. To investigate the effect of HIF- α on CCN2 promoter activity, cells were co-transfected with 100–300 ng of CA-HIF-1 α , CA-HIF-2 α , siHIF-1 α , shHIF-2 α or the respective

Cross-talk between HIF-1 α and CCN2 in the Nucleus Pulposus

backbone vector along with 400 ng of *CCN2* reporter and 300 ng of pRL-TK plasmid. Lipofectamine 2000 (Invitrogen) was used as the transfection reagent; for each transfection, plasmids were premixed with transfection reagent. The next day, the cells were harvested and a Dual-LuciferaseTM reporter assay system (Promega) was used for sequential measurements of firefly and *Renilla* luciferase activities. Quantification of luciferase activities and calculation of relative ratios were carried out using a luminometer (TD-20/20, Turner Designs, CA). At least three independent transfections were performed, and all analyses were carried out in triplicate.

Site-directed Mutagenesis—Site-directed mutagenesis of the human and mouse *CCN2* promoters was performed according to the manufacturer's protocol using the In-Fusion HD Cloning Kit (Clontech). Primers used for human *CCN2* promoter mutants with mutated HRE sites underlined are: HRE MT1 F, 5'-AGAGA-ACAAAGCAACGTGTGACTCAGGATGCAGTCTCCTG-3'; HRE MT2 F, 5'-GAAGGGTAGGGCCTTGCAGTGGCAGTCTCACCTAAGGTGG-3'; HRE MT3 F, 5'-CAGGGAAGTC-ATGTGTAGGAGCCATATTCCCATTCTGTT-3'. Primers used for mouse *CCN2* promoter mutants with the mutated HRE site underlined were: HRE MT1 F, 5'-TGGCTTTGAGTTCGAA-TTCCACCAGTATGTTTCCCTGAGAC-3'; HRE MT2 F, 5'-CACACACACACAAAAGCAAAGAGAGACAGAGAGAGA-GAGA-3'. Mutations were verified by sequencing using the Applied Biosystems 3730 DNA Sequencer.

Lentiviral Particle Production and Viral Transduction—HEK 293T cells were seeded in 10-cm plates (1.3×10^6 cells/plate) in DMEM with 10% heat-inactivated FBS 2 days before transfection. Cells were transfected with 2.5 μ g of pLKO.1-Ctr, shHIF-1 α , or shCCN2 plasmids along with 1.875 μ g of psPAX2 and 0.625 μ g of pMD2.G. After 16 h, transfection media was removed and replaced with DMEM with 5% heat-inactivated FBS and penicillin-streptomycin. Lentiviral particles were harvested at 48 and 60 h post-transfection. Nucleus pulposus cells were plated in DMEM with 5% heat-inactivated FBS 1 day before transduction. Cells in 10-cm plates were transduced with 5 ml of conditioned media containing viral particles along with 6 μ g/ml of Polybrene. After 24 h, conditioned media was removed and replaced with DMEM, 5% heat-inactivated FBS. Cells were harvested for protein extraction 5 days after viral transduction.

Dimethylmethylene Blue Assay—The proteoglycan content of conditioned media was measured as sulfated glycosaminoglycan by colorimetric assay with 1,9-dimethylmethylene blue (Blyscan, Biolor Ltd., Carrickfergus, UK) with chondroitin-4-sulfate as a standard following the manufacturer's instructions. GAGs were precipitated from conditioned media and stained with dimethylmethylene blue and staining was quantified by measuring absorbance at 656 nm. Results were calculated as GAG (μ g)/total DNA (ng) and expressed relative to the value obtained for untreated controls.

Immunohistochemistry of Disc Tissue—Paraffin-embedded sections of wild type and mutant mice were boiled for 15 min in citrate buffer to reverse cross-links and unmask epitopes. Sections were blocked with 5% goat serum for 1 h and incubated with anti-CCN2 (CCN2) (Abcam, Cambridge MA) or anti-aggrexin (Millipore, Danvers, MA) at a dilution of 1:250 over-

night at 4 °C. The following day sections were incubated with secondary antibody (Alexa Fluor 555 or 488 goat anti-rabbit, Invitrogen) for 1 h at room temperature. Sections were counterstained with DAPI (Vectashield, Vector Laboratories, Burlingame, CA). FAST staining was performed as described by Leung *et al.* (35).

Statistical Analysis—All measurements were performed in triplicate, data are presented as mean \pm S.E. Differences between groups were analyzed by the Student's *t* test; *, *p* < 0.05.

RESULTS

Hypoxia Decreases CCN2 Expression in Nucleus Pulposus Cells—Nucleus pulposus cells were cultured in hypoxia (1% O₂) and expression of *Ccn2* was analyzed using real time RT-PCR. Fig. 1A shows that hypoxia results in a significant decrease in *Ccn2* mRNA expression in nucleus pulposus cells. Western blot analysis of cellular lysates and secreted protein in conditioned media shows that *Ccn2* levels are decreased by hypoxia as well (Fig. 1B). Densitometric analysis of Western blot experiments confirmed a significant decrease in both cellular and secreted CCN2 in hypoxia (Fig. 1, C and D). Immunofluorescence microscopy of cells cultured in hypoxia for 24 h confirmed that there is a decrease in CCN2 levels compared with normoxic controls (Fig. 1E).

CCN2 Promoter Contains Conserved HREs—To investigate the mechanism of transcriptional regulation of *CCN2* by hypoxia, we examined the response of both human and mouse *CCN2* promoters to 1% O₂. First, using the Evolutionarily Conserved Region Browser and UCSC genome browser, we observed that the first 5 kb of the *CCN2* promoter is highly conserved between several vertebrate species including human, mouse, and rat (Fig. 2A). Next, we scanned the first 5 kb of the human *CCN2* promoter for the presence of HREs using the JASPAR core database (36). Previous studies have experimentally validated two functional HREs within the first 5 kb of the mouse *Ccn2* promoter; thus, the profile score threshold used was first optimized by analyzing the mouse promoter sequence in JASPAR as a positive control (22). At an 85% profile score threshold, the JASPAR database returned three putative HRE sites at -640/-634, -2210/-2006, and -2264/-2258 bp on the human *CCN2* promoter, whose specific sequences are shown in bold in Fig. 2B. The HREs in the mouse *Ccn2* promoter, however, are not conserved in location in the human promoter and vice versa, as verified by the Multiz alignment (Fig. 2B).

Hypoxia and HIF Regulation of CCN2 Promoter Activity—We then used plasmids containing either the human or mouse *CCN2* promoter driving luciferase expression to measure the effect of hypoxia on promoter activity in nucleus pulposus cells (Fig. 3, A and B). Fig. 3, C and D, shows that hypoxia significantly decreases the activity of the human and mouse *CCN2* promoter fragments. Serial deletion analysis of the mouse *Ccn2* promoter showed that activity of smaller promoter fragments including a 0.5-kb reporter that lacked HREs is suppressed by hypoxia (Fig. 3D). To test the hypothesis that HIFs were involved in mediating the hypoxia-induced decrease in promoter activity we performed loss- and gain-of-function exper-

Cross-talk between HIF-1 α and CCN2 in the Nucleus Pulposus

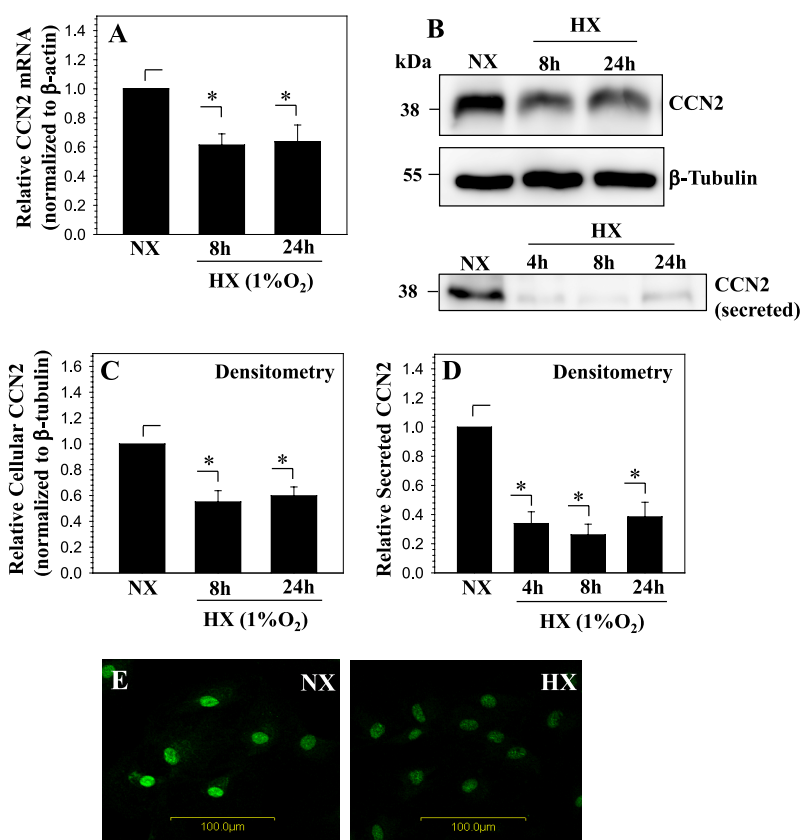


FIGURE 1. Hypoxia decreases CCN2 expression in nucleus pulposus cells. *A*, real time RT-PCR analysis of *CCN2* expression by nucleus pulposus cells cultured in hypoxia (HX) for 8 and 24 h. *CCN2* expression decreases with hypoxia. *B*, Western blot analysis shows a decrease in both cellular and secreted CCN2 in nucleus pulposus cells cultured in hypoxia up to 24 h. *C* and *D*, densitometric analysis of three independent experiments described in *B* confirms a significant decline in levels of cellular (*C*) and secreted (*D*) CCN2 in hypoxia. *E*, immunofluorescent analysis of CCN2 expression in nucleus pulposus cells cultured in hypoxia for 24 h, CCN2 staining decreases in hypoxia. Magnification $\times 20$. Values shown are mean \pm S.E. from three independent experiments, *, $p < 0.05$. NX, normoxia.

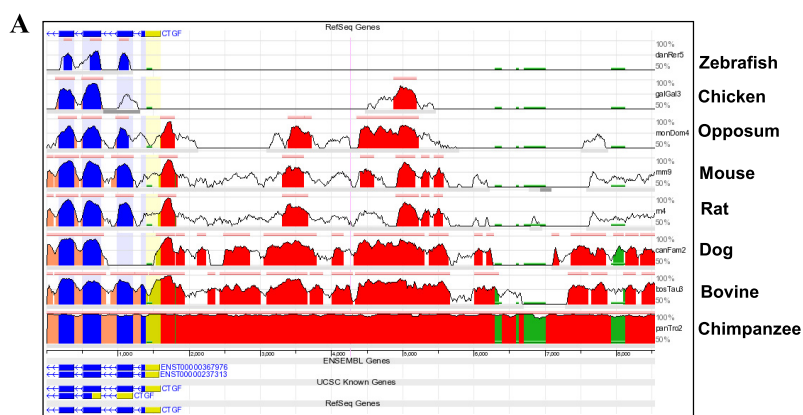
iments by co-transfecting cells with siHIF- α plasmid. Both human and mouse promoters show an increase in promoter activity in the presence of siHIF-1 α (Fig. 3*E*). Similarly, overexpression of HIF-1 α or HIF-2 α strongly suppresses the activity of both human and mouse *CCN2* promoters (Fig. 3, *F* and *G*).

HIF-1 Suppresses CCN2 Promoter Activity Independent of HREs—To further examine if the HREs are necessary for promoter regulation by hypoxia, we performed site-directed mutagenesis to mutate HREs individually or in combination. Fig. 4*A* shows a schematic of the wild type and mutant human *CCN2* promoter constructs. Cells were transfected with these constructs and luciferase activity was measured following a 24-h culture in hypoxia (Fig. 4*B*) or co-transfection with HIF-1 α (Fig. 4*C*). Results show that neither individual nor any combination of HRE mutations cause a difference in response to hypoxia or HIF-1 α overexpression compared with the wild type promoter (Fig. 4, *B* and *C*). We also mutated mouse *Ccn2* promoter constructs (Fig. 4*D*) and similarly observed hypoxic suppression of the wild type and mutant reporters (Fig. 4*E*). Additionally, overexpression of HIF-1 α caused a decrease in promoter activity despite the mutation of one or both of the HREs, indicating HRE independent regulation of the promoter activity by HIF-1 α (Fig. 4*F*). To delineate the possible mecha-

nisms of this indirect regulation of *CCN2* expression by hypoxia and HIF-1, we examined if hypoxia decreases the responsiveness of nucleus pulposus cells to TGF- β , an autocrine factor that maintains the *CCN2* expression levels in these cells (23). Our results clearly show that hypoxia diminishes the effect of TGF- β on *CCN2* expression by NP cells (Fig. 4, *G* and *H*). We then measured the activity of a wild type or *CCN2* reporter containing a mutation in the Smad binding element (Fig. 4*I*) following co-transfection with HIF-1 α . It is noteworthy that the activity of both the reporters was strongly suppressed by HIF-1 α (Fig. 4*J*).

HIF-1 α Is a Negative Regulator of CCN2 Expression in Nucleus Pulposus Cells—To confirm the involvement of HIF-1 α in hypoxic regulation of *CCN2* expression, we performed HIF-1 α loss-of-function studies. First, HIF-1 α was stably knocked down in nucleus pulposus cells using lentiviral transduction of shHIF-1 α . Fig. 5*A* shows the robust expression of YFP in lentivirus-infected cells, indicating high transduction efficiency. As expected, the mRNA expression of HIF-1 α and its target gene, *GAPDH*, is significantly decreased following shHIF-1 α expression (Fig. 5*B*). Correspondingly, *CCN2* mRNA expression is significantly increased in HIF-1 α -silenced cells (Fig. 5*C*). Interestingly, we found that *CCN3* mRNA expression

Cross-talk between HIF-1 α and CCN2 in the Nucleus Pulposus



B Multiz Alignment of HRE in the CCN2 promoter:

HRE 1 (-634/-640bp):

Human ... A G A C G C G T G...
 Rhesus ... A G C C*G G G T C...
 Dog ... A G C C*G G G T C ...
 Mouse ... G - - - - -

HRE2 (-2006/-2010 bp):

Human ... G G A T G T G C A...
 Rhesus ... G G A T G T G C A...
 Dog ... G G A T G T G A A...
 Mouse ... G G A A G G G A A...

HRE 3 (-2258/-2264 bp):

Human ... T C A C A C G T A G...
 Rhesus ... T C A C A C G T A G ...
 Dog ... - - - - A A G T A A...
 Mouse ... T C A C A G A G A G ...

FIGURE 2. **Analysis of human CCN2 promoter for conserved HREs.** A, evolutionarily conserved regions of the CCN2 gene between several vertebrate species, including chimpanzee, bovine, dog, rat, and mouse, are shown using the Evolutionarily Conserved Region (ECR) genome browser. ECR threshold is set at 80%. CCN2 promoter: red, 5' UTR; yellow, exons; blue, introns; peach, transposons; and simple repeats, green. B, Multiz alignment from UCSC genome database of the three HREs located by the JASPAR database in the human CCN2 promoter (HRE1, HRE2, and HRE3). Non-conserved bases are underlined. *, gaps in alignment; -, no alignment.

responded in a reciprocal manner to CCN2 (Fig. 5D). Furthermore, suppression of HIF-1 α protein levels results in a significant increase in both cellular and secreted CCN2 (Fig. 6, A and B). To complement the loss-of-function experiments, we perform gain-of-function studies by treating cells with the prolyl hydroxylase inhibitor DMOG. As expected, this treatment causes an accumulation of HIF-1 α ; there is a simultaneous decline in CCN2 expression. Densitometric analysis of three independent experiments confirms significant induction of HIF-1 α and concomitant decrease in CCN2 protein levels at 4, 8, and 24 h (Fig. 6D).

CCN2 Antagonizes HIF-1 in Nucleus Pulposus Cells—Next, we sought to determine the effect of CCN2 on the regulation of HIF-1 α expression and activity. To suppress endogenous CCN2, cells were transduced with a lentiviral construct expressing shRNA against CCN2 (shCCN2-LV) or shRNA control (Ctr-LV). Real time RT-PCR analysis shows that CCN2 mRNA is decreased with shCCN2-LV transduction (Fig. 7A), whereas mRNA expression of HIF-1 α and its target genes,

ENOLASE 1 and VEGF, increased (Fig. 7, B–D). In contrast to HIF-1 α , HIF-2 α mRNA levels declined in CCN2-silenced cells (Fig. 7B). Western blot analysis was then used to follow changes at the protein level. Results show that CCN2 levels are significantly decreased in shCCN2-LV-transduced cells (Fig. 7, E and F). Moreover, in agreement to changes in mRNA expression, HIF-1 α protein levels increased in CCN2-silenced cells (Fig. 7, E and F).

Next, we treated cells with recombinant CCN2 to examine if endogenous HIF-1 α activity and expression is affected in a corresponding manner. Treatment with recombinant CCN2 for 24 h results in a significant decrease in HRE reporter activity (Fig. 8A). We then examined the expression of HIF-1 α target genes, VEGF and ENOLASE 1, in response to CCN2 treatment and found that the expression of both genes is significantly decreased (Fig. 8B). Interestingly, Western blot and corresponding densitometric analysis showed that HIF-1 α protein expression is not significantly affected by CCN2 treatment (Fig. 8, C and D). Next, we examined the mechanism by which CCN2

Cross-talk between HIF-1 α and CCN2 in the Nucleus Pulposus

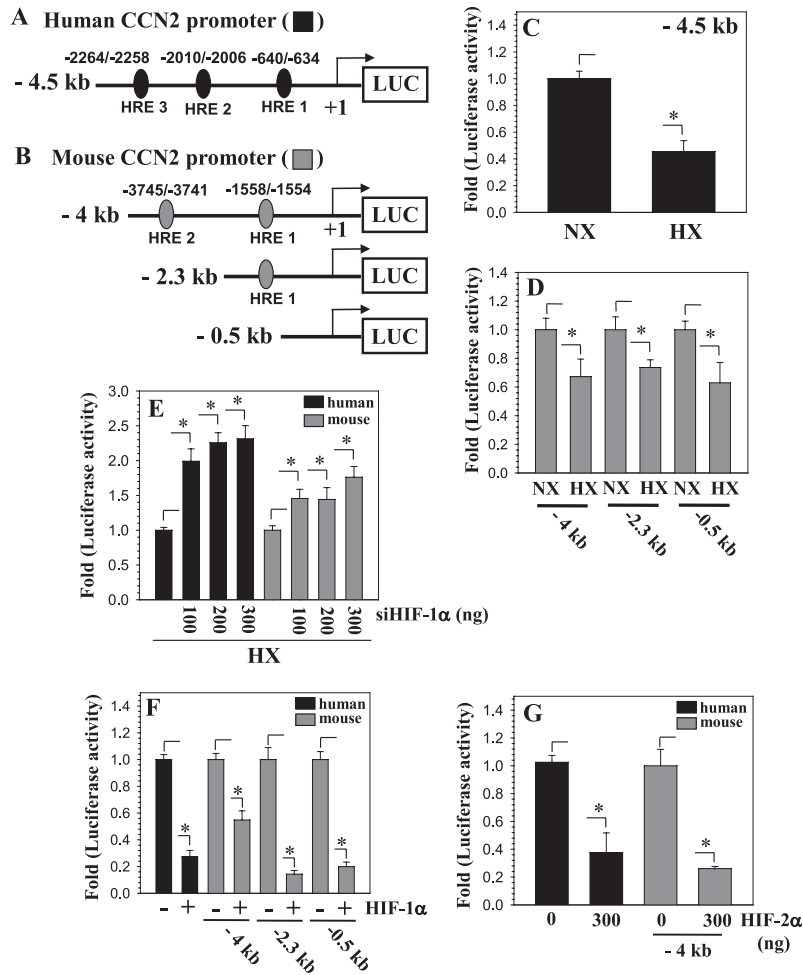


FIGURE 3. Hypoxia and HIF regulation of CCN2 promoter activity. A and B, schematic of human CCN2 promoter construct with putative HRE at -640/-634, -2010/-2006, and -2264/-2258 bp (A) and of mouse Ccn2 promoter constructs with HRE at -3745/-3741 and -1558/-1554 bp (B). C and D, NP cells transfected with human or mouse Ccn2 promoter constructs and activity were measured following a 24-h culture in hypoxia (black and gray bars, respectively). Activity of both human (C) and mouse (D) CCN2 reporters was decreased in hypoxia. E and F, nucleus pulposus cells were co-transfected with siHIF-1 α (E) or shHIF-2 α (F) and CCN2 reporter activities were measured in hypoxia. Both human and mouse CCN2 promoter activities increased with siHIF-1 α (E). Overexpression of HIF-1 α (F) or HIF-2 α (G) suppressed activities of human and mouse CCN2 promoter. Values shown are mean \pm S.E. from three independent experiments, *, $p < 0.05$. HX, hypoxia; NX, normoxia.

regulates HIF-1 α activity. For this purpose, we tested if CCN2 treatment affects interactions between the transactivation domain of HIF-1 α and its co-activators. Reporter constructs expressing both the N- and C-terminal TAD (Fig. 8E) were transfected into cells and their activity was measured following CCN2 treatment. Fig. 8, F and G, shows that the addition of CCN2 caused a significant decrease in the activity of all HIF-1 α -TAD reporters, indicating a decline in transcriptional activity. As expected the empty Gal4-DBD showed almost undetectable activity that remained unaffected by CCN2 treatment.

Finally, we measured the role of CCN2 in controlling the expression of AGGRECAN and COLLAGEN II, two important extracellular matrix genes for nucleus pulposus cells. Fig. 9, A and B, confirms that the lentiviral shCCN2 efficiently surpasses the level of cellular and secreted CCN2. Results show that the suppression of endogenous CCN2 results in a significant

decrease in AGGRECAN (Fig. 9C) and COLLAGEN II (Fig. 9D) and COLLAGEN I (Fig. 9E) mRNA expression. Moreover, the level of sulfated glycosaminoglycans is significantly declined in CCN2-suppressed cells (Fig. 9F).

CCN2 Promotes Extracellular Matrix Production by Nucleus Pulposus Cells—To support these *in vitro* silencing studies, we measured expression levels of proteoglycans in general and aggrecan in particular in discs of Ccn2 null mice. Fig. 9G shows that Ccn2 is expressed in the nucleus pulposus of the developing intervertebral disc. At E16.5, the nucleus pulposus is present in both WT and Ccn2 null littermates, and there are no obvious differences. However, differences were apparent in E18.5 by safranin-o (Fig. 9H) and FAST staining (Fig. 9I). FAST staining is a multiple dye staining procedure that includes fast green, Alcian blue, safranin-o, and tartrazine, and thus detects collagens and proteoglycans. As shown in Fig. 9, H and I, there

Cross-talk between HIF-1 α and CCN2 in the Nucleus Pulposus

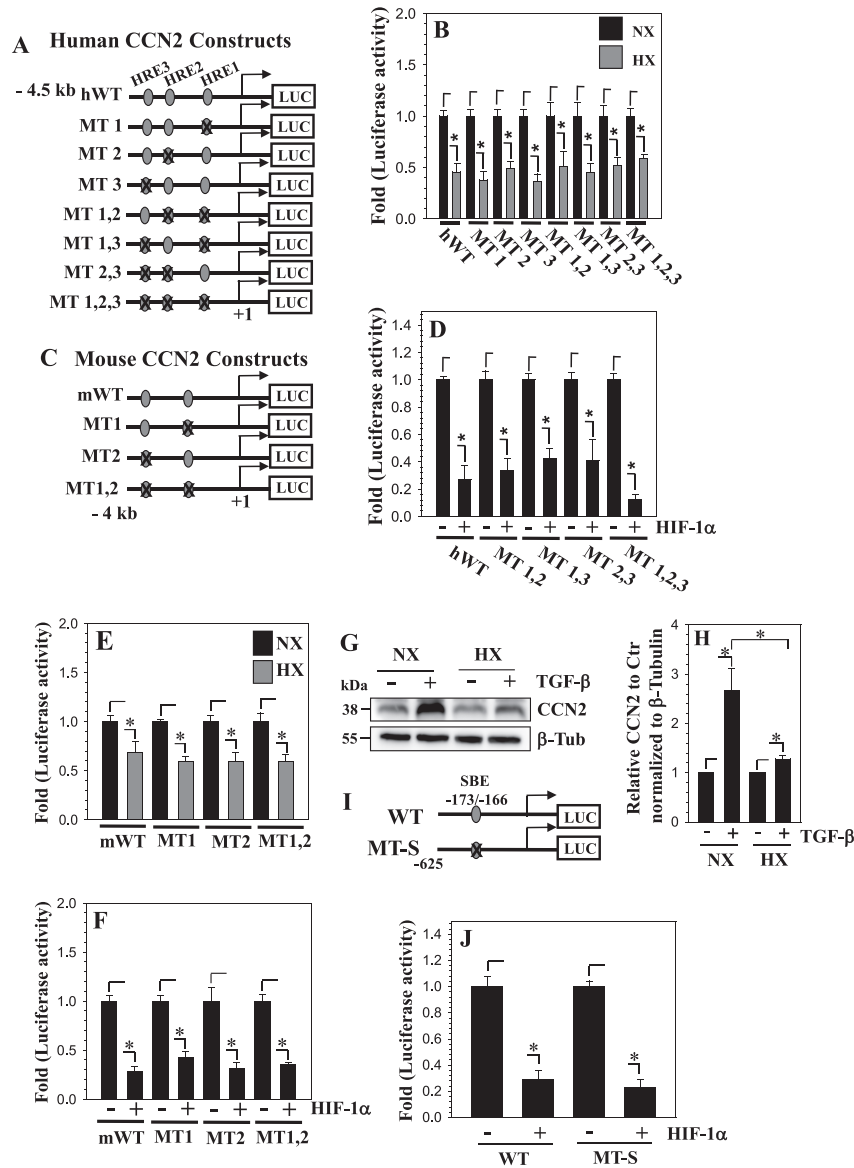


FIGURE 4. HIF-1 suppresses CCN2 promoter activity independent of HREs. *A*, schematic of human *CCN2* promoter constructs with putative HREs located at -640/-632, -2010/-2006, and -2264/-2258 bp. HREs were mutated individually (*MT1*, *MT2*, and *MT3*) or in combination (*MT1,2*; *MT1,3*; and *MT1,2,3*). *B* and *C*, human *CCN2* reporters were transfected into NP cells and cultured under normoxia (black) or hypoxia (gray). Individual HRE mutations or mutations in combination did not change the response of the *CCN2* promoter to hypoxia (*B*) or overexpression of HIF-1 α (*C*) when compared with wild type reporter. *D*, schematic of the mouse *Ccn2* promoter constructs used (WT, wild type; *MT1*, HRE 1 mutant; *MT2*, HRE 2 mutant; *MT1,2*, HRE 1 and 2 double mutant). *E* and *F*, cells were transfected with wild type or mutant promoter constructs and cultured under normoxia (black) or hypoxia (gray). Both hypoxia (*E*) and HIF-1 α overexpression (*F*) decreased activity of WT as well as all the HRE mutant constructs. *G* and *H*, nucleus pulposus cells were treated with TGF- β (10 ng/ml) for 24 h in either normoxia or hypoxia and CCN2 expression was measured by Western blot. *H*, densitometric analysis shows that in hypoxia, a much smaller increase in CCN2 levels by TGF- β was seen compared with normoxia. *I*, schematic of the 625-bp Smad3 wild type (WT) and mutant (MT-S) human CCN2 promoter constructs used in transfection. *J*, activity of Smad3 WT and MT-S construct was measured in nucleus pulposus cells following co-transfection with HIF-1 α . HIF-1 suppressed activity of both the reporters. Values shown are mean \pm S.E. from three independent experiments, *, $p < 0.05$. HX, hypoxia; NX, normoxia.

is a relative paucity of safranin-o-stained proteoglycan in the nucleus pulposus of the mutant. Finally, we examined aggrecan levels by immunofluorescence (Fig. 9J). Consistent with the FAST staining analysis, lower levels of aggrecan are seen in the nucleus pulposus in *Ccn2*^{-/-} mutants. Other details of the phenotypic analysis will be reported elsewhere, but the above

results support the hypothesis that CCN2 is a regulator of aggrecan expression in the nucleus pulposus.

DISCUSSION

The experiments described in this investigation show that hypoxia regulates CCN2 expression through HIF-1 α in nucleus

Cross-talk between HIF-1 α and CCN2 in the Nucleus Pulposus

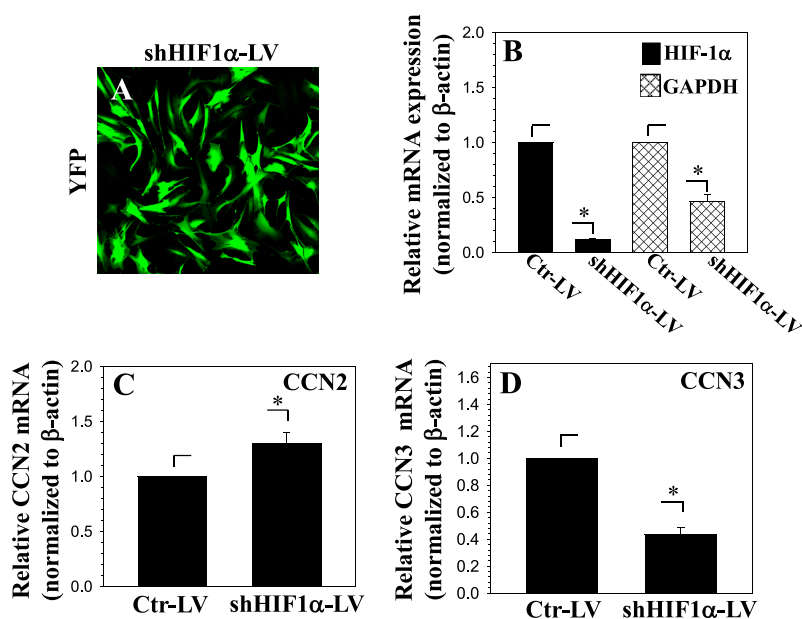


FIGURE 5. **Suppression of HIF-1 α increases CCN2 expression in nucleus pulposus cells.** A, YFP expression by nucleus pulposus cells infected with a lentivirus co-expressing shHIF-1 α and YFP shows high transduction efficiency. B–D, nucleus pulposus cells transduced with shHIF-1 α show significantly decreased mRNA expression of HIF-1 α (black bars) and a corresponding HIF-1 α target gene, GAPDH (hatched bars) (B). Correspondingly, CCN2 expression is significantly increased (C), whereas CCN3 expression is decreased (D). Values shown are mean \pm S.E. from three independent experiments, *, $p < 0.05$.

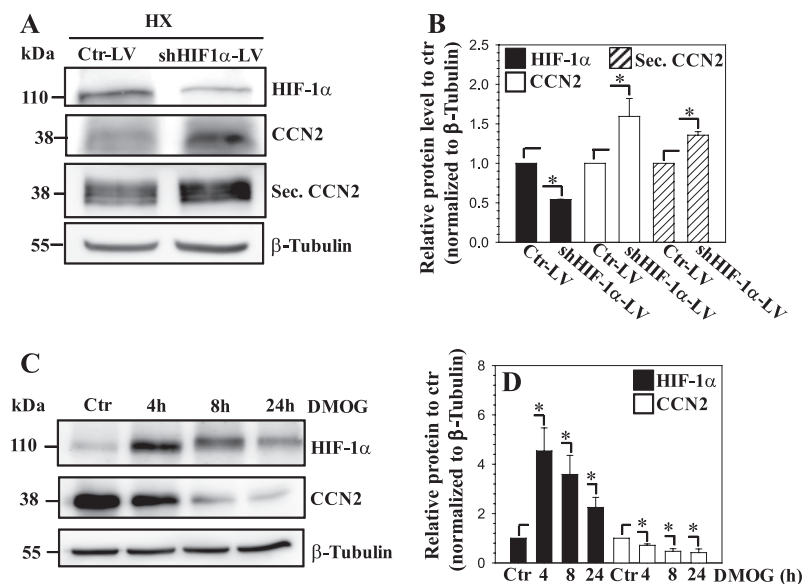


FIGURE 6. **Knockdown of HIF-1 α in nucleus pulposus cells increases CCN2 protein levels.** A and B, Western blot analysis of nucleus pulposus cells transduced with control-shRNA (Ctr-LV) or shHIF-1 α (shHIF-1 α -LV) expressing lentivirus. Cellular and secreted CCN2 levels were increased in HIF-1 α -silenced cells (A). Densitometric analysis of three independent experiments shows that transduction of cells with shHIF-1 α significantly decreases HIF-1 α (black bars), whereas increasing cellular CCN2 (open bars) and secreted CCN2 (diagonally striped bars) levels (B). C, Western blot of cellular lysate of cells treated with DMOG for 4, 8, and 24 h. HIF-1 α shows accumulation at 4, 8, and 24 h, whereas CCN2 expression is correspondingly decreased. D, densitometric analysis of three independent experiments shows that DMOG treatment increases HIF-1 α protein levels (black bars), whereas decreasing CCN2 protein expression (open bars) at all time points. Values shown are mean \pm S.E. from three independent experiments, *, $p < 0.05$.

pulposus cells. We demonstrate that although hypoxia decreases CCN2 expression and promoter activity in a HIF-1 α -dependent manner, direct binding of HIF-1 to HREs in the proximal CCN2 promoter is not required. We also observed that

CCN2 regulates HIF-1 α expression and activity, which may play a role in tissue homeostasis in both normal and degenerate discs.

Initially, we focused on the regulation of CCN2 by hypoxia. We and others have shown that hypoxia is an overriding aspect

Cross-talk between HIF-1 α and CCN2 in the Nucleus Pulposus

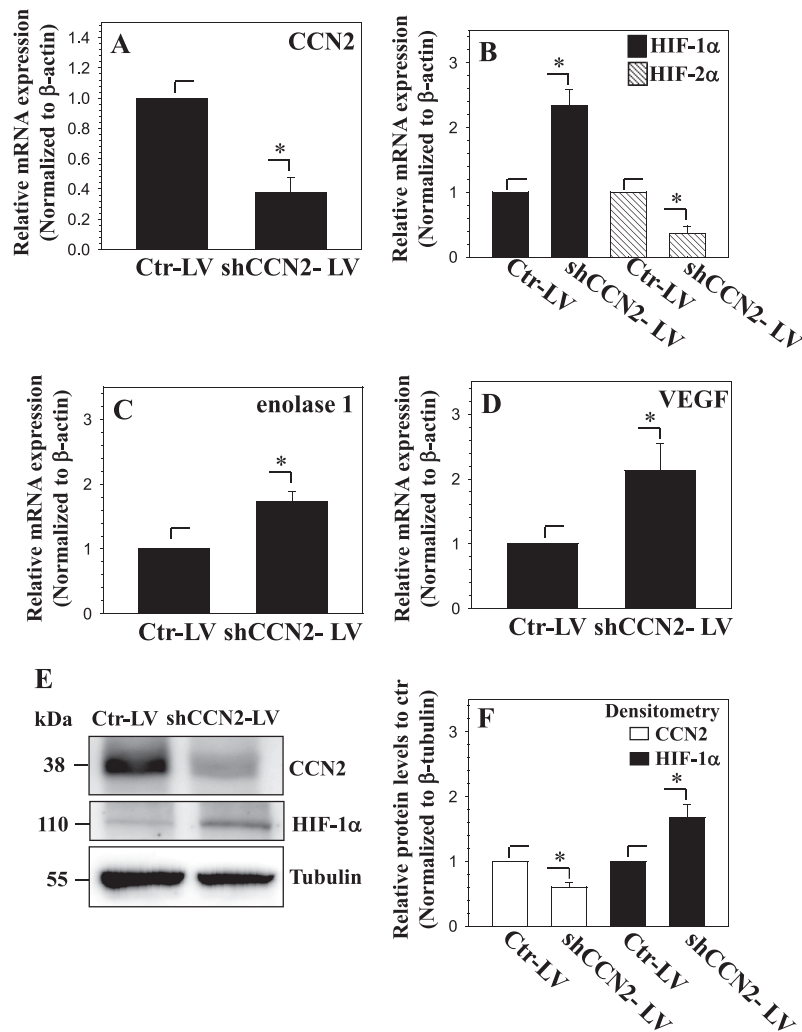


FIGURE 7. Knockdown of CCN2 in nucleus pulposus cells increases HIF-1 α . A–C, real time RT-PCR analysis of cells transduced with control (Ctr-LV) or shCCN2 (shCCN2-LV) expressing lentivirus shows that CCN2 expression is decreased (A). Correspondingly, whereas HIF-1 α expression is increased, that of HIF-2 α is decreased (B). Expression of HIF-1 target genes, *ENOLASE 1* (C) and *VEGF* expression (D), is increased in CCN2-silenced cells. E, Western blot analysis of nucleus pulposus cells transduced with control shRNA (Ctr-LV) or shCCN2 lentivirus (shCCN2-LV). HIF-1 α protein increases with knockdown of CCN2. F, densitometric analysis of three independent experiments shows that transduction of cells with shCCN2 significantly decreases CCN2 expression (open bars), whereas increasing HIF-1 α (black bars). Values shown are mean \pm S.E. from three independent experiments, *, $p < 0.05$.

of disc biology that regulates the expression of important cell survival and matrix genes in this tissue (7–10). Results of this study show that hypoxia decreased *CCN2* transcription and protein levels in nucleus pulposus cells. Interestingly, in HCS-2/8 chondrosarcoma cells that are used to model chondrocyte behavior, hypoxia stabilizes *CCN2* expression (37). Similarly, in several other cell types hypoxia was also shown to increase *CCN2* expression (12, 27, 38); which in turn mediated the downstream effects of pathological hypoxia. Evidence to support the notion that *CCN2* expression must be tightly regulated in tissues is apparent from transgenic mice that overexpress *CCN2*. Mice with two copies of *Col1a2-Ccn2*, which drives expression in fibroblasts, developed accelerated systemic multiorgan fibrosis compared with mice with only one copy of the transgene, which showed a much later onset of fibrosis and

longer lifespan (39). Likewise, increased fibrosis was observed in mice with liver-specific *CCN2* overexpression, but only upon tissue injury. This observation suggests that perhaps induced inflammatory mediators could interact with *CCN2* to promote increased fibrosis or that the inflammatory microenvironment could change the response of cells to *CCN2* (40). This is relevant because *CCN2* levels are elevated during disc degeneration, a condition characterized by tissue inflammation (23). Thus, it is reasonable to assume that whereas *CCN2* is expressed in the developing nucleus pulposus and plays a role in maintenance of normal levels of aggrecan in this hypoxic niche, tight control of *CCN2* expression is necessary to prevent excessive accumulation and to regulate its biological function (18, 23, 32, 34).

We next examined the mechanism by which hypoxia suppresses *CCN2* expression in nucleus pulposus cells. For this

Cross-talk between HIF-1 α and CCN2 in the Nucleus Pulposus

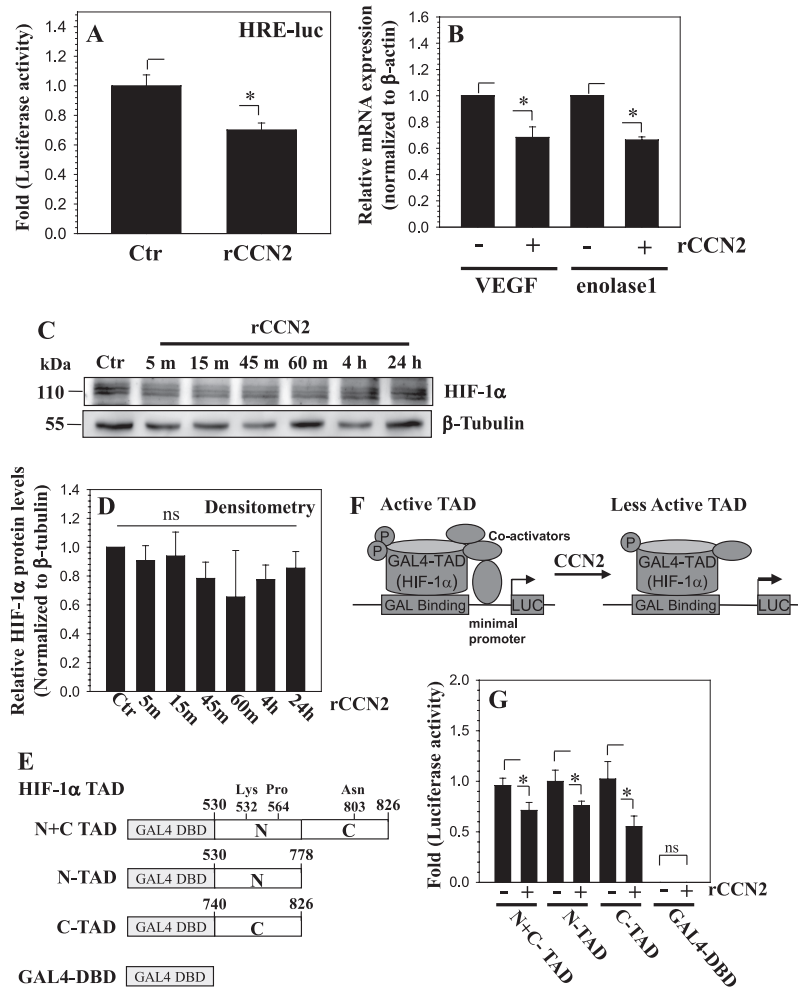


FIGURE 8. CCN2 treatment decreases the activity of HIF-1 α in nucleus pulposus cells. *A*, cells were transfected with a HIF-1 responsive luciferase reporter (HRE-luc) and activity measured following treatment with 100 ng/ml of rCCN2. CCN2 treatment significantly decreases HRE reporter activity. *B*, real time RT-PCR analysis of *VEGF* and *ENOLASE 1* mRNA expression in cells treated with rCCN2. Both *VEGF* and *ENOLASE 1* expression decreases with rCCN2 treatment. *C*, Western blot of HIF-1 α in cells treated with rCCN2 for 5 min to 24 h. HIF-1 α levels were largely unaffected by the treatment. *D*, densitometric analysis of three independent experiments in *C* shows that rCCN2 treatment does not significantly affect HIF-1 α levels. *E*, schematic of TAD constructs used for transactivation studies of HIF-1 α . *F*, schematic summarizing the role of CCN2 in controlling HIF-1 α -TAD activity. *G*, cells were transfected with a Gal4 binary reporter system consisting of Gal4-HIF1 α -TAD (HIF-1 α N+C TAD, amino acids 530–826; N-TAD, amino acids 530–778; and C-TAD, amino acids 740–826) and pFR-Luc reporter and luciferase activity measured following rCCN2 treatment. Gal4DBD (empty vector pM) was used to measure background pFR-Luc activity. rCCN2 decreased the reporter activity indicating a decreased ability of all HIF-1 α -TAD fusion proteins to recruit transcriptional co-activators. Background activity of Gal4DBD was almost undetectable and remained unaffected by CCN2 treatment. Values shown are mean \pm S.E. from three independent experiments, *, $p < 0.05$.

purpose, we chose to examine 4.0-kb proximal promoters of mouse and human *CCN2*. Importantly, studies of transgenic mice in which expression of nuclear-localized lacZ is driven by the 4-kb *CCN2* proximal promoter have shown that this region is sufficient to drive high expression in the nucleus pulposus (34). We found that HIF-1 α overexpression decreased *CCN2* promoter activity, whereas siHIF-1 α relieved hypoxic suppression of promoter activity. Further support for the role of HIF-1 α in controlling *CCN2* expression was forthcoming from loss- and gain-of-function experiments, which clearly showed a reciprocal relationship between HIF-1 α and *CCN2* levels in nucleus pulposus cells. These results were in accordance with previous studies showing the involvement of HIF-1 α in hypoxic regulation of *CCN2* in other cell types (12, 22, 27, 30, 42). Note-

worthy, deletion and mutation analysis showed that the binding of HIF-1 α to HREs contained within the studied promoter was not necessary for hypoxic repression of the activity.

The observation that CCN2 expression was less responsive to TGF- β treatment in hypoxia raised the possibility that hypoxia and HIF-1 may modulate canonical Smad signaling that is critical in maintenance of *CCN2* expression in nucleus pulposus cells (23). Surprisingly, suppressive effects of hypoxia/HIF-1 did not involve interfering with the binding of Smad3 to the *CCN2* promoter. This clearly suggests that in nucleus pulposus cells, regulation of *CCN2* by HIF-1 α is complex and may occur indirectly through modulation of binding of other regulatory factor(s) beside Smad3. This mode of regulation is similar to what we have previously observed in the context of HIF-1 α

Cross-talk between HIF-1 α and CCN2 in the Nucleus Pulposus

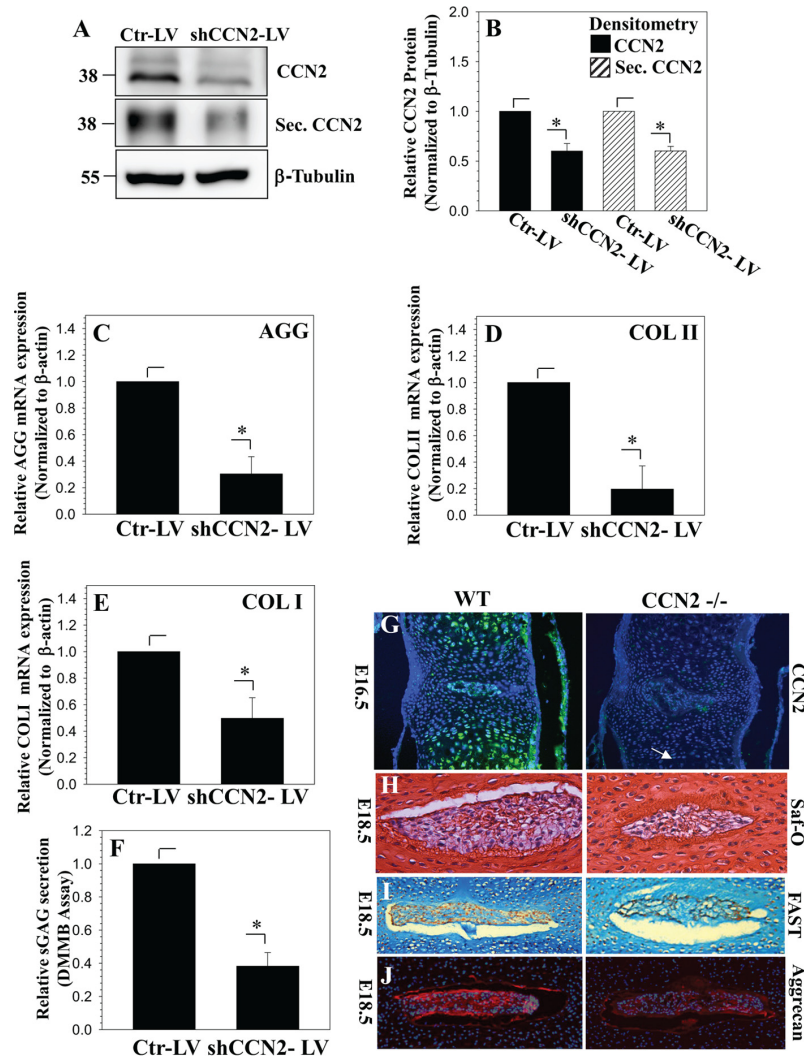


FIGURE 9. CCN2 controls expression of extracellular matrix genes and accumulation of the proteoglycan matrix in nucleus pulposus cells. *A*, Western blot analysis of nucleus pulposus cells transduced with control shRNA (Ctr-LV) or shCCN2 (shCCN2-LV) lentivirus. *B*, densitometric analysis shows that cellular and secreted CCN2 is significantly decreased in cells transduced with shCCN2-LV (CCN2, black; secreted CCN2, diagonally striped). *C* and *D*, real time RT-PCR analysis shows that suppression of CCN2 results in a decrease of AGGREGAN (*C*), COLLAGEN II (*D*), and COLLAGEN I (*E*) expression. *F*, dimethylmethylene blue (DMMB) assay shows that knockdown of CCN2 results in decreased accumulation of sulfated glycosaminoglycan. Values shown are mean \pm S.E. from three independent experiments, *, $p < 0.05$. *G*, immunofluorescence analysis of CCN2 expression in vertebral bodies from E16.5 WT (left) and CCN2^{-/-} littermates (right). In the WT mouse, CCN2 is abundant in the hypertrophic cartilage of the vertebral body and in the nucleus pulposus. Hypertrophy of chondrocytes in the vertebral bodies appears to be delayed in mutants (arrow), but there are no obvious differences in the nucleus pulposus. *H*, sections through the spines of E18.5 WT (left) and mutant (right) littermates, stained with safranin-o (Safr-O). The relative level of safranin-o-stained material is decreased in mutants in the nucleus pulposus. *I*, images of the nucleus pulposus at E18.5 stained using the FAST protocol. *J*, immunofluorescence staining for aggrecan demonstrates decreased expression in the nucleus pulposus of CCN2 mutants.

regulation of *Hsp70* and *GlcAT-I* promoters in nucleus pulposus cells (6, 11). Related to this discussion, one possibility is that hypoxia may exert its effects on CCN2 through the modulation of Fli1 or Ets-1, members of the Ets family of transcription factors. These factors function as molecular switches regulating a subset of target genes in response to physiological stimuli including hypoxia (43–45). Nakerakanti *et al.* (46) showed that Fli1 and Ets1 had differential effects on CCN2 expression in fibroblasts through differential occupancy of the Ets binding site, located at -114 bp in the proximal CCN2 promoter. Occu-

pancy of this site by Fli1 had a suppressive effect on CCN2 gene expression, whereas occupancy by Ets-1 had a positive effect (46). It will be of interest to examine if, in nucleus pulposus cells, hypoxia controls the levels and binding ability of these factors to the CCN2 promoter in a HIF-1 α -dependent fashion. This possibility is currently being examined.

We then investigated whether HIF-1 α expression and activity is in turn controlled by CCN2. We observed an increase in HIF-1 α and target gene expression with CCN2 knockdown. Correspondingly, decreased HRE reporter activity and

Cross-talk between HIF-1 α and CCN2 in the Nucleus Pulposus

decreased HIF-1 α target gene expression following treatment of cells with rCCN2 suggested that CCN2 may be involved in the maintenance of basal HIF-1 α levels. Although these results are in contradiction to studies that reported a CCN2-mediated increase in HIF-1 α levels in stromal fibroblasts and chondrosarcoma cells (24, 47), they are in agreement with a previous report of human lung adenocarcinoma (31). These investigators showed that lung adenocarcinomas with high levels of CCN2 exhibited lower HIF-1 α levels and that in cultured cells, CCN2 decreased HIF-1 α levels by enhancing its degradation through acetylation of Lys-532 and subsequent association with pVHL. Noteworthy, in nucleus pulposus cells, unlike previous studies, CCN2 treatment decreased the activity of HIF-1 α -TAD reporters, suggesting that in addition to maintenance of basal levels it may affect the activity of the HIF-1 α transcriptional complex. Furthermore, our study shows that in contrast to HIF-1 α , CCN2 is a positive regulator of HIF-2 α expression. This is relevant, as we have previously reported that in nucleus pulposus, HIF-2 α controls the expression of *cited2*, a p300 interacting protein (29). By competing with HIF-1 α for p300 binding, *cited2* suppresses transcriptional activity of HIF (29). Thus, it is possible that through induction of the HIF-2 α -*cited2* circuit, CCN2 may decrease HIF-1 α activity and target gene expression. The details of the mechanism by which CCN2 controls HIF-1 α levels/activity in the nucleus pulposus is not yet known and is a subject of future investigation.

Last, our study provided some insight into the role of endogenous CCN2 in nucleus pulposus cells. Both *in vitro* loss-of-function studies using postnatal nucleus pulposus cells and analysis of *Ccn2* null mouse embryos showed a decrease in proteoglycan levels and a specific decrease in aggrecan accumulation, although the effect on proteoglycan matrix levels in the embryonic discs seemed modest. However, as matrix accumulation and turnover in a healthy disc is a slow process (41), it is possible that the cumulative effect of a small but continuous decrease in matrix production over time will have a significant impact on the structure and function of postnatal discs. Because *Ccn2* global null is perinatally lethal, a nucleus pulposus-specific deletion of *Ccn2* will be required to further investigate this possibility in postnatal tissue. Taken together, our results confirm that basal CCN2 levels in nucleus pulposus cells play a role in maintenance of proteoglycan-rich extracellular matrix and tissue homeostasis. However, as both CCN2 and HIF-1 α have anabolic function in nucleus pulposus cells (10, 23, 32), it is plausible that their effect on matrix production is likely to be independent of each other. Importantly, this negative feedback loop may serve to tightly control both CCN2 and HIF-1 α levels in the healthy disc. In summary, we show for the first time that in the nucleus pulposus, hypoxia regulates CCN2 in a HIF-1 α -dependent manner, whereas CCN2 controls HIF-1 α levels and activity. Further studies are needed to determine how HIF-1 α regulation of CCN2 and vice versa could impact the progression of degenerative disc disease.

REFERENCES

1. Bartels, E. M., Fairbank, J. C., Winlove, C. P., and Urban, J. P. (1998) Oxygen and lactate concentrations measured *in vivo* in the intervertebral discs of patients with scoliosis and back pain. *Spine (Phila Pa 1976)* **23**, 1–7
2. Hassler, O. (1969) The human intervertebral disc. A micro-angiographical study on its vascular supply at various ages. *Acta Orthop. Scand.* **40**, 765–772
3. Rudert, M., and Tillmann, B. (1993) Lymph and blood supply of the human intervertebral disc. Cadaver study of correlations to discitis. *Acta Orthop. Scand.* **64**, 37–40
4. Rajpurohit, R., Risbud, M. V., Ducheyne, P., Vresilovic, E. J., and Shapiro, I. M. (2002) Phenotypic characteristics of the nucleus pulposus. Expression of hypoxia inducing factor-1, glucose transporter-1 and MMP-2. *Cell Tissue Res.* **308**, 401–407
5. Fujita, N., Chiba, K., Shapiro, I. M., and Risbud, M. V. (2012) HIF-1 α and HIF-2 α degradation is differentially regulated in nucleus pulposus cells of the intervertebral disc. *J. Bone Miner. Res.* **27**, 401–412
6. Gogate, S. S., Fujita, N., Skubutyte, R., Shapiro, I. M., and Risbud, M. V. (2012) Tonicity enhancer binding protein (TonEBP) and hypoxia-inducible factor (HIF) coordinate heat shock protein 70 (Hsp70) expression in hypoxic nucleus pulposus cells. Role of Hsp70 in HIF-1 α degradation. *J. Bone Miner. Res.* **27**, 1106–1117
7. Risbud, M. V., Guttapalli, A., Stokes, D. G., Hawkins, D., Danielson, K. G., Schaefer, T. P., Albert, T. J., and Shapiro, I. M. (2006) Nucleus pulposus cells express HIF-1 α under normoxic culture conditions. A metabolic adaptation to the intervertebral disc microenvironment. *J. Cell. Biochem.* **98**, 152–159
8. Zeng, Y., Danielson, K. G., Albert, T. J., Shapiro, I. M., and Risbud, M. V. (2007) HIF-1 α is a regulator of Galectin-3 expression in the intervertebral disc. *J. Bone Miner. Res.* **22**, 1851–1861
9. Skubutyte, R., Markova, D., Freeman, T. A., Anderson, D. G., Dion, A. S., Williams, C. J., Shapiro, I. M., and Risbud, M. V. (2010) Hypoxia-inducible factor regulation of ANK expression in nucleus pulposus cells. Possible implications in controlling dystrophic mineralization in the intervertebral disc. *Arthritis Rheum.* **62**, 2707–2715
10. Agrawal, A., Guttapalli, A., Narayan, S., Albert, T. J., Shapiro, I. M., and Risbud, M. V. (2007) Normoxic stabilization of HIF-1 α drives glycolytic metabolism and regulates aggrecan gene expression in nucleus pulposus cells of the rat intervertebral disk. *Am. J. Physiol. Cell Physiol.* **293**, C621–631
11. Gogate, S. S., Nasser, R., Shapiro, I. M., and Risbud, M. V. (2011) Hypoxic regulation of β -1,3-glucuronyltransferase 1 expression in nucleus pulposus cells of the rat intervertebral disc. Role of hypoxia-inducible factor proteins. *Arthritis Rheum.* **63**, 1950–1960
12. Shimo, T., Kubota, S., Kondo, S., Nakanishi, T., Sasaki, A., Mese, H., Matsumura, T., and Takigawa, M. (2001) Connective tissue growth factor as a major angiogenic agent that is induced by hypoxia in a human breast cancer cell line. *Cancer Lett.* **174**, 57–64
13. Ivkovic, S., Yoon, B. S., Popoff, S. N., Safadi, F. F., Libuda, D. E., Stephenson, R. C., Daluiski, A., and Lyons, K. M. (2003) Connective tissue growth factor coordinates chondrogenesis and angiogenesis during skeletal development. *Development* **130**, 2779–2791
14. Braig, S., Wallner, S., Junglas, B., Fuchshofer, R., and Bosserhoff, A. (2011) CTGF is overexpressed in malignant melanoma and promotes cell invasion and migration. *Br. J. Cancer.* **105**, 231–238
15. Hall-Glenn, F., De Young, R. A., Huang, B. L., van Handel, B., Hofmann, J. J., Chen, T. T., Choi, A., Ong, J. R., Benya, P. D., Mikkola, H., Iruela-Arispe, M. L., and Lyons, K. M. (2012) CCN2/connective tissue growth factor is essential for pericyte adhesion and endothelial basement membrane formation during angiogenesis. *PLoS One* **7**, e30562–e30562
16. Hoshijima, M., Hattori, T., Inoue, M., Araki, D., Hanagata, H., Miyauchi, A., and Takigawa, M. (2006) CT domain of CCN2/CTGF directly interacts with fibronectin and enhances cell adhesion of chondrocytes through integrin α 5 β 1. *FEBS Lett.* **580**, 1376–1382
17. Inoki, I., Shiomi, T., Hashimoto, G., Enomoto, H., Nakamura, H., Makino, K., Ikeda, E., Takata, S., Kobayashi, K., and Okada, Y. (2002) Connective tissue growth factor binds vascular endothelial growth factor (VEGF) and inhibits VEGF-induced angiogenesis. *FASEB J.* **16**, 219–221
18. Aoyama, E., Hattori, T., Hoshijima, M., Araki, D., Nishida, T., Kubota, S., and Takigawa, M. (2009) N-terminal domains of CCN family 2/connective tissue growth factor bind to aggrecan. *Biochem. J.* **420**, 413–420
19. Gao, R., and Brigstock, D. R. (2004) Connective tissue growth factor

Cross-talk between HIF-1 α and CCN2 in the Nucleus Pulposus

- (CCN2) induces adhesion of rat activated hepatic stellate cells by binding of its C-terminal domain to integrin $\alpha_3\beta_3$ and heparan sulfate proteoglycan. *J. Biol. Chem.* **279**, 8848–8855
20. Nishida, T., Kawaki, H., Baxter, R. M., Deyoung, R. A., Takigawa, M., and Lyons, K. M. (2007) CCN2 (connective tissue growth factor) is essential for extracellular matrix production and integrin signaling in chondrocytes. *J. Cell. Commun. Signal.* **1**, 45–58
 21. Abreu, J. G., Ketpura, N. I., Reversade, B., and De Robertis, E. M. (2002) Connective-tissue growth factor (CTGF) modulates cell signalling by BMP and TGF- β . *Nat. Cell Biol.* **4**, 599–604
 22. Higgins, D. F., Biju, M. P., Akai, Y., Wutz, A., Johnson, R. S., and Haase, V. H. (2004) Hypoxic induction of Ctgf is directly mediated by Hif-1. *Am. J. Physiol. Renal Physiol.* **287**, F1223–1232
 23. Tran, C. M., Markova, D., Smith, H. E., Susarla, B., Ponnappan, R. K., Anderson, D. G., Symes, A., Shapiro, I. M., and Risbud, M. V. (2010) Regulation of CCN2/CTGF expression in the nucleus pulposus of the intervertebral disc. Role of Smad and AP1 signaling. *Arthritis Rheum.* **62**, 1983–1992
 24. Nishida, T., Kondo, S., Maeda, A., Kubota, S., Lyons, K. M., and Takigawa, M. (2009) CCN family 2/connective tissue growth factor (CCN2/CTGF) regulates the expression of Vegf through Hif-1 α expression in a chondrocytic cell line, HCS-2/8, under hypoxic condition. *Bone* **44**, 24–31
 25. Ponticos, M., Holmes, A. M., Shi-wen, X., Leoni, P., Khan, K., Rajkumar, V. S., Hoyles, R. K., Bou-Gharios, G., Black, C. M., Denton, C. P., Abraham, D. J., Leask, A., and Lindahl, G. E. (2009) Pivotal role of connective tissue growth factor in lung fibrosis. MAPK-dependent transcriptional activation of type I collagen. *Arthritis Rheum.* **60**, 2142–2155
 26. Lee, C. H., Shah, B., Moioili, E. K., and Mao, J. J. (2010) CTGF directs fibroblast differentiation from human mesenchymal stem/stromal cells and defines connective tissue healing in a rodent injury model. *J. Clin. Invest.* **120**, 3340–3349
 27. Hong, K. H., Yoo, S. A., Kang, S. S., Choi, J. J., Kim, W. U., and Cho, C. S. (2006) Hypoxia induces expression of connective tissue growth factor in scleroderma skin fibroblasts. *Clin. Exp. Immunol.* **146**, 362–370
 28. Bennewith, K. L., Huang, X., Ham, C. M., Graves, E. E., Erlar, J. T., Kambham, N., Feazell, J., Yang, G. P., Koong, A., and Giaccia, A. J. (2009) The role of tumor cell-derived connective tissue growth factor (CTGF/CCN2) in pancreatic tumor growth. *Cancer Res.* **69**, 775–784
 29. Agrawal, A., Gajghate, S., Smith, H., Anderson, D. G., Albert, T. J., Shapiro, I. M., and Risbud, M. V. (2008) Cited2 modulates hypoxia-inducible factor-dependent expression of vascular endothelial growth factor in nucleus pulposus cells of the rat intervertebral disc. *Arthritis Rheum.* **58**, 3798–3808
 30. Kroening, S., Neubauer, E., Wullich, B., Aten, J., and Goppelt-Struebe, M. (2010) Characterization of connective tissue growth factor expression in primary cultures of human tubular epithelial cells. Modulation by hypoxia. *Am. J. Physiol. Renal Physiol.* **298**, F796–806
 31. Chang, C. C., Lin, M. T., Lin, B. R., Jeng, Y. M., Chen, S. T., Chu, C. Y., Chen, R. J., Chang, K. J., Yang, P. C., and Kuo, M. L. (2006) Effect of connective tissue growth factor on hypoxia-inducible factor 1 α degradation and tumor angiogenesis. *J. Natl. Cancer Inst.* **98**, 984–995
 32. Erwin, W. M., Ashman, K., O'Donnel, P., and Inman, R. D. (2006) Nucleus pulposus notochord cells secrete connective tissue growth factor and up-regulate proteoglycan expression by intervertebral disc chondrocytes. *Arthritis Rheum.* **54**, 3859–3867
 33. Chiou, M. J., Chao, T. T., Wu, J. L., Kuo, C. M., and Chen, J. Y. (2006) The physiological role of CTGF/CCN2 in zebrafish notochord development and biological analysis of the proximal promoter region. *Biochem. Biophys. Res. Commun.* **349**, 750–758
 34. Huang, B. L., Brugger, S. M., and Lyons, K. M. (2010) Stage-specific control of connective tissue growth factor (CTGF/CCN2) expression in chondrocytes by Sox9 and β -catenin. *J. Biol. Chem.* **285**, 27702–27712
 35. Leung, V. Y., Chan, W. C., Hung, S. C., Cheung, K. M., and Chan, D. (2009) Matrix remodeling during intervertebral disc growth and degeneration detected by multichromatic FAST staining. *J. Histochem. Cytochem.* **57**, 249–256
 36. Sandelin, A., Alkema, W., Engström, P., Wasserman, W. W., and Lenhard, B. (2004) JASPAR. An open-access database for eukaryotic transcription factor binding profiles. *Nucleic Acids Res.* **32**, D91–4
 37. Kondo, S., Kubota, S., Mukudai, Y., Nishida, T., Yoshihama, Y., Shirota, T., Shintani, S., and Takigawa, M. (2011) Binding of glyceraldehyde-3-phosphate dehydrogenase to the cis-acting element of structure-anchored repression in ccn2 mRNA. *Biochem. Biophys. Res. Commun.* **405**, 382–387
 38. Gupta, S., Clarkson, M. R., Duggan, J., and Brady, H. R. (2000) Connective tissue growth factor. Potential role in glomerulosclerosis and tubulointerstitial fibrosis. *Kidney Int.* **58**, 1389–1399
 39. Sonnylal, S., Shi-Wen, X., Leoni, P., Naff, K., Van Pelt, C. S., Nakamura, H., Leask, A., Abraham, D., Bou-Gharios, G., and de Crombrughe, B. (2010) Selective expression of connective tissue growth factor in fibroblasts *in vivo* promotes systemic tissue fibrosis. *Arthritis Rheum.* **62**, 1523–1532
 40. Tong, Z., Chen, R., Alt, D. S., Kemper, S., Perbal, B., and Brigstock, D. R. (2009) Susceptibility to liver fibrosis in mice expressing a connective tissue growth factor transgene in hepatocytes. *Hepatology* **50**, 939–947
 41. Sivan, S. S., Tsitron, E., Wachtel, E., Roughley, P. J., Sakke, N., van der Ham, F., DeGroot, J., Roberts, S., and Maroudas, A. (2006) Aggrecan turnover in human intervertebral disc as determined by the racemization of aspartic acid. *J. Biol. Chem.* **281**, 13009–13014
 42. Rimon, E., Chen, B., Shanks, A. L., Nelson, D. M., and Sadovsky, Y. (2008) Hypoxia in human trophoblasts stimulates the expression and secretion of connective tissue growth factor. *Endocrinology* **149**, 2952–2958
 43. Oikawa, M., Abe, M., Kurosawa, H., Hida, W., Shirato, K., and Sato, Y. (2001) Hypoxia induces transcription factor ETS-1 via the activity of hypoxia-inducible factor-1. *Biochem. Biophys. Res. Commun.* **289**, 39–43
 44. Aryee, D. N., Niedan, S., Kauer, M., Schwentner, R., Bennani-Baiti, I. M., Ban, J., Muehlbacher, K., Kreppel, M., Walker, R. L., Meltzer, P., Poremba, C., Kofler, R., and Kovar, H. (2010) Hypoxia modulates EWS-FLI1 transcriptional signature and enhances the malignant properties of Ewing's sarcoma cells *in vitro*. *Cancer Res.* **70**, 4015–4023
 45. Klappacher, G. W., Lunyak, V. V., Sykes, D. B., Sawka-Verhelle, D., Sage, J., Brard, G., Ngo, S. D., Gangadharan, D., Jacks, T., Kamps, M. P., Rose, D. W., Rosenfeld, M. G., and Glass, C. K. (2002) An induced Ets repressor complex regulates growth arrest during terminal macrophage differentiation. *Cell* **109**, 169–180
 46. Nakerakanti, S. S., Kapanadze, B., Yamasaki, M., Markiewicz, M., and Trojanowska, M. (2006) Fli1 and Ets1 have distinct roles in connective tissue growth factor/CCN2 gene regulation and induction of the profibrotic gene program. *J. Biol. Chem.* **281**, 25259–25269
 47. Capparelli, C., Whitaker-Menezes, D., Guido, C., Balliet, R., Pestell, T. G., Howell, A., Sneddon, S., Pestell, R. G., Martinez-Outschoorn, U., Lisanti, M. P., and Sotgia, F. (2012) CTGF drives autophagy, glycolysis and senescence in cancer-associated fibroblasts via HIF1 activation, metabolically promoting tumor growth. *Cell Cycle* **11**, 2272–2284

A.3 CCN2/CTGF is required for matrix organization and cellular survival during chondrogenesis

I facilitated with the optimization of the TUNEL stain (Figure 1) and replicated the BiP immunofluorescence (Figure 2D).

CCN2/CTGF is required for matrix organization and to protect growth plate chondrocytes from cellular stress

Faith Hall-Glenn · Armen Aivazi · Lusi Akopyan ·
Jessica R. Ong · Ruth R. Baxter · Paul D. Benya ·
Roel Goldschmeding · Frans A. van Nieuwenhoven ·
Ernst B. Hunziker · Karen M. Lyons

Received: 8 January 2013 / Accepted: 22 April 2013
© The Author(s) 2013. This article is published with open access at Springerlink.com

Abstract CCN2 (connective tissue growth factor (CTGF/CCN2)) is a matricellular protein that utilizes integrins to regulate cell proliferation, migration and survival. The loss of CCN2 leads to perinatal lethality resulting from a severe chondrodysplasia. Upon closer inspection of *Ccn2* mutant mice, we observed defects in extracellular matrix (ECM) organization and hypothesized that the severe chondrodysplasia caused by loss of CCN2 might be associated with defective chondrocyte survival. *Ccn2* mutant growth plate chondrocytes exhibited enlarged endoplasmic reticulum (ER), suggesting cellular stress. Immunofluorescence analysis confirmed elevated stress in *Ccn2* mutants, with reduced stress observed in *Ccn2* overexpressing transgenic mice. In vitro studies revealed that *Ccn2* is a stress responsive gene in chondrocytes. The elevated stress

observed in *Ccn2*^{-/-} chondrocytes is direct and mediated in part through integrin $\alpha 5$. The expression of the survival marker NF κ B and components of the autophagy pathway were decreased in *Ccn2* mutant growth plates, suggesting that CCN2 may be involved in mediating chondrocyte survival. These data demonstrate that absence of a matricellular protein can result in increased cellular stress and highlight a novel protective role for CCN2 in chondrocyte survival. The severe chondrodysplasia caused by the loss of CCN2 may be due to increased chondrocyte stress and defective activation of autophagy pathways, leading to decreased cellular survival. These effects may be mediated through nuclear factor κ B (NF κ B) as part of a CCN2/integrin/NF κ B signaling cascade. These studies highlight a novel protective role of CCN2 in chondrocyte stress and survival.

Electronic supplementary material The online version of this article (doi:10.1007/s12079-013-0201-y) contains supplementary material, which is available to authorized users.

F. Hall-Glenn · A. Aivazi · L. Akopyan · J. R. Ong · K. M. Lyons
Department of Molecular, Cell and Developmental Biology,
University of California, Los Angeles, Los Angeles,
CA 90095, USA

R. R. Baxter · P. D. Benya · K. M. Lyons
Department of Orthopaedic Surgery, University of California,
Los Angeles, Los Angeles, CA 90095, USA

R. Goldschmeding
Department of Pathology, University of Utrecht, Utrecht,
Netherlands

F. A. van Nieuwenhoven
Maastricht University, Maastricht, Netherlands

E. B. Hunziker
Centre of Regenerative Medicine for Skeletal Tissues, Department
of Clinical Research, University of Bern, Bern, Switzerland

K. M. Lyons (✉)
Department of Orthopaedic Surgery, Orthopaedic Hospital
Research Center, University of California Los Angeles,
615 Charles E Young Drive South 501,
Los Angeles, CA 90095, USA
e-mail: klyons@mednet.ucla.edu

Present Address:
A. Aivazi
School of Medicine, Stony Brook University, East Loop Road,
Stony Brook, NY, USA

Present Address:
L. Akopyan
Western University of Health Sciences College of Pharmacy,
309 E. Second street,
Pomona, CA, USA

Keywords Cartilage · CCN2/CTGF · Chondrocytes · Cellular stress · Nuclear factor κ B · Autophagy

Introduction

Chondrocytes secrete large amounts of extracellular matrix (ECM) as they differentiate. Disruptions in this process often result in chondrodysplasias, a diverse group of congenital birth defects characterized by short stature and skeletal deformity. The most common causes of chondrodysplasias are mutations that lead to structural alterations in genes that encode ECM proteins. These alterations prevent proper protein folding and maturation, leading to their retention in the endoplasmic reticulum (ER), and/or the incorporation of the mutated product into the ECM, interfering with matrix structure and function (Bateman et al. 2009).

ER enlargement is a hallmark of defective protein folding and cellular stress. ER and other forms of cellular stress activate the Unfolded Protein Response (UPR), an adaptive mechanism to restore cell homeostasis and viability (Rasheva and Domingos 2009). The UPR ameliorates cellular stress by attenuating protein synthesis and increasing chaperone protein levels to facilitate correct protein folding and clearing of misfolded protein aggregates. The glucose-regulated protein 78 (GRP78) also known as BiP, is a resident ER chaperone and the main initiator of the UPR (Bertolotti et al. 2000). BiP activates UPR effector molecules that function to restore cellular homeostasis. ER and other forms of cellular stress also activate anti-oxidative stress genes, which promote cell survival; however, prolonged stress can lead to activation of CCAAT/enhancer-binding protein-homologous protein (CHOP) and caspases to induce cell death (Rasheva and Domingos 2009). Although ER sensing of unfolded proteins is the most common inducer of ER stress, the UPR is activated by multiple stress pathways, including hypoxia and ECM detachment (Avivar-Valderas et al. 2011; Walter and Ron 2011). Stress pathways are major players in multiple pathologies including osteoarthritis (Rasheva and Domingos 2009) and identifying proteins involved in cellular stress pathways may provide new therapeutic targets.

Nuclear factor κ B (NF κ B/p65/relA) is a transcription factor that plays pivotal roles in cell proliferation, differentiation and survival (Marcu et al. 2010). ER stress activates NF κ B via tumor necrosis factor- α (TNF- α) receptor associated factor 2 (TRAF2) and inositol requiring enzyme 1 (IRE1) *in vitro* (Kaneko et al. 2003). The role of NF κ B activation in various forms of cellular stress is unclear, but several studies show that NF κ B exerts pro-survival functions (Nozaki et al. 2001; Sirabella et al. 2009). In the growth plate, NF κ B is essential for chondrocyte viability (Park et al. 2007; Wu et al. 2007). However, the mechanisms that control NF κ B activity in the growth plate are unknown.

Autophagy is a lysosomal degradation pathway used to recycle cellular components and activate cell survival under conditions of starvation and stress (Mehrpour et al. 2010). Autophagy is essential for maintaining ER homeostasis, and evidence indicates that during prolonged ER stress, autophagy is activated to assist in the removal of misfolded proteins (Li et al. 2008). Crosstalk between cellular stress pathways, autophagy and NF κ B-mediated cellular survival has been confirmed previously (Copetti et al. 2009; Sirabella et al. 2009), but whether such crosstalk occurs in chondrocytes is unknown.

The term “matricellular” was coined to encompass a structurally diverse group of proteins that reside in the ECM, but serve no structural functions (Bornstein 2009). Members of the CCN (Cyr61/CTGF/Nov) family of matricellular proteins are critical regulators of cell-ECM interactions. The six members of the CCN family contain four conserved domains that mediate interactions with integrins, growth factors, and ECM components including heparin sulfate proteoglycans, fibronectin and aggrecan (Jun and Lau 2011). Connective tissue growth factor (CTGF/CCN2) is best known for its role in fibrosis, where its overexpression exacerbates excess collagen deposition in multiple organs (Brigstock 2010). CCN2 overexpression is involved in many other pathological processes, such as atherosclerosis, osteoarthritis and cancer (Chen and Lau 2009).

Although most studies have focused on the mechanisms by which CCN2 overexpression leads to pathological changes, CCN2 is indispensable for endochondral bone formation. Global loss of CCN2 in mice results in severe chondrodysplasia and lethality at birth (Ivkovic et al. 2003). This phenotype is accompanied by a significant decrease in chondrocyte proliferation, delayed chondrocyte differentiation, impaired ECM production and insufficient vascular invasion (Hall-Glenn et al. 2012; Ivkovic et al. 2003).

CCN2 induces NF κ B activity in ATDC5 chondrocytic cells through integrin α v β 3-mediated mechanisms to enhance migration (Tan et al. 2009). Reciprocally, the CCN2 promoter contains an NF κ B responsive element that activates CCN2 expression during the mechanical stretch response in smooth muscle cells (Chaouar et al. 2006). These studies raise the possibility that CCN2 may regulate NF κ B in the growth plate. Given the essential role of NF κ B in chondrocyte survival, and evidence that CCN2 induces its expression and activity in multiple cell types, we investigated whether CCN2 plays a role in survival of growth plate chondrocytes. We show that CCN2 is essential for chondrocyte survival, protecting growth plate chondrocytes from pro-apoptotic pathways activated by cellular stress, and promoting chondrocyte survival. We provide evidence

consistent with the possibility that CCN2 enhances chondrocyte survival through activation of NF κ B and autophagy. Additionally, we provide evidence that these effects are mediated in part through the ability of CCN2 to engage integrins.

Materials and methods

Mouse strains and cell lines *Ccn2* knockout mice were generated, genotyped and maintained as described (Ivkovic et al. 2003). *Ccn2*^{-/-} embryos were obtained from timed heterozygote matings, with embryonic day (E) 0.5 representing the detection of a post-copulatory plug.

CCN2 floxed inducible transgenic mice (*Ccn2*^{flxTg}) were generated by pronuclear injection as described (Araki et al. 1995; Voncken 2011). These mice were crossed to *Col2a1Cre* mice (Ovchinnikov et al. 2000) to induce overexpression of CCN2 in chondrocytes. Genotyping was performed on DNA isolated from tail biopsies with the following primers: Forward: 5'-TCTTCTGCGATTCGGCTCC-3'; Reverse: 5'-AATGTGTCTTCCAGTCGGTAG-3'. Mouse embryonic fibroblasts (MEFs) from *Ccn2*^{flxTg} embryos were isolated and cultured as described (Lengner et al. 2004). MEFs were infected for 24 hours with adenoviral Cre-recombinase (Ad-CRE) and empty vector controls (Ad-CNT) (University of Iowa Gene Transfer Vector Core) at a multiplicity of infection of 300. RNA was isolated using Qiagen RNeasy Kit, and quantitative RT-PCR (qRT-PCR) was used to quantify relative CCN2 expression normalized to glyceraldehyde-3-phosphate dehydrogenase (GAPDH) as described (Kawaki et al. 2008).

Experiments on mice were performed with four sets of WT and *Ccn2*^{-/-} littermates at E16.5, E18.5 and postnatal day (P) 0 (*N*=8 per genotype). Animals were treated in accordance with the National Institutes of Health guidelines for care and use of animals, and approved by the UCLA Institutional Animal Care and Use Committee.

Transmission electron microscopy WT and *Ccn2*^{-/-} E18.5 hindlimbs (*N*=3 per genotype) were prepared for electron microscopy as previously described (Szafranski et al. 2004). The ultrastructural analysis was performed at the Center of Regenerative Medicine for Skeletal Tissues (Department of Clinical Research, University of Bern), in Bern, Switzerland.

Terminal deoxynucleotidyl transferase dUTP nick end labeling (TUNEL) assays TUNEL assays (Roche) were performed on WT and *Ccn2*^{-/-} growth plates according to the manufacturer's protocol. Cellular counts of chondrocytes were quantitated and normalized to total DAPI counts.

Immunofluorescent staining Embryos were fixed and embedded as described (Ivkovic et al. 2003). 7 μ m sections were generated using a Lecia GM40 Microtome. For fluorescent staining, Tyramide Signal Amplification was performed according to the manufacturer's protocol (Invitrogen). The following antibodies were used: CCN2 L-20 (1:1,000; Santa Cruz Biotechnology), BiP (1:500; Cell Signaling), CHOP (1:400; Cell Signaling), Calnexin (1:300; Chemicon), NF κ B/RelA/p65 (1:400; Cell Signaling), Apg/Atg12 (1:400; Chemicon) and Apg8b/LC3 (1:200; Abgent). Secondary antibodies were conjugated with AlexaFluor-594 and 488 (Invitrogen). Sections were counterstained with DAPI (Sigma) and mounted with Prolong Gold reagent (Sigma). Immunofluorescence was visualized on an Olympus Bx60 Microscope.

Sternal chondrocyte isolation E16.5 sterna were isolated and pooled by genotype into conical tubes. Garnet bead mix (Invitrogen) was added to 15 ml of HEPES (Sigma) buffered DMEM (HDMEM) (GIBCO). The connective tissue from the sterna was removed by mechanical shaking for 30 min. The media was aspirated, and 0.03 % bacterial collagenase (*Chlostridium*; Sigma) in HDMEM was added. Additional shaking was performed for 10 min. Cleared sterna were further digested in 0.01 % collagenase overnight. The following day, chondrocytes were filtered (70 μ m Fisher) and plated.

Alginate chondron cultures Isolated sternal chondrocytes were suspended in 1.1 % sodium alginate in 1X Phosphate Buffered Saline (PBS) (Sigma) (Lee et al. 1997). The cell/alginate suspension was extruded drop-wise into 0.1 M Calcium Chloride (Sigma) and beads were polymerized at room temperature for 10–15 min. The beads were then washed with 1X PBS, transferred to T25 flasks and incubated in differentiation media containing 50 ng/ml ascorbic acid (Sigma). After 7–10 days in culture, the chondrons were released using 10 mM sodium citrate (Sigma). Chondron clusters were plated using Cell-tak adhesive (BD Biosciences) and cultured for 1–3 days for immunofluorescence (Hamamura et al. 2009).

Thapsigargin-induced ER stress in ATDC5 cells ATDC5 chondrosarcoma cells (RCB0565-Riken Cell Bank) were cultured as described (Altaf et al. 2006). ER stress was induced by a 24 h treatment with thapsigargin (THG, Sigma) diluted in DMSO at the following concentrations: 0, 40, 80 and 160nM (Hamamura et al. 2009). All experiments were performed in triplicate and repeated twice.

Integrin blocking and recombinant CCN2 assays Sternal chondrocytes were isolated as described above. Integrin blocking assays were performed as previously described

(Nishida et al. 2007). Briefly, sternal chondrocytes were plated and serum starved for 6–8 h. Chondrocytes were then treated for 24 h with an anti-rat integrin $\alpha 5$ blocking antibody (1:100; CD49e BD Pharmingen) or 5 % rat control serum (Sigma). In a separate set of experiments, ATDC5 cells were serum starved followed by a 1 h treatment with recombinant protein containing only the C terminal (CT) domain of CCN2 (150 ng/ml; Peprotech) or BSA added to the media, and then by a 1 h treatment with integrin $\alpha 5$ blocking antibody and/or 80nM THG or DMSO control. Cells were lysed and RNA extracted using a Qiagen RNA purification kit following the manufacturer's instructions. cDNA was generated using Superscript III (Invitrogen). The following primer sequences were used: Integrin alpha 5 Forward: 5'-AGCGCATCTCTCACCATCTT-3' and Reverse: 3'-TCAGGTTCAAGTGC GTTCTTGT-5', and normalized to GAPDH as described (Nishida et al. 2007).

CCN2 overexpression in ATDC5 cells ATDC5 cells were infected with a bicistronic adenovirus expressing CCN2 and green fluorescent protein (AdCCN2-GFP) adenovirus or an adenoviral control (Ad-CNT) vector for 24 h at a multiplicity of infection of 200 (University of Iowa) (Hall-Glenn et al. 2012). After 24 h, cells were analyzed by immunofluorescence. Experiments were performed in triplicate and repeated twice.

Western blot analysis Proteins were isolated from *Ccn2*^{fxTg} and WT sterna through lysis in RIPA buffer with 1X protease (Roche) and 1X phosphatase inhibitors (Sigma). 30 μ g of protein lysates were separated by gel electrophoresis and transferred to 0.45 μ m nitrocellulose membranes (Biorad). Membranes were blocked in milk and incubated at a 1:2,000 dilution of the following primary antibodies overnight at 4 °C: CCN2 (L-20; Santa Cruz Biotech) and β -actin (Sigma). The blots were incubated with the following secondary antibodies: Donkey anti-goat horseradish peroxidase (HRP) and Goat anti-rabbit HRP (1:5,000; Biorad). Membranes were developed using Pierce ECL HRP chemoluminescent reagent (ThermoScientific). The blots were repeated twice.

Quantitative reverse transcriptase PCR (qRT-PCR) All qRT-PCR reactions were performed with a SYBR Green Real-time PCR Master Mix (Fermentas) with a Mx3005P QPCR System (Stratagene). Relative expression of *Ccn2*, *Bip* and *Chop* were quantitated and normalized to *Gapdh* as described and performed in triplicate (Hamamura et al. 2009; Kawaki et al. 2008). *Atg12* and *Lc3* levels were quantitated and normalized to *Gapdh* as previously described (Kouroku et al. 2007; Marino et al. 2010).

Statistical analysis

Immunofluorescent quantitation of the levels of CCN2, BiP and CHOP expression was performed through ImageJ analysis and calculated as a percentage of DAPI positive total cell counts. Three images were taken per independent experiment, followed by quantitation and averaging. At least three independent WT and mutant littermate growth plates were examined with each marker. All in vitro experiments were performed in triplicate and repeated twice. All graphs are represented as fold induction over normalized untreated controls. A normal distribution of the data was assumed, and statistical analysis was performed using Student's *t*-test (95 % confidence interval).

Results

Loss of CCN2 results in cellular stress in the growth plate

Ccn2 mutant growth plates and cultured chondrocytes exhibit decreased ECM production (Ivkovic et al. 2003; Nishida et al. 2007). However, the consequences on the overall organization of the cartilage ECM were not previously investigated. Therefore, transmission electron microscopy was performed on E18.5 WT and *Ccn2* mutant growth plates. Unexpectedly, ultrastructural examination revealed enlarged and distended ERs in proliferating and hypertrophic chondrocytes in *Ccn2* mutants (Fig. 1a–d). WT proliferating (Fig. 1a) and hypertrophic (Fig. 1c) chondrocytes contained an organized rough ER (rER) with a limited amount of protein evenly distributed throughout the cisternae. However, in *Ccn2* mutants, rER cisternae were dilated (Fig. 1b, d). Large vacuoles filled with an electron-lucid granular substance were also observed in mutants, indicative of accumulated intracellular proteins (Fig. 1b, d). Moreover, the nuclear chromatin in mutant chondrocytes was condensed (Fig. 1d), indicating most chondrocytes were undergoing cell death. The mechanism by which chondrocytes undergo physiological cell death is a matter of debate, but condensed chromatin and TUNEL labeling are reliable markers of chondrocyte death (Ahmed et al. 2007). TUNEL staining showed that *Ccn2*^{-/-} growth plates exhibited an increase in the percent of chondrocytes undergoing cell death in both the proliferative and hypertrophic zones compared to WT growth plates (Fig. 1e–g). Ultrastructural analysis also revealed major defects in ECM assembly in mutants. Fewer collagen fibrils were observed throughout the growth plate in *Ccn2* mutants compared to WT littermates (Fig. S1).

Because we noted distended ER in proliferative as well as hypertrophic chondrocytes, we examined CCN2 expression and confirmed that CCN2 protein is expressed both in the

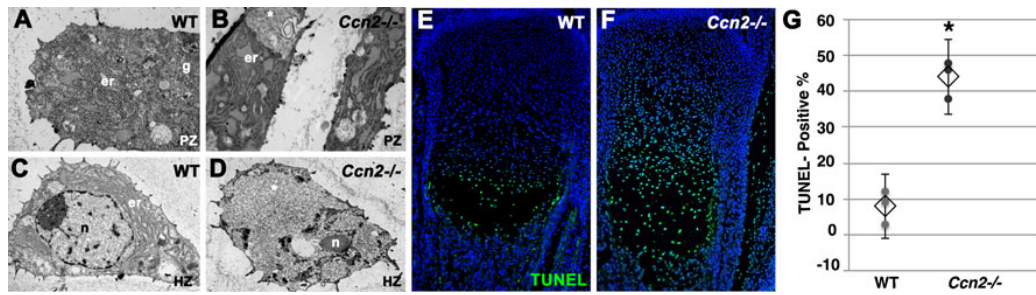


Fig. 1 The Loss of CCN2 results in chondrocyte stress and death. Electron microscopy was performed on WT and *Ccn2* mutant chondrocytes in E18.5 growth plates. **a, b** WT and *Ccn2*^{-/-} proliferative chondrocytes, respectively. **c, d** WT and *Ccn2*^{-/-} hypertrophic chondrocytes, respectively. The *Ccn2* mutant ER appears devoid of ribosomes and is engorged with an electron lucid substance, which is presumably composed of misfolded protein aggregates. Large vacuoles

are also present and filled with granulated material (asterisk). **e, f** WT and *Ccn2* mutant growth plates analyzed by TUNEL staining showing increased cell death in the proliferative zone in mutants. **g** Quantitation of TUNEL-positive cells. Open triangles represent the average of the data points. **g** golgi, **n** nucleus; **r** endoplasmic reticulum. Representative images are shown

proliferative and hypertrophic zones (Ivkovic et al. 2003) (Fig. 2a), and that CCN2 protein is absent in mutant growth plates (Fig. 2b) (Ivkovic et al. 2003). Next, we tested whether the distended ER in *Ccn2* mutant chondrocytes is associated with activation of ER stress pathways by examining expression of the UPR activator, BiP, and the apoptosis inducing protein, CHOP. Consistent with previous studies (Tsang et al. 2007), low levels of BiP were observed

in the hypertrophic zone (Fig. 2c), and CHOP (Fig. 2e) was undetectable in E16.5 WT growth plates. Increased expression of BiP (Fig. 2d) and CHOP (Fig. 2f) was observed in the hypertrophic zones of *Ccn2* mutant growth plates, but not in the proliferative zone. Expression of calnexin, a calcium dependent ER chaperone, was elevated throughout the proliferative and prehypertrophic zones in *Ccn2* mutants (Fig. 2g, h). Although calnexin is upregulated by ER stress in chondrocytes (Vranka et al. 2001), the observation that BiP and CHOP were not elevated in the proliferative zone in *Ccn2* mutants indicates that these chondrocytes are not undergoing a classical UPR. Nonetheless, these results show that the absence of CCN2 in the growth plate results in defective ECM assembly, increased cellular stress, and chondrocyte cell death in both the proliferative and hypertrophic zones.

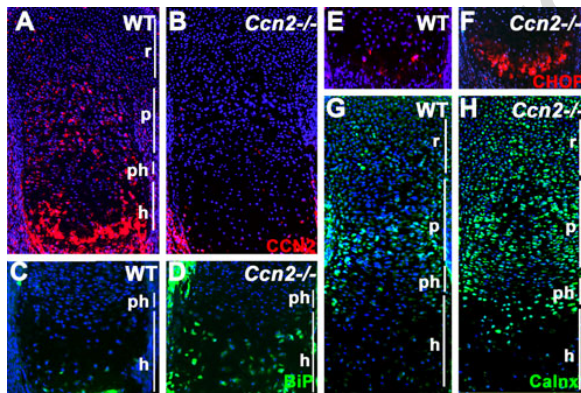


Fig. 2 Depletion of CCN2 results in increased cellular stress and defective chaperone expression in vivo. All images are E16.5 tibial growth plates. **a, b** Immunofluorescence staining for CCN2 in WT and *Ccn2*^{-/-} growth plates, respectively, showing expression of CCN2 in proliferative chondrocytes in addition to hypertrophic chondrocytes. **b** The *Ccn2* mutant allele is transcriptionally null, and in accordance, no CCN2 expression is observed in *Ccn2*^{-/-} growth plates. **c, d** Immunofluorescence staining for BiP reveals very low levels of expression in WT growth plates (**c**), and elevated expression in the hypertrophic zones of *Ccn2* mutant littermates (**d**). **e, f** The pro-apoptotic marker CHOP is seen at very low levels, restricted to the hypertrophic zone, in WT growth plates (**e**), but is strongly upregulated in the hypertrophic zone in *Ccn2* mutant littermates (**f**). **g, h** Expression of the resident ER chaperone calnexin is restricted to lower proliferative zone chondrocytes in WT growth plates (**g**), but is upregulated throughout the growth plates of *Ccn2* mutants (**h**). Representative images are shown

CCN2 Is a stress responsive gene in vitro

The finding that loss of CCN2 was associated with increased chondrocyte stress raised the possibility that CCN2 may be responsive to cellular stress in chondrocytes. Therefore, we tested whether CCN2 is upregulated in chondrocytes during chemically induced ER stress. Thapsigargin (THG) induces cellular stress by inhibiting sarco/endoplasmic reticulum calcium ATPases, thus blocking calcium release from ER stores (Yang et al. 2005). Prior to cell death, the transcription of ECM components is downregulated and protective ER stress response genes such as BiP are activated by THG in chondrocytes (Yang et al. 2005). ATDC5 chondrocytic cells were treated with increasing concentrations of THG. *Bip* and *Chop* levels were examined using qRT-PCR. Consistent with previous studies, THG induced dose-dependent increases in *BiP* (Fig. 3a) and *Chop* mRNA (Fig. 3b) (Hamamura et al. 2009). In contrast to the expression of ECM components,

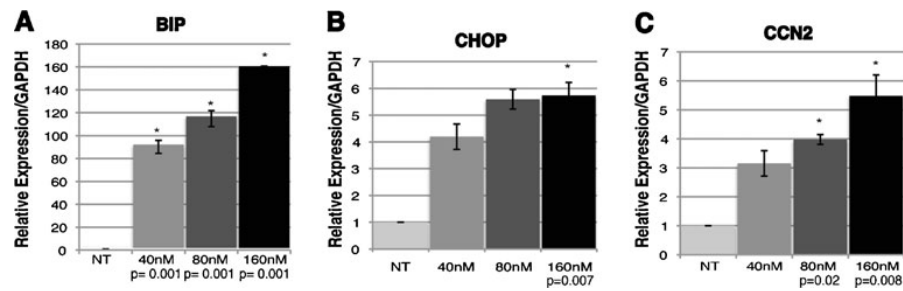


Fig. 3 CCN2 is a stress responsive gene in chemically induced cellular stress. ATDC5 chondrocytes were cultured for 24 h in the presence of Thapsigargin (THG) at the indicated concentrations. mRNA expression levels of *Ccn2* (A), *BiP* (B) and *Chop* (C) were assayed by

Quantitative Reverse Transcriptase PCR (qRT-PCR). Assays were performed in triplicate and a p value of >0.05 was considered significant compared to no THG (*). p values shown are for 160nM THG

which are downregulated by THG (Nugent et al. 2011), *Ccn2* mRNA levels were increased by THG with the same kinetics as *BiP* and *Chop* (Fig. 3c), suggesting that CCN2 is a stress-responsive gene in chondrocytes in vitro.

CCN2 depletion induces cellular stress in chondron cultures

The above experiments demonstrate that CCN2 expression is induced by stress in vitro. However, they do not demonstrate that the cellular stress observed in *Ccn2*^{-/-} growth plates is due to a direct role for CCN2 in chondrocytes. Recent studies have shown that the presence of ECM protects chondrocytes from ER stress (Nugent et al. 2011). Therefore, a 3-dimensional culture system was developed in which chondrocytes were maintained in alginate, yielding chondrocyte clusters (chondrons) (Fig. S2) (Lee et al. 1997). The accumulation of ECM components can be observed (Fig. S2A, B). THG treatment induced cellular stress in chondrons, with BiP localization transitioning from the ER lumen in control cells (Fig. S2C), to the nucleus/perinuclear region in THG treated chondrons (Fig. S2D). The re-localization of BiP to the nucleus has not been reported previously in chondrocytes, but is consistent with previous reports in other cell types (Ni et al. 2011). CHOP levels were also increased in THG treated chondrons (Fig. S2F), compared to untreated controls (Fig. S2E). Therefore, chondrons in alginate are sensitive to THG-induced stress. Next, the impact of loss of *Ccn2* on THG-induced stress was tested. First, we confirmed that CCN2 is expressed in WT chondrons (Fig. 4a) and is absent in *Ccn2*^{-/-} chondrons (Fig. 4b, c). WT chondrons expressed low levels of BiP (Fig. 4d). *Ccn2*^{-/-} chondrons displayed upregulated BiP expression and a higher proportion of nuclear BiP-positive cells (Fig. 4e, f). CCN2 mutant chondrons also exhibit increased expression of CHOP (Fig. 4h-i). These results suggest that CCN2 plays a direct role in the protection of chondrocytes against THG-induced stress in vitro.

The protective effect of CCN2 against chondrocyte stress may be mediated through integrin $\alpha 5$

CCN2 is thought to mediate its functions by acting as a ligand for integrins (Jun and Lau 2011). CCN2 induces expression of integrin $\alpha 5$, and binds to integrin $\alpha 5\beta 1$ to promote chondrocyte proliferation and ECM secretion (Nishida et al. 2007). Integrin $\alpha 5\beta 1$ is also required for chondrocyte survival (Pulai et al. 2002). Recent data demonstrate that multiple stress pathways are activated as a survival mechanism during cell detachment from the ECM (Avivar-Valderas et al. 2011). Taken together, these findings suggest that one of the pro-survival functions of integrin $\alpha 5\beta 1$ in chondrocytes may be the suppression of cellular stress. To test this possibility, sternal chondrocytes were treated with or without an integrin $\alpha 5$ -blocking antibody for 24 h (Fig. 5a). *BiP* and *Chop* mRNA expression levels were upregulated in response to treatment with the integrin $\alpha 5$ -blocking antibody (Fig. 5a). Consistent with our findings that loss of *Ccn2* leads to increased cellular stress in chondron cultures (Fig. 4), recombinant C-terminal CCN2 (rCCN2)-treated ATDC5 cells exhibited a decrease in *Chop* mRNA levels compared to BSA treated controls in the presence of THG (Fig. 5b). The C-terminal domain of rCCN2 contains the integrin $\alpha 5\beta 1$ -binding domain (Gao and Brigstock 2006). Next, ATDC5 cells were pre-treated for 1 h with recombinant C-terminal rCCN2 added to the medium prior to stress induction for 1 h in the presence of the $\alpha 5$ -blocking antibody. As in Fig. 5a, treatment with integrin $\alpha 5$ -blocking antibody led to increased *Chop* mRNA expression (Fig. 5c, columns 1 and 2), whereas treatment of ATDC5 cells with THG leads to an approximately 2-fold induction in *Chop* mRNA (Fig. 5b, columns 1 and 2). Also, treatment with THG in the presence of the integrin $\alpha 5$ -blocking antibody leads to an approximately 10-fold induction of *Chop* (Fig. 5c, columns 1 and 3). Moreover, while rCCN2 prevented THG-induced *Chop* expression (Fig. 5b, columns 2 and 4), treatment with integrin $\alpha 5$ -blocking antibody prevented the protective effect of rCCN2 (Fig. 5c,

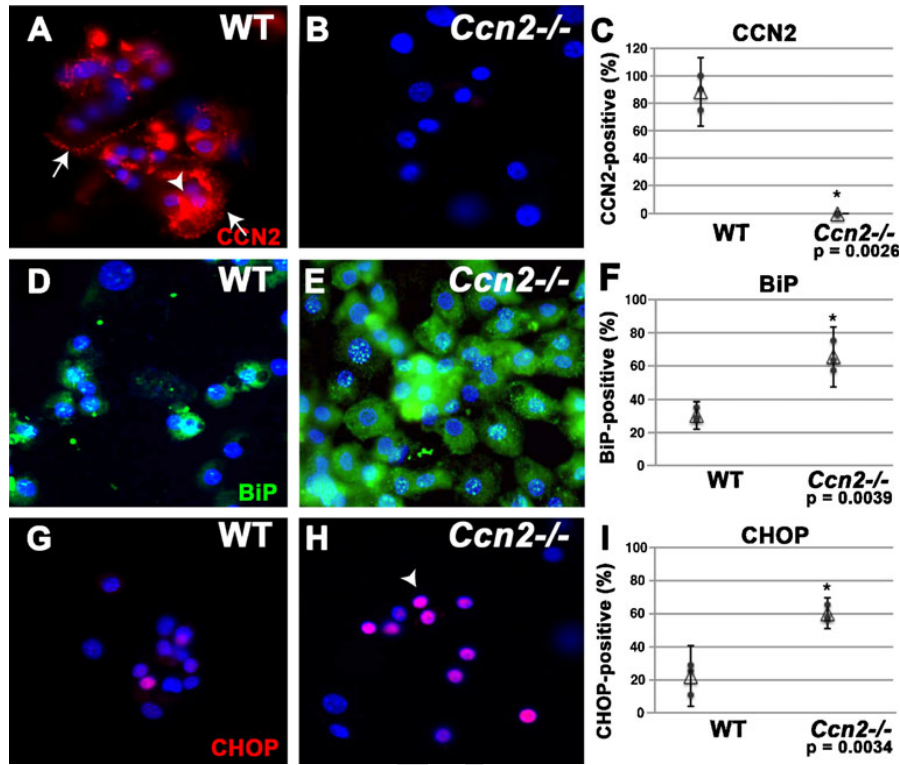


Fig. 4 CCN2 depleted chondrons exhibit elevated cellular stress. Primary sternal chondrocytes were isolated from E16.5 WT and *Ccn2*^{-/-} sterna, and cultured in alginate for 10 days to yield chondrons. CCN2, BiP and CHOP protein expression were analyzed through immunofluorescence. **a-c** CCN2 expression. CCN2 protein expression was abundant in WT chondrons (**a**), where punctate CCN2 protein expression was observed intracellularly (*arrowhead*) and pericellularly (*arrows*). CCN2 protein was not detected in *Ccn2* mutant chondrons. **b, c** Quantitation of number of CCN2-expressing cells. **d-f** BiP expression in WT and *Ccn2*^{-/-} chondrons. **d** BiP is detected in the ER in some cells in WT chondron clusters. **e** Nearly all *Ccn2*^{-/-}

chondrocytes express BiP, and many nuclei are positive. **f** Quantitation of the percentage of nuclear BiP-expressing cells. **g-i** CHOP expression. **g** Few WT chondrocytes express CHOP. In contrast, most *Ccn2*^{-/-} chondrocytes express CHOP (**h**). **i** Quantitation of the percentage of CHOP-expressing chondrocytes. **e, f, i** CCN2, BiP, and CHOP expression was analyzed in triplicate using ImageJ analysis and calculated as a percentage of DAPI positive total cell counts. *Asterisks* indicate statistical significance with a *p*-value of 0.003. *Open triangles* in (**c**), (**f**), and (**i**) represent the averages of the data points. Representative images are shown

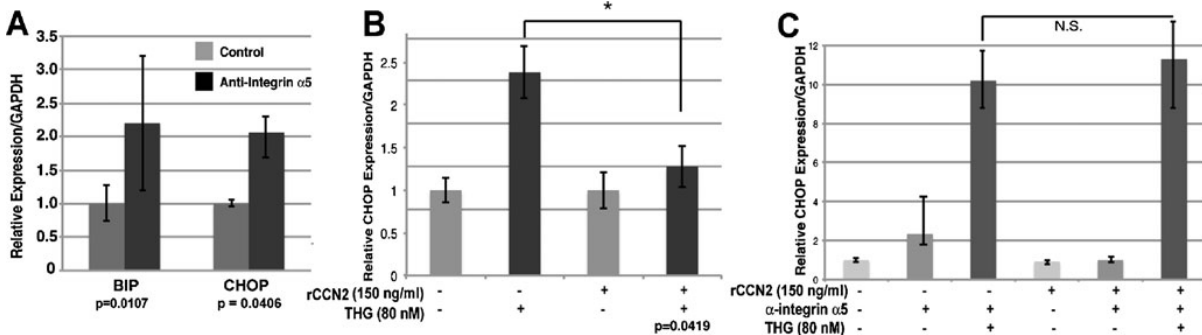


Fig. 5 Blocking Integrin $\alpha 5$ results in chondrocyte stress. Primary sternal chondrocytes were serum starved and treated with anti-integrin $\alpha 5$ blocking antibody or goat serum (control) for 24 h, after which BiP and CHOP mRNA levels were quantitated by qRT-PCR and normalized to GAPDH. BiP and CHOP expression were increased by

treatment with the blocking antibody. **b** rCCN2 protects against THG-induced stress, resulting in *Chop* mRNA induction. **c** This affect is attenuated upon treatment with $\alpha 5$ blocking antibody and THG compared to DMSO and rat serum controls

columns 3 and 6). These results, although preliminary, suggest that integrin $\alpha 5$ may be required for the ability of CCN2 to protect against cellular stress in chondrocytes in vitro.

Overexpression of CCN2 attenuates chondrocyte stress

Since loss of CCN2 induces cellular stress in cartilage, we generated transgenic mice that overexpress CCN2 in chondrocytes to determine whether increased CCN2 could lead to reduced stress. An inducible transgenic construct was generated, consisting of a floxed transcriptional STOP signal placed upstream of the *Ccn2* coding sequence (Fig 6a). Transgenic lines were established and mated to *Col2Cre* mice (Ovchinnikov et al. 2000) to induce chondrocyte-specific overexpression of CCN2 (Fig 6a). A 3–5 fold induction of CCN2 protein was observed in *Ccn2fxTg;Col2Cre* mice (Fig. 6b). The specificity of induction was confirmed in isolated mouse embryonic fibroblasts (MEFs) from *Ccn2fxTg* embryos infected with adenoviral Cre (Ad-CRE) (Fig. 6c). *Ccn2fxTg;Col2Cre* mice were viable with no obvious morphological differences at birth

(Fig. 6d), but exhibited progressive overgrowth of cartilage elements (data not shown). A complete characterization of these transgenics will be presented elsewhere. The growth plates of P0 *Ccn2fxTg* tibiae had normal chondrocyte organization, although both the hypertrophic zone and chondrocytes within it were slightly smaller than in WT littermates (Fig. 6e, f). Consistent with a protective function for CCN2, levels of BiP were reduced in *Ccn2fxTg;Col2Cre* mice compared to WT controls (Fig. 6g, h).

CCN2 regulates NF κ B expression and autophagy

NF κ B is required for chondrocyte survival (Park et al. 2007; Wu et al. 2007). CCN2 induces nuclear localization of NF κ B and activates pro-survival mechanisms, while inhibiting stress-mediated apoptosis in a number of cell types (Gao and Brigstock 2005). NF κ B is activated by integrin $\alpha 5\beta 1$ in breast cancer epithelial cells (Sen et al. 2010) and $\alpha 5\beta 1$ is a major receptor for CCN2 in chondrocytes (Sen et al. 2010). Our earlier results suggested that CCN2 protects against chondrocyte stress through

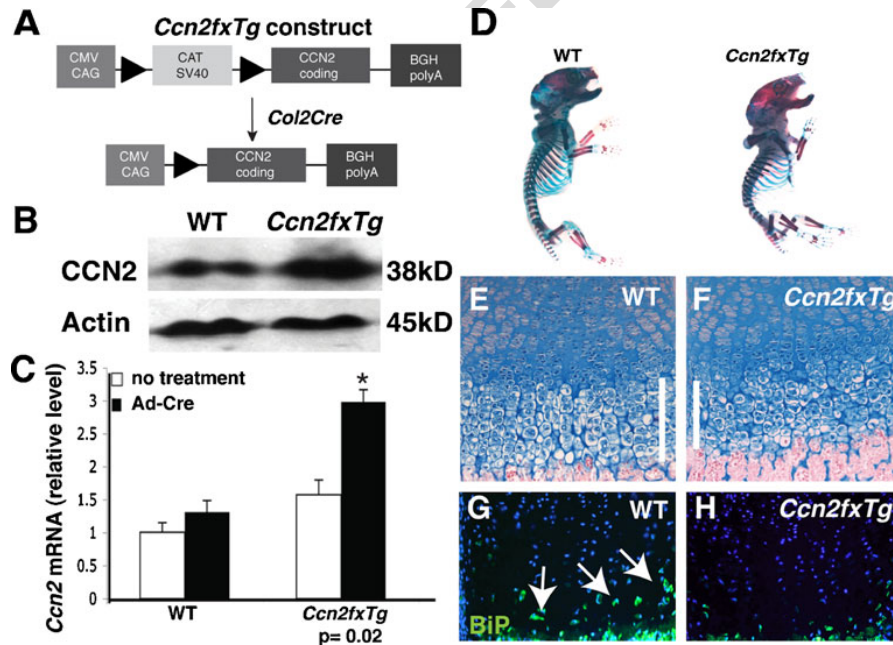


Fig. 6 CCN2 overexpression attenuates ER stress in vivo. **a** Schematic of the CCN2 floxed transgenic construct. A floxed cassette consisting of a STOP cassette and a chloroacetyltransferase (CAT) gene is flanked by loxP sites and inserted between the CMV/chicken β actin (CAG) promoter and the murine CCN2 coding sequence, followed by a bovine growth hormone polyA signal sequence. Upon crossing to a *Col2Cre* mouse, the silencer is excised, leading to transcription of CCN2 from the transgene in cartilage. **b** Western blot of protein isolated from sterna of WT and *Ccn2fxTg;Col2Cre* P0 pups with actin controls. **c** *Ccn2* mRNA levels in mouse embryonic fibroblasts (MEFs) from E11.5

Ccn2fxTg E11.5 embryos infected with AdCre or Adcontrol. *Ccn2* mRNA levels are not significantly different in WT vs. *Ccn2fxTg* MEFs in the absence of Cre, but are increased approximately 2.5-fold in *Ccn2fxTg* mice in the presence of Cre. **(D)** Skeletal preparations of postnatal day 0 (P0) *Ccn2fxTg;Col2Cre* and WT littermates, showing no apparent morphological differences. **(E, F)** Growth plate histology of P0 WT **(e)** and *Ccn2fxTg;Col2Cre* **(f)** littermate. The hypertrophic zone is slightly shorter and hypertrophic chondrocytes are smaller in transgenics. **(g, h)** Overexpression of *Ccn2* results in decreased BiP expression **(h)** compared to WT littermate **(g)** in P0 growth plates

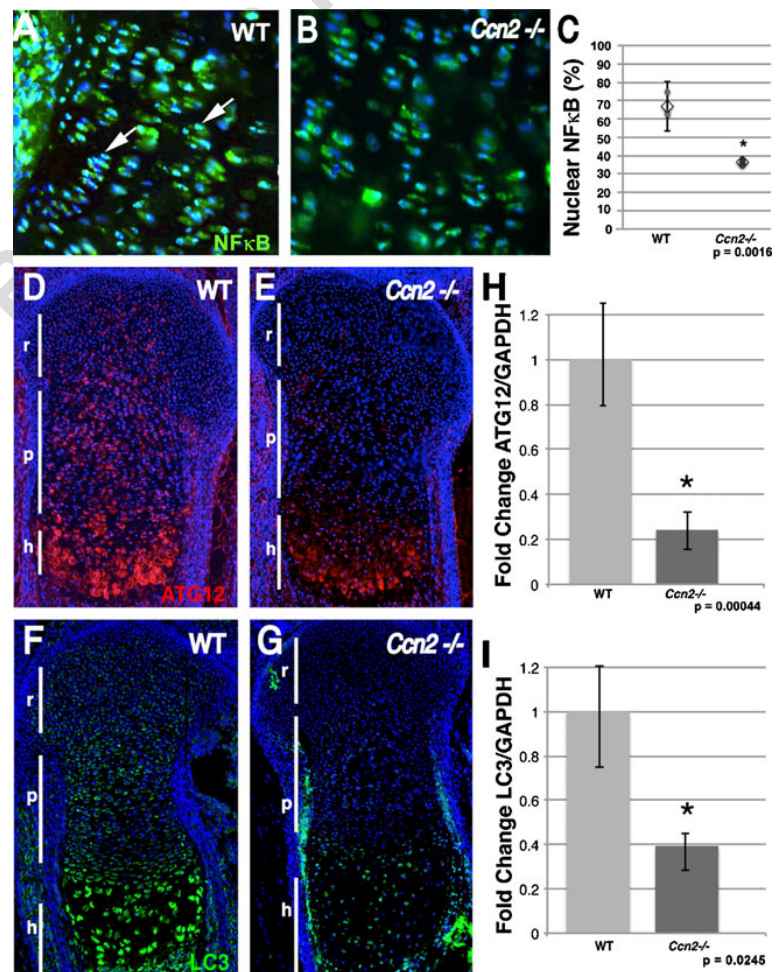
integrin $\alpha 5$ in vitro (Fig. 5). We therefore investigated whether CCN2 might exert pro-survival functions in chondrocytes at least in part through regulation of NF κ B. NF κ B localization was examined in E16.5 WT and mutant growth plates. In WT proliferative zones, NF κ B was predominantly localized to the nucleus (Fig. 7a), similar to previous reports (Park et al. 2007; Wu et al. 2007). In *Ccn2*^{-/-} growth plates, NF κ B was present in the cytoplasm, but the number of cells exhibiting nuclear localization was decreased (Fig. 7b,c). These data are thus consistent with previous in vitro studies showing that CCN2 induces NF κ B activation (Gao and Brigstock 2005), and raise the possibility that CCN2 exerts pro-survival effects in chondrocytes at least in part through NF κ B.

Autophagy is an important survival mechanism in normal chondrocytes and in response to stress (Lotz and Carames 2011). We examined the expression of autophagosome markers Atg12 and LC3 (Atg8), which conjugate with one another to stabilize autophagosome formation (Mehrpour et

al. 2010). In E16.5 WT growth plates, Atg12 and LC3 were expressed throughout the growth plate, with the highest levels in the hypertrophic zone (Fig. 7d, f), consistent with previous literature showing that autophagy is required for terminal chondrocyte differentiation (Srinivas et al. 2009). However, in *Ccn2*^{-/-} growth plates Atg12 and LC3 protein (Fig. 7e,g) and mRNA (Fig. 7h, i) levels were decreased.

Because NF κ B and autophagy have pro-survival functions in chondrocytes, we investigated whether CCN2 can induce NF κ B and the expression of autophagy genes. ATDC5 cells infected with a CCN2 overexpressing adenovirus (Ad-CCN2-GFP) exhibited increased CCN2 expression within 24 h after infection (Fig. 8a, b). Consistent with in vivo studies (Fig. 7), CCN2 expression induced nuclear NF κ B expression (Fig. 8c, d). Furthermore, CCN2 stimulated the expression of LC3 (Fig. 8e, f). These data suggest that CCN2 may protect against chondrocyte stress by upregulating pro-survival NF κ B and autophagy pathways.

Fig. 7 Decreased NF κ B and autophagy-mediated cell survival in *Ccn2* mutants. NF κ B expression was visualized by immunofluorescence in E16.5 WT and *Ccn2* mutant growth plates. **a** In WT growth plates, NF κ B was primarily localized to the nucleus throughout the proliferative zone. **b** In *Ccn2*^{-/-} growth plates, NF κ B expression in the proliferative zone was decreased and localized mainly to the cytoplasm. **c** NF κ B nuclear expression throughout the growth plate was quantitated using Image J analysis as the percentage of DAPI positive nuclei. Growth plate immunostaining was performed in triplicate; asterisk denotes a *p*-value of 0.003, indicating statistical significance. Open triangle indicates the average of the data points. **d, e** E16.5 WT (D) and *Ccn2*^{-/-} (e) growth plates immunostained for Atg12. **f, g** E16.5 WT (F) and *Ccn2*^{-/-} (g) growth plates immunostained for Atg8 (LC3). All sections were counterstained with DAPI. Stains were performed at least twice and representative images are shown. **h, i** *Atg12* and *LC3* mRNA levels were quantitated by qRT-PCR in WT and *Ccn2*^{-/-} sternal chondrocytes



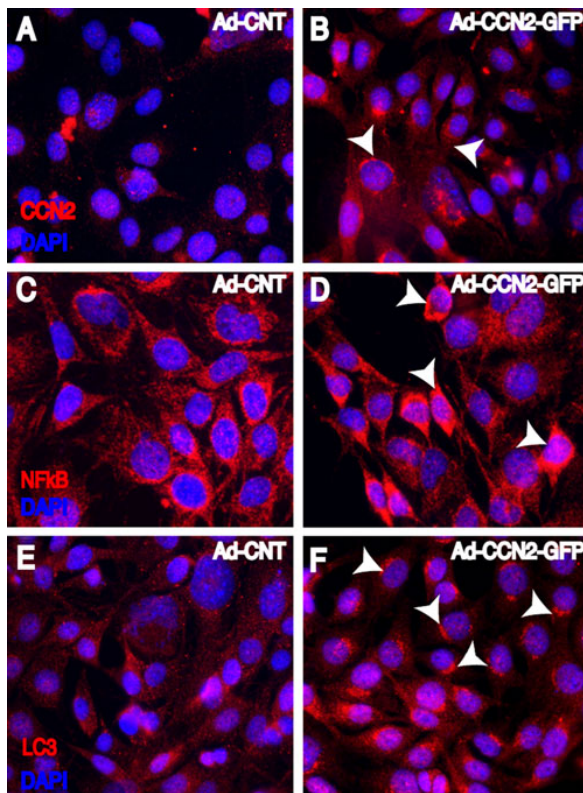


Fig. 8 Ectopic CCN2 expression results in increased NF κ B and expression of autophagy genes in ATDC5 cells. NF κ B and autophagy marker LC3 were examined in ATDC5 cells infected with Ad-CCN2-green fluorescent protein (Ad-CCN2-GFP) and Ad-control (Ad-CNT) constructs. **a, b** CCN2 expression is upregulated in Ad-CCN2-GFP ATDC5 cells (**b**) compared to Ad-CNT treated cells (**a**). **c, d** Nuclear NF κ B is increased in Ad-CCN2-GFP cells (**d**) compared to control cells (**c**). **e, f** Expression of LC3/Atg8 is increased in Ad-CCN2-GFP cells (**f**) compared to Ad-CNT treated cells (**e**). (Red = CCN2, NF κ B and LC3); (Blue = DAPI counterstain). Representative images are shown

Discussion

The data reported here provide evidence that CCN2 is important for ECM assembly and chondrocyte survival in the growth plate. Ultrastructural analysis revealed that loss of CCN2 leads to defective ECM organization and chondrocyte death, accompanied by increased cellular stress. The activation of stress pathways *in vivo* was confirmed by elevated levels of BiP and CHOP in *Ccn2*^{-/-} growth plates. These results were recapitulated *in vitro*, where loss of *Ccn2* in chondron cultures also resulted in cellular stress. This finding suggests that the role of CCN2 in protecting chondrocytes from stress is direct, rather than an indirect consequence of defective growth plate angiogenesis. The finding that *Ccn2* expression is induced by stress, unlike structural ECM proteins, whose expression is downregulated,

suggests that an important function of CCN2 may be to mediate chondrocyte survival.

The precise mechanisms by which CCN2 protects against cellular stress remain unclear. Integrin α 5 β 1 is essential for chondrocyte survival *in vitro* (Pulai et al. 2002). Integrin α 5 expression was decreased in *Ccn2*^{-/-} chondrocytes, leading to defective chondrocyte adhesion and downstream integrin signaling (Nishida et al. 2007). Evidence that CCN2 may exert a pro-survival effect through modulation of cell-ECM attachment comes from the finding that treatment of chondrocytes with an integrin α 5-blocking antibody leads to increased cellular stress, while treatment of ATDC5 cells with C-terminal rCCN2 (which contains the α 5 β 1 binding site) (Gao and Brigstock 2006) mediates a modest protective effect during chemically induced stress, which is attenuated in the presence of an integrin α 5-blocking antibody. Currently, no *in vivo* studies have been conducted to assess the role of α 5 containing integrins in cartilage. However, the loss of β 1 integrin leads to reduced ECM production, growth plate disorganization and impaired survival (Aszodi et al. 2003), consistent with a potential role for α 5 β 1 in ECM organization and chondrocyte survival.

In addition to induction of pro-apoptotic stress pathways, the loss of *Ccn2* also results in decreased expression of nuclear NF κ B and autophagy genes *in vivo*. In accordance, overexpression of *Ccn2* in chondrocytes resulted in induction of nuclear NF κ B and autophagy gene expression. A limitation of these experiments is that the ability of overexpression of CCN2 to rescue NF κ B and autophagy gene expression in *Ccn2*^{-/-} chondrocytes was not tested *in vitro*. Thus, we cannot determine whether the effect of CCN2 is direct or indirect. However, both NF κ B and autophagy exert pro-survival functions in growth plate chondrocytes (Srinivas et al. 2009; Wu et al. 2007). The mechanism by which CCN2 induces the expression of NF κ B in chondrocytes is unknown but probably occurs through integrin signaling, as previously observed in other cell types (Gao and Brigstock 2005; Zahir et al. 2003).

CCN2 expression is correlated with the onset of osteoarthritis (OA) and synovial damage (Blaney Davidson et al. 2006; Omoto et al. 2004). Paradoxically, recombinant CCN2 expedites repair of articular cartilage during chemically induced knee OA (Nishida et al. 2004). These opposing effects of CCN2 may be due to its ability to modulate NF κ B. While NF κ B has pro-survival functions in chondrocytes (Park et al. 2007; Wu et al. 2007), it also promotes the expression of pro-inflammatory genes in OA chondrocytes (Marcu et al. 2010). Whether NF κ B has a pro-survival function in OA chondrocytes is unknown. Further investigations of the mechanism by which CCN2 promotes

survival in growth plate chondrocytes, and its role in the maintenance of articular cartilage may provide new avenues to treat and prevent OA.

Acknowledgments We thank Jeannine Wagner for expert technical assistance. This work was supported by grants: F31 AR060687-01 (FHG), R01 AR052686 (KML), Beckman Foundation (JSO), and the Swiss National Science Foundation (EBH).

Author contributions KML, PB, EBH and FHG were involved in the conception and design of the experiments. FHG, AD, AA, LA, RRB and EBH performed the experiments and analyzed the data. FFS, FvN and RG generated crucial reagents. FHG and KML wrote the article.

Open Access This article is distributed under the terms of the Creative Commons Attribution License which permits any use, distribution, and reproduction in any medium, provided the original author(s) and the source are credited.

References

- Ahmed YA, Tatarczuch L, Pagel CN, Davies HM, Mirams M, Mackie EJ (2007) Physiological death of hypertrophic chondrocytes. *Osteoarthr Cartil OARS Osteoarthr Res Soc* 15(5):575–586
- Altaf FM, Hering TM, Kazmi NH, Yoo JU, Johnstone B (2006) Ascorbate-enhanced chondrogenesis of ATDC5 cells. *Eur Cell Mater* 12:64–69, discussion 69–70
- Araki K, Araki M, Miyazaki J, Vassalli P (1995) Site-specific recombination of a transgene in fertilized eggs by transient expression of Cre recombinase. *Proc Natl Acad Sci U S A* 92(1):160–164
- Aszodi A, Hunziker EB, Brakebusch C, Fassler R (2003) Beta1 integrins regulate chondrocyte rotation, G1 progression, and cytokinesis. *Genes Dev* 17(19):2465–2479
- Avivar-Valderas A, Salas E, Bobrovnikova-Marjon E, Diehl JA, Nagi C, Debnath J, Aguirre-Ghiso JA (2011) PERK integrates autophagy and oxidative stress responses to promote survival during extracellular matrix detachment. *Mol Cell Biol* 31(17):3616–3629
- Barbieri O, Astigiano S, Morini M, Tavella S, Schito A, Corsi A, Di Martino D, Bianco P, Cancedda R, Garofalo S (2003) Depletion of cartilage collagen fibrils in mice carrying a dominant negative Col2a1 transgene affects chondrocyte differentiation. *Am J Physiol Cell Physiol* 285(6):C1504–C1512
- Bateman JF, Boot-Handford RP, Lamande SR (2009) Genetic diseases of connective tissues: cellular and extracellular effects of ECM mutations. *Nature reviews. Genetics* 10(3):173–183
- Bertolotti A, Zhang Y, Hendershot LM, Harding HP, Ron D (2000) Dynamic interaction of BiP and ER stress transducers in the unfolded-protein response. *Nat Cell Biol* 2(6):326–332
- Blaney Davidson EN, Vitters EL, Mooren FM, Oliver N, Berg WB, van der Kraan PM (2006) Connective tissue growth factor/CCN2 overexpression in mouse synovial lining results in transient fibrosis and cartilage damage. *Arthritis Rheum* 54(5):1653–1661
- Bornstein P (2009) Matricellular proteins: an overview. *J Cell Commun Signal* 3(3–4):163–165
- Brigstock DR (2010) Connective tissue growth factor (CCN2, CTGF) and organ fibrosis: lessons from transgenic animals. *J Cell Commun Signal* 4(1):1–4
- Chaquor B, Yang R, Sha Q (2006) Mechanical stretch modulates the promoter activity of the profibrotic factor CCN2 through increased actin polymerization and NF-kappaB activation. *J Biol Chem* 281(29):20608–20622
- Chen CC, Lau LF (2009) Functions and mechanisms of action of CCN matricellular proteins. *Int J Biochem Cell Biol* 41(4):771–783
- Copetti T, Bertoli C, Dalla E, Demarchi F, Schneider C (2009) p65/RelA modulates BECN1 transcription and autophagy. *Mol Cell Biol* 29(10):2594–2608
- Gao R, Brigstock DR (2005) Activation of nuclear factor kappa B (NF-kappaB) by connective tissue growth factor (CCN2) is involved in sustaining the survival of primary rat hepatic stellate cells. *Cell Commun Signal* 3:14
- Gao R, Brigstock DR (2006) A novel integrin alpha5beta1 binding domain in module 4 of connective tissue growth factor (CCN2/CTGF) promotes adhesion and migration of activated pancreatic stellate cells. *Gut* 55(6):856–862
- Hall-Glenn F, De Young RA, Huang BL, van Handel B, Hofmann JJ, Chen TT, Choi A, Ong JR, Benya PD, Mikkola H, Iruela-Arispe ML, Lyons KM (2012) CCN2/connective tissue growth factor is essential for pericyte adhesion and endothelial basement membrane formation during angiogenesis. *PLoS One* 7(2):e30562
- Hamamura K, Goldring MB, Yokota H (2009) Involvement of p38 MAPK in regulation of MMP13 mRNA in chondrocytes in response to surviving stress to endoplasmic reticulum. *Arch Oral Biol* 54(3):279–286
- Ivkovic S, Yoon BS, Popoff SN, Safadi FF, Libuda DE, Stephenson RC, Daluiski A, Lyons KM (2003) Connective tissue growth factor coordinates chondrogenesis and angiogenesis during skeletal development. *Development* 130(12):2779–2791
- Jun JI, Lau LF (2011) Taking aim at the extracellular matrix: CCN proteins as emerging therapeutic targets. *Nat Rev Drug Discov* 10(12):945–963
- Kaneko M, Niinuma Y, Nomura Y (2003) Activation signal of nuclear factor-kappa B in response to endoplasmic reticulum stress is transduced via IRE1 and tumor necrosis factor receptor-associated factor 2. *Biol Pharm Bull* 26(7):931–935
- Kawaki H, Kubota S, Suzuki A, Lazar N, Yamada T, Matsumura T, Ohgawara T, Maeda T, Perbal B, Lyons KM, Takigawa M (2008) Cooperative regulation of chondrocyte differentiation by CCN2 and CCN3 shown by a comprehensive analysis of the CCN family proteins in cartilage. *J Bone Miner Res* 23(11):1751–1764
- Kourouk Y, Fujita E, Tanida I, Ueno T, Isoai A, Kumagai H, Ogawa S, Kaufman RJ, Kominami E, Momoi T (2007) ER stress (PERK/eIF2alpha phosphorylation) mediates the polyglutamine-induced LC3 conversion, an essential step for autophagy formation. *Cell Death Differ* 14(2):230–239
- Lee GM, Poole CA, Kelley SS, Chang J, Caterson B (1997) Isolated chondrons: a viable alternative for studies of chondrocyte metabolism in vitro. *Osteoarthr Cartil* 5(4):261–274
- Lengner CJ, Lepper C, van Wijnen AJ, Stein JL, Stein GS, Lian JB (2004) Primary mouse embryonic fibroblasts: a model of mesenchymal cartilage formation. *J Cell Physiol* 200(3):327–333
- Li J, Ni M, Lee B, Barron E, Hinton DR, Lee AS (2008) The unfolded protein response regulator GRP78/BiP is required for endoplasmic reticulum integrity and stress-induced autophagy in mammalian cells. *Cell Death Differ* 15(9):1460–1471
- Lotz MK, Carames B (2011) Autophagy and cartilage homeostasis mechanisms in joint health, aging and OA. *Nat Rev Rheumatol* 7(10):579–587
- Marcu KB, Otero M, Olivetto E, Borzi RM, Goldring MB (2010) NF-kappaB signaling: multiple angles to target OA. *Current Drug Targets* 11(5):599–613
- Marino G, Fernandez AF, Cabrera S, Lundberg YW, Cabanillas R, Rodriguez F, Salvador-Montoliu N, Vega JA, Germana A, Fueyo A, Freije JM, Lopez-Otin C (2010) Autophagy is essential for mouse sense of balance. *J Clin Invest* 120(7):2331–2344
- Mehrpour M, Esclatine A, Beau I, Codogno P (2010) Overview of macroautophagy regulation in mammalian cells. *Cell Res* 20(7):748–762

- Ni M, Zhang Y, Lee AS (2011) Beyond the endoplasmic reticulum: atypical GRP78 in cell viability, signalling and therapeutic targeting. *Biochem J* 434(2):181–188
- Nishida T, Kubota S, Kojima S, Kuboki T, Nakao K, Kushibiki T, Tabata Y, Takigawa M (2004) Regeneration of defects in articular cartilage in rat knee joints by CCN2 (connective tissue growth factor). *J Bone Miner Res* 19(8):1308–1319
- Nishida T, Kawaki H, Baxter RM, Deyoung RA, Takigawa M, Lyons KM (2007) CCN2 (Connective Tissue Growth Factor) is essential for extracellular matrix production and integrin signaling in chondrocytes. *J Cell Commun Signal* 1(1):45–58
- Nozaki S, Sledge GW Jr, Nakshatri H (2001) Repression of GADD153/CHOP by NF-kappaB: a possible cellular defense against endoplasmic reticulum stress-induced cell death. *Oncogene* 20(17):2178–2185
- Nugent AE, McBurney DL, Horton WE Jr (2011) The presence of extracellular matrix alters the chondrocyte response to endoplasmic reticulum stress. *J Cell Biochem* 112(4):1118–1129
- Omoto S, Nishida K, Yamaai Y, Shibahara M, Nishida T, Doi T, Asahara H, Nakanishi T, Inoue H, Takigawa M (2004) Expression and localization of connective tissue growth factor (CTGF/Hcs24/CCN2) in osteoarthritic cartilage. *Osteoarthr Cartil* 12(10):771–778
- Ovchinnikov DA, Deng JM, Ogunrinu G, Behringer RR (2000) Col2a1-directed expression of Cre recombinase in differentiating chondrocytes in transgenic mice. *Genesis* 26(2):145–146
- Park M, Yong Y, Choi SW, Kim JH, Lee JE, Kim DW (2007) Constitutive RelA activation mediated by Nkx3.2 controls chondrocyte viability. *Nat Cell Biol* 9(3):287–298
- Pulai JJ, Del Carlo M Jr, Loeser RF (2002) The alpha5beta1 integrin provides matrix survival signals for normal and osteoarthritic human articular chondrocytes in vitro. *Arthritis Rheum* 46(6):1528–1535
- Rasheva VI, Domingos PM (2009) Cellular responses to endoplasmic reticulum stress and apoptosis. *Apoptosis* 14(8):996–1007
- Sen T, Dutta A, Chatterjee A (2010) Epigallocatechin-3-gallate (EGCG) regulates gelatinase-B (MMP-9) by involvement of FAK/ERK/NFkappaB and AP-1 in the human breast cancer cell line MDA-MB-231. *Anti-cancer drugs* 21(6):632–644
- Sirabella R, Secondo A, Pannaccione A, Scorziello A, Valsecchi V, Adornetto A, Bilo L, Di Renzo G, Annunziato L (2009) Anoxia-induced NF-kappaB-dependent upregulation of NCX1 contributes to Ca²⁺ refilling into endoplasmic reticulum in cortical neurons. *Stroke J Cereb Circ* 40(3):922–929
- Srinivas V, Bohensky J, Shapiro IM (2009) Autophagy: a new phase in the maturation of growth plate chondrocytes is regulated by HIF, mTOR and AMP kinase. *Cells Tissues Organs* 189(1–4):88–92
- Szafrański JD, Grodzinsky AJ, Burger E, Gaschen V, Hung HH, Hunziker EB (2004) Chondrocyte mechanotransduction: effects of compression on deformation of intracellular organelles and relevance to cellular biosynthesis. *Osteoarthr Cartil* 12(12):937–946
- Tan TW, Lai CH, Huang CY, Yang WH, Chen HT, Hsu HC, Fong YC, Tang CH (2009) CTGF enhances migration and MMP-13 up-regulation via alpha5beta3 integrin, FAK, ERK, and NF-kappaB-dependent pathway in human chondrosarcoma cells. *J Cell Biochem* 107(2):345–356
- Tsang KY, Chan D, Cheslett D, Chan WC, So CL, Melhado IG, Chan TW, Kwan KM, Hunziker EB, Yamada Y, Bateman JF, Cheung KM, Cheah KS (2007) Surviving endoplasmic reticulum stress is coupled to altered chondrocyte differentiation and function. *PLoS Biol* 5(3):e44
- Voncken JW (2011) Genetic modification of the mouse: general technology—pronuclear and blastocyst injection. *Methods Mol Biol* 693:11–36
- Vranka J, Mokashi A, Keene DR, Tufa S, Corson G, Sussman M, Horton WA, Maddox K, Sakai L, Bachinger HP (2001) Selective intracellular retention of extracellular matrix proteins and chaperones associated with pseudoachondroplasia. *Matrix Biol* 20(7):439–450
- Walter P, Ron D (2011) The unfolded protein response: from stress pathway to homeostatic regulation. *Science* 334(6059):1081–1086
- Wu S, Flint JK, Rezvani G, De Luca F (2007) Nuclear factor-kappaB p65 facilitates longitudinal bone growth by inducing growth plate chondrocyte proliferation and differentiation and by preventing apoptosis. *J Biol Chem* 282(46):33698–33706
- Yang L, Carlson SG, McBurney D, Horton WE Jr (2005) Multiple signals induce endoplasmic reticulum stress in both primary and immortalized chondrocytes resulting in loss of differentiation, impaired cell growth, and apoptosis. *J Biol Chem* 280(35):31156–31165
- Zahir N, Lakins JN, Russell A, Ming W, Chatterjee C, Rozenberg GI, Marinkovich MP, Weaver VM (2003) Autocrine laminin-5 ligates alpha6beta4 integrin and activates RAC and NFkappaB to mediate anchorage-independent survival of mammary tumors. *J Cell Biol* 163(6):1397–1407